August 28, 2009

Dr. Michael Berndt
Research Scientist II
Minnesota Department of Natural Resources
Division of Lands and Minerals
500 Lafayette Road
St. Paul, MN 55155-4045

Dear Dr. Berndt:

Subject: Revised Final Report Entitled "Assessment of Potential Corrosion Induced by Bromine Species Used for Mercury Reduction in a Taconite Facility"; Work Order Contract No. B24812; EERC Fund 14783

Enclosed please find the subject report. If you have any questions, please contact me by phone at (701) 777-5236 or by e-mail at yzhuang@undeerc.org.

Sincerely,

Ye Zhuang
Research Engineer

YZ/sah

Enclosure

ASSESSMENT OF POTENTIAL CORROSION INDUCED BY BROMINE SPECIES USED FOR MERCURY REDUCTION IN A TACONITE FACILITY

Final Report

(for the period of February 6 through June 30, 2009)

Prepared for:

Michael Berndt

Minnesota Department of Natural Resources
Division of Lands and Minerals
500 Lafayette Road
St. Paul, MN 55155-4045

Work Order Contract No. B24812

Prepared by:

Ye Zhuang
David J. Dunham
John H. Pavlish

Energy & Environmental Research Center
University of North Dakota
15 North 23rd Street, Stop 9018
Grand Forks, ND 58202-9018

2009-EERC-08-07 August 2009

EERC DISCLAIMER

TABLE OF CONTENTS

LIST OF FIGURES

Continued . . .

LIST OF FIGURES (continued)

LIST OF TABLES

ASSESSMENT OF POTENTIAL CORROSION INDUCED BY BROMINE SPECIES USED FOR MERCURY REDUCTION IN A TACONITE FACILITY

EXECUTIVE SUMMARY

Bromine-related mercury control technology has been considered an effective mercury reduction option for the taconite industry even though its impact on taconite facility operation is not well understood. The EERC conducted bench-scale exposure experiments where metal coupons were exposed in simulated taconite flue gas in 40-ppm HBr processing environments. To understand how bromine-induced corrosion may occur in different temperature zones, the designed static-exposure experiments were performed at 500°, 300°, and 150°C to mimic the preheat zone, the drying/cooling zone, and the discharge zone, respectively. The coupons were exposed to flue gas for 30 days and were removed every 10 days during the test for weight measurement. The weight gain/loss was determined by comparing present tested weights to previous weight measurements. The coupons were treated following the ASTM International Standard G1-03 method before the weight measurement. Similar metal coupons were also exposed in taconite flue gas without bromine present for comparison. The metal coupons provided by the taconite industry represented process grate materials used in United Taconite Mine (also U), Minorca Mines (also M), and U.S. Steel (USS) Minntac Mine (UM). At the end of the exposure experiments, morphology as well as the elemental compositions of the corrosion product were then characterized using scanning electron microscopy–energy-dispersive x-ray analysis (SEM–EDX).

The preliminary test results indicated that 1) 40 ppm HBr in taconite process flue gas appears to cause slight surface corrosion of the test coupons. SEM surface microscopy showed small pitting, cracking, and blistering occurred with bromine deposition and losses of Fe, Cr, and Ni; 2) however, coupon cross-sectional analyses indicated that bromine deposition and losses of Fe, Ni, and Cr were mainly confined to the surface of the coupons, and no significant bromine penetration and subsequent elemental changes were observed below the coupon surface after the 30-day exposure experiments; 3) coupon surface corrosion appears to be less with decreasing temperature; 4) three coupon sets showed resistance to bromine attack under testing environments during the 30-day testing period; and 5) deposits of iron oxide and sodium sulfate seem to induce slight chemistry changes on U and M coupons but not on UM coupons.

It should be noted that, because of limited time and scope of work, the completed corrosion exposure tests were carried out in simplified simulated flue gas environments that did not 100% represent 100% actual operating conditions in the taconite process. The original objective of this project was to see if bromine could cause any possible corrosion under selected testing conditions; however, the 30-day exposure testing period may not necessarily be long enough to attain a complete perspective of possible bromine-induced corrosion issues in a taconite facility. Therefore, the project results can be regarded as the first step in the effort to address potential bromine-induced corrosion when bromine is applied to a taconite facility for mercury reduction. Additional bench-scale coupon corrosion tests under continuous thermal cycling with wider temperature regimes and extended exposure times are needed before any large-scale field testing.

ASSESSMENT OF POTENTIAL CORROSION INDUCED BY BROMINE SPECIES USED FOR MERCURY REDUCTION IN A TACONITE FACILITY

BACKGROUND

The state of Minnesota is targeting an overall mercury reduction of 90%. In Minnesota, taconite plants are the second largest source of mercury emissions in the state, while stack emissions are the dominant pathway of mercury release from taconite processing.

Mercury in a typical taconite flue gas has three basic forms: 1) elemental mercury (Hg^0), 2) oxidized mercury (Hg^{2+}), and 3) particulate-bound mercury (Hg[p]). It is widely known that both Hg(p) and Hg^{2+} can be removed from the gas stream with particulate matter (PM) control devices and/or wet scrubbers, while Hg^0 is not readily removed by existing air pollution control devices (APCDs). Since most taconite facilities are equipped with a wet venturi-type scrubber to control PM emissions (1), the most convenient mercury reduction approach for the taconite industry is to improve conversion of Hg^0 to Hg^{2+} and/or Hg(p), so that the mercury can then be removed with existing APCDs without adding new control devices.

Among various mercury reduction technologies being developed, halogens have been widely applied and proven effective in mercury oxidation and adsorption in coal flue gas environments (2–7). However, with the difference between coal flue gas and taconite flue gas, these Hg control technologies have to be tested in taconite flue gas before full-scale application. Both chloride and bromide compounds have been added into the induration furnace, the green ball feed system, and the scrubber liquids to evaluate their effectiveness on mercury reduction in taconite flue gas. So far, bromine compounds have been shown to be the most promising mercury reduction agent that can be directly applied to taconite facilities (1, 8, 9). However, one concern about applying bromide as a mercury reduction agent is that it will induce corrosion and/or accelerate corrosion rates on taconite equipment, such as the feed grate.

Bromine-induced corrosion has been observed in a coal flue gas environment (10) and may be classified as dew point corrosion or active oxidation, depending on the flue gas conditions. Hydrobromic acid is formed with water through multicomponent condensation when flue gas temperature is below a corresponding hydrobromic acid dew point; subsequently, dew point corrosion occurs on the metal surface. At temperatures over the hydrobromic acid dew point, gaseous bromine is capable of diffusing through the oxide layer to the scale–metal interface where it reacts with the iron to form iron bromide through Reactions 1 and/or 2:

$$Fe(s) + Br_2(g) \rightarrow FeBr_2(s) \quad [1]$$

$$Fe(s) + 2HBr(g) \rightarrow FeBr_2(s) + H_2(g) \quad [2]$$

The volatile iron bromide potentially then diffuses outward to the scale surface where it is converted to a solid oxide at the elevated oxygen concentration (Reaction 4):

$$FeBr_2(s) \rightarrow FeBr_2\ (g) \quad [3]$$

$$2FeBr_2(g) + 3/2O_2(g) \rightarrow Fe_2O_3(s) + 2Br_2(g) \quad [4]$$

By Reaction 4, the formed free bromine is either released to the bulk gas or diffuses back to the scale–metal interface, and thus a cycle is formed.

The same bromine corrosion and regeneration cycles may proceed via $FeBr_3$, and it is possible for the ferrous iron to be oxidized to the ferric state while the oxidation liberates bromine as well:

$$4FeBr_2 + 4HBr + O_2 \rightarrow 4FeBr_3 + 2H_2O \quad [5]$$

$$4FeBr_3 + 3O_2 \rightarrow 2Fe_2O_3 + 4Br_2 \quad [6]$$

Although direct injection of bromide salts, so far, has been shown to be a relatively easy, convenient, and cost-effective mercury control option applicable to the taconite industry (8, 9), most of these tests have been short in duration and have not addressed process concerns and potential impacts to the process and/or processing equipment, including potential bromine-induced corrosion. This project was undertaken to evaluate this potential as a prerequisite to applying bromide salts as a mercury control option for the taconite industry. Therefore, the exposure experiments will help the taconite industry to understand and evaluate the potential side effects that may result from applying bromide-related mercury control technology to the taconite industry.

OBJECTIVES

The objectives of this project included the following:

- Determine if bromine induces and/or increases the metal corrosion of equipment exposed to a typical taconite flue gas environment.
- Determine if the rate of bromine-related corrosion is a function of exposure temperature.
- Determine the mechanisms of bromine-related induced corrosion.

EXPERIMENTAL APPROACH

To meet proposed objectives, the EERC conducted bench-scale exposure experiments where metal coupons were placed in a temperature-controlled chamber filled with simulated taconite flue gas. Table 1 shows the simulated flue gas composition used in the exposure experiments.

Table 1. Simulated Taconite Flue Gas Baseline Composition

Flue Gas Constituent	Concentration[1]
O_2, %	14
CO_2, %	4.0
H_2O, %	20
N_2, %	Balance
NO, ppm	600
NO_2, ppm	10
CO, ppm	40
SO_2, ppm	10
HBr, ppm[2]	40

[1] Average value measured in taconite flue gas.
[2] HBr included in Test Series 2 only.

It should be noted that the taconite flue gas usually has high concentrations of O_2 (~14%) and H_2O (~20%) and small amounts of SO_2 as a result of taconite plants using low-sulfur fuel and moisture from drying the green balls. For the bromine-induced corrosion testing, HBr is added to the matrix in a 40-ppm concentration.

The metal coupons used were provided by three taconite mines and were chosen to closely represent the material of each process grate. The companies supplying coupons were United Taconite Mine (also U), Minorca Mines (also M), and U.S. Steel (USS) Minntac Mine (also UM). In general, the Minorca coupon has a lower Ni content and a higher Fe content than the United and Minntac coupons, while their Cr contents are similar. Each testing coupon was approximately 1 in. × 1 in. The metal coupons were covered with iron oxides to simulate the taconite-processing environment. A parallel exposure experiment was also conducted in which the metal coupons were not covered with iron oxides. The experimental results will determine if iron oxide will affect potential bromine-induced corrosion in taconite flue gas.

It is likely that the grate material will be exposed to bromine species, most likely HBr, throughout the drying zone, preheat zone, firing zone, cooling zone, and stack. Plotted in Figure 1 is a diagram of a typical grate–kiln taconite process. To understand how bromine-induced corrosion may occur at these different temperature zones, the designed static-exposure experiments were performed at 500°, 300°, and 150°C to mimic the preheat zone, the drying/cooling zone, and the discharge zone, respectively. In addition to the bromine-induced corrosion testing, similar metal coupons were also exposed in taconite flue gas without bromine present for comparison. The detailed test matrix is shown in Table 2. The coupons were exposed to flue gas for 30 days and were removed every 10 days during the test for weight measurement. The weight gain/loss was determined through comparison to previous weight measurements. The coupons were treated following the ASTM International Standard G1-03 method before the weight measurement.

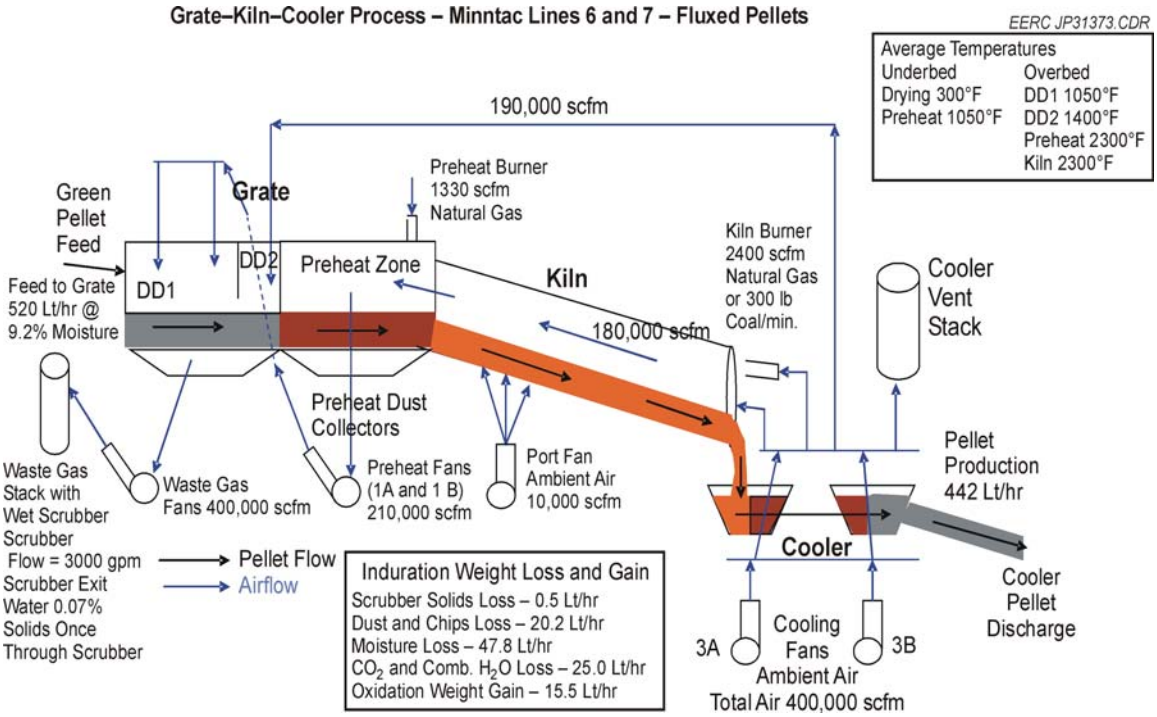

Figure 1. Diagram of a typical taconite process.

Table 2. Exposure Test Matrix

Test No.	Flue Gas Composition	Iron Oxides	Exposure Temperature, °C
I-1	Taconite flue gas baseline	None	500
I-2a	Taconite flue gas baseline plus 40 ppm HBr	None	500
I-2b	Taconite flue gas baseline plus 40 ppm HBr	Yes	500
II-1	Taconite flue gas baseline	None	300
II-2a	Taconite flue gas baseline plus 40 ppm HBr	None	300
II-2b	Taconite flue gas baseline plus 40 ppm HBr	Yes	300
III-1	Taconite flue gas baseline	None	150
III-2a	Taconite flue gas baseline plus 40 ppm HBr	None	150
III-2b	Taconite flue gas baseline plus 40 ppm HBr	Yes	150

At the end of the exposure experiments, the metal coupons were removed and treated following a standard metallographic preparation procedure. Morphology as well as the elemental compositions of the corrosion product was then characterized using scanning electron microscopy–energy-dispersive x-ray analysis (SEM–EDX). This information is presented in the results section of this report.

EXPERIMENTAL SETUP

Bench-scale exposure chambers were designed and set up to provide temperature zones that mimic the taconite process. Two 90-in. ceramic tubes were used as test chambers. One chamber carried flue gas, while a second chamber carried 40 ppm HBr in addition to the flue gas. A tube furnace was used to heat the 500° and 300°C temperature zones. The final zone was wrapped with heat tape and controlled at 150°C. The temperature zones were monitored with a thermocouple/heater controller system. A schematic of the test system is shown in Figure 2.

The gas delivery system of the EERC's Environmental Control Laboratory was used to provide the flue gas matrix for the test. The system uses mass flow controllers (MFCs) to meter appropriate amounts of each gas constituent. The MFCs are backed up by rotameters to provide a visual check on the gas flows into the mixing manifold. A National Instruments LabVIEW program was written for the test and directed the MFCs to provide required flow rates for each flue gas constituent. The program also logged system temperatures throughout the test. The acid gases, air, nitrogen balance, and carbon dioxide were mixed in a heated manifold before being sent to the test tubes in a heated line. The moisture for the gas matrix was created in a steam generator and combined with a small portion of the nitrogen balance before being sent to the test apparatus in a heated line. The moisture content was regulated with a peristaltic pump which fed the steam generator. It is important to note that heated lines were used to bring all components of the flue gas matrix to the system to allow for preheat and mixing time before entering the test chambers.

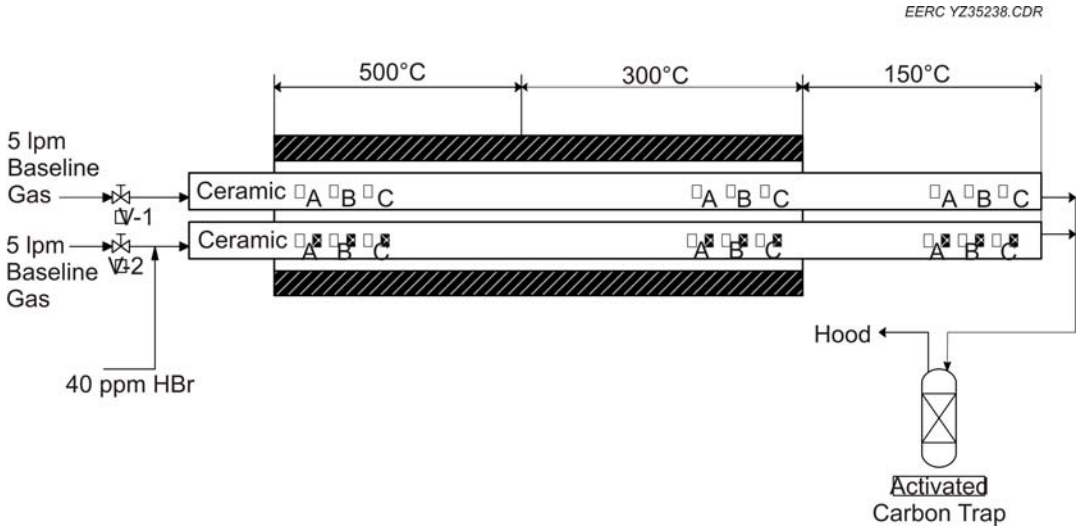

Figure 2. Schematic of the exposure testing system.

EXPERIMENTAL PROCEDURE

The three sets of 1-in. × 1-in. coupons tested were provided by the taconite industry. Before testing, the coupons were prepared by the EERC in the following steps:

1) Stamped for identification purposes and labeled 1–9
2) Coupons 1–3 of each set drilled to receive iron oxide/sodium sulfate deposit
3) Immersed in an acetone bath
4) Ultrasonically cleansed for 30 minutes
5) Dried in desiccators for 30 minutes
6) Weighed

The coupons were loaded into the ceramic test tubes, with the polished surface facing up. Coupons labeled 1–3 received a deposit of iron oxide/sodium sulfate powder (90/10). Table 3 summarizes the layout of testing coupons within the system.

Upon loading, the furnace and heaters were brought up to operating temperature. When the process temperatures were reached, the gases and moisture were turned on. The test ran from April 15 until June 2, 2009. Upon completion of 10 days of testing, the unit was turned off and the coupons removed for weighing and inspection. Because the USS Minntac coupons were received late, they were not included in the first 10 days of testing. Another 10 days of exposure were added at the end of the test to accommodate the Minntac coupon 30-day exposure time. Table 4 lists the start/end date of testing for each coupon set.

Table 3. Coupon Test Layout

		Flue Gas with HBr			Flue Gas Without HBr		
Coupons	Deposit	500°C	300°C	150°C	500°C	300°C	150°C
United	Yes	U1	U2	U3			
	No	U4	U5	U6	U7	U8	U9
Minorca	Yes	M1	M2	M3			
	No	M4	M5	M6	M7	M8	M9
USS Minntac	Yes	UM1	UM2	UM3			
	No	UM4	UM5	UM6	UM7	UM8	UM9

Table 4. Test Dates

	Start Date	End Date
United	4/15/09	5/22/09
Minorca	4/15/09	5/22/09
USS Minntac	4/27/09	6/2/09

Throughout the testing, gas flows, temperatures, and water flows were checked periodically to assure that the test parameters were being met. The gas flows were checked by comparing the rotameter flows with the software readouts from the mass flow controllers. The gas flows remained at their set points throughout the duration of the test. Temperature control was verified several times a day by visual inspection of digital heater control readouts. Water flow input to the system through the steam generator was cross-checked by measuring the mass of water per minute through the peristaltic pump. The water flow was steady at its set point throughout the test.

RESULTS AND DISCUSSIONS

Upon completion of 30 days of testing the coupons were removed and prepared for analysis. The coupons were photographed, weighed, and sent to the EERC's Materials Analysis Laboratory (MAL) for analysis. The MAL used SEM–EDX to determine morphology as well as the elemental compositions of the corrosion product.

Macroscopic Surface Analysis

Figures 3–5 are surface photographs of each coupon after 30 days of flue gas exposure.

United Coupons U1–6 were exposed to flue gas containing HBr while coupons U7–9 were exposed to flue gas only. All of the coupons changed color although the flue gas containing HBr caused more surface discoloration than non-HBr-containing flue gas. Also, the coupons subjected to higher temperatures—U1, 4, and 7—show more surface oxidation than the lower-temperature coupons. The iron oxide/sodium sulfate deposit on U1–3 does not appear to have affected the surface coloration of the United coupons.

For the Minorca coupons, it appears that the exposure to HBr affected surface discoloration but not as greatly as what was seen in the United coupons. Unlike the United coupons, it does not appear that the temperature gradient caused greater surface discoloration across the set. The iron oxide/sodium sulfate deposits on M1–3 appear to have only caused significant surface discoloration on the M1 coupon, which was sitting in the 500°C chamber of the test apparatus.

The surfaces of the USS Minntac coupons are shown in Figure 5. Exposure to higher temperatures caused more discoloration than lower temperatures. The effect of HBr exposure did not induce any additional surface oxidation compared to non-HBr-containing flue gas. A deposit of iron oxide/sodium sulfate on coupons UM1–3 did not cause any additional discoloration when compared to the other coupons.

Microscopic Analysis

Each coupon surface was scanned with SEM–EDX to characterize detailed surface morphology and quantify distribution of metal elements on the coupon surface. Moreover, cross section SEM–EDX analysis was also performed for each coupon to determine degree of potential

Figure 3. Surface of United coupons after testing.

corrosion. Although all coupons were analyzed, only figures and analyses showing corrosion or other notable characteristics are included in the body of this report. The complete data set of SEM results is included in Appendices A–C for each coupon set.

United Coupons

Table 5 summarizes the elemental distribution on the surfaces of United coupons for the testing conditions. Only averaged data were reported since they best represent the random nature in which the scans were completed. The elemental weight percentage of the United coupons before testing is also included for comparison.

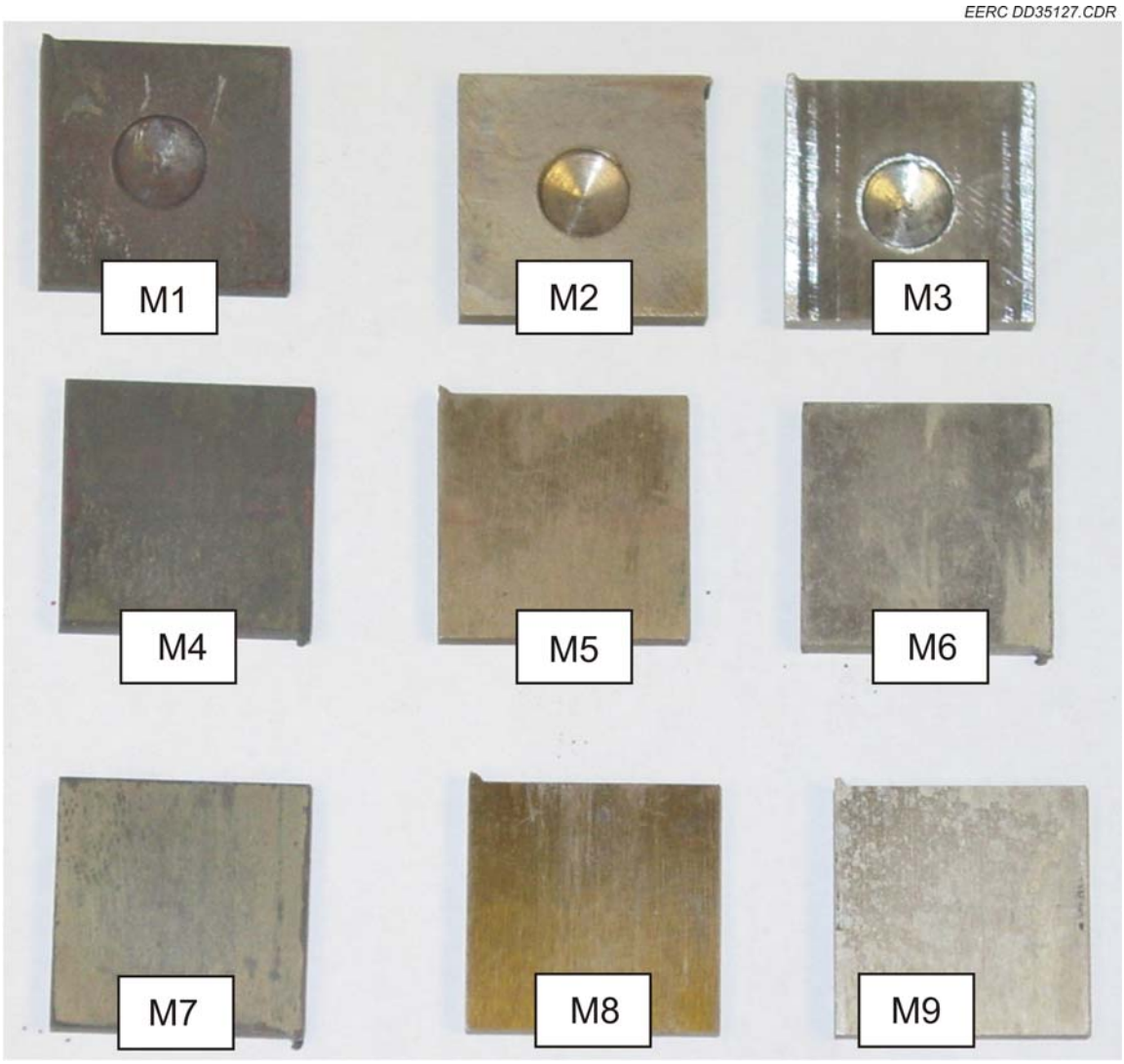

Figure 4. Surface of Minorca coupons after testing.

Compared to the elemental pretest composition, all exposed United coupons experienced some surface corrosion. Coupons exposed to taconite flue gas only, U8 and 9, experienced very few elemental changes, while U7 indicated measurable loss of Ni. The Ni loss can be attributed to sulfur attack. Figures 6 and 7 show SEM images of the U7 surface and cross section, respectively. Table 6 lists measured elemental concentrations along the U7 cross section. The U7 surface appears to have slight surface striations. Although the U7 surface suffered Ni loss, there is no further corrosion penetration.

SEM analyses on the surface and cross section of U8 and U9 show little change in morphology and elemental compositions. The complete analysis details have been included in Appendix A.

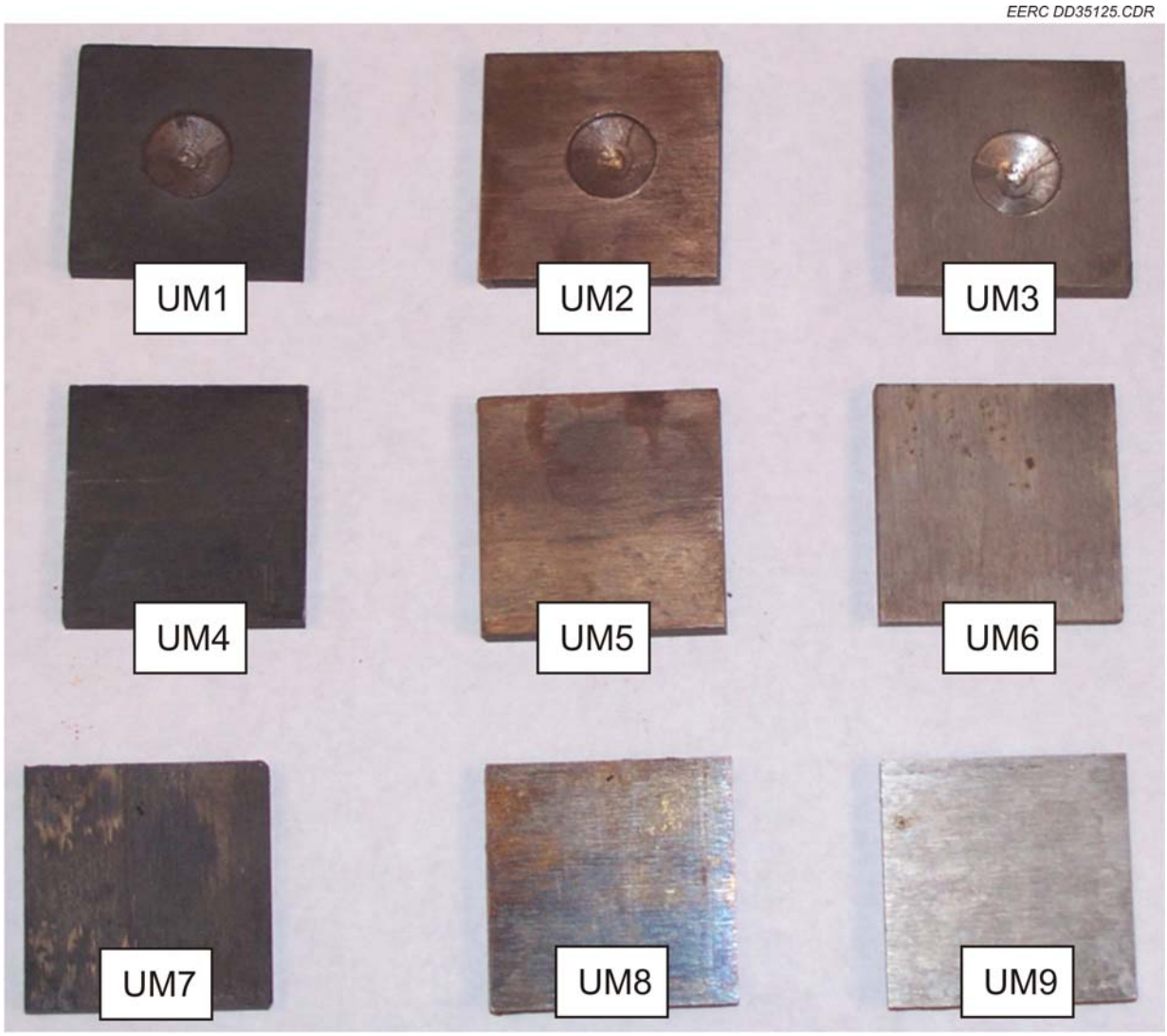

Figure 5. Surface of USS Minntac coupons after testing.

Table 5. Normalized Distribution of Elements on United Coupon Surface, wt%

	Temp., °C	Si	S	Cr	Mn	Fe	Co	Ni	Br
Pretest		4.26	0.50	27.81	0.25	52.42	0.00	14.91	0.00
U1	500	6.18	1.18	21.60	1.69	58.01	0.03	9.00	2.25
U2	300	2.50	0.84	17.90	0.76	67.75	0.20	7.05	2.91
U3	150	1.99	0.57	22.75	0.44	64.81	0.08	7.92	1.35
U4	500	3.09	0.49	21.43	0.90	59.49	0.17	9.09	5.23
U5	300	3.26	1.20	29.98	0.38	48.77	0.00	13.53	2.85
U6	150	3.80	2.86	33.47	0.46	45.47	0.01	12.36	1.31
U7	500	6.44	8.28	39.57	2.90	39.30	0.11	3.22	0.00
U8	300	4.47	2.42	27.09	0.63	52.07	0.09	12.52	0.00
U9	150	4.17	6.34	25.68	0.48	49.82	0.04	13.38	0.00

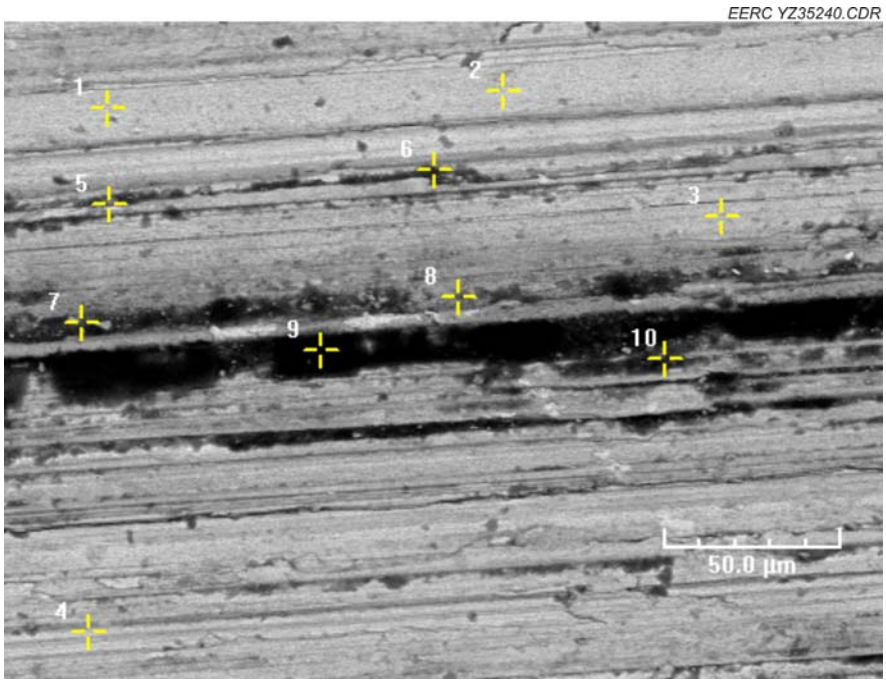

Figure 6. U7 surface SEM image.

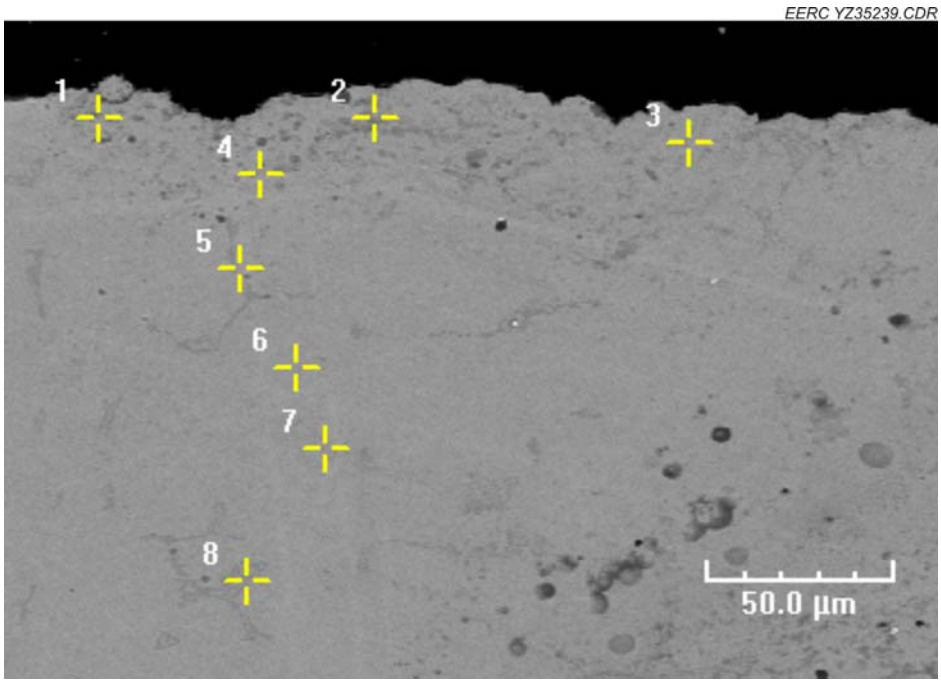

Figure 7. U7 cross-sectional SEM image.

Table 6. Elemental Analysis of U7 Cross Section, wt%

Tag	Si	S	Cr	Mn	Fe	Co	Ni
1	1.78	0.50	50.52	0.71	37.11	0.00	9.34
2	5.68	2.01	26.56	0.23	51.25	0.00	14.02
3	3.19	0.50	26.32	0.43	54.76	0.00	14.71
4	6.63	0.52	26.84	0.15	51.56	0.00	14.29
5	4.23	1.02	28.45	0.17	52.28	0.00	13.81
6	4.69	0.30	24.75	0.37	55.35	0.00	14.45
7	3.04	0.45	26.36	0.18	54.15	0.00	15.72
8	3.73	0.43	27.20	0.78	52.81	0.00	14.96

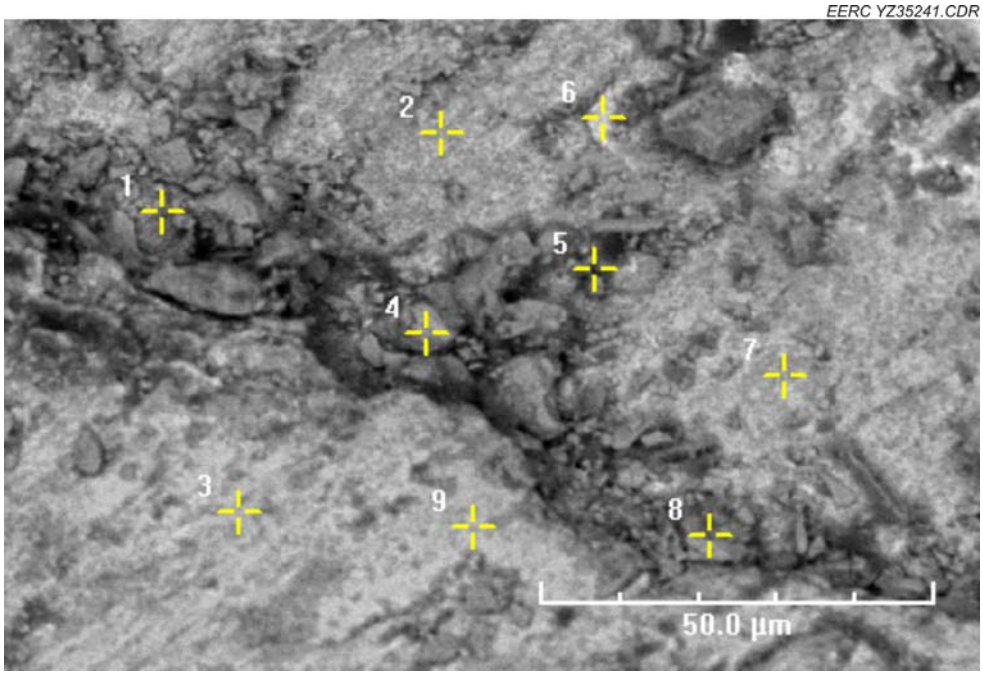

Figure 8. U1 surface SEM image.

Coupons that have been exposed to bromine and taconite flue gas, U1–6, all showed Br deposition in small percentages. As a result, iron, chromium, and nickel elemental averages show small gains/losses depending on the testing conditions. Sulfur and silicon were affected in very small percentages in some coupons. Plotted in Figures 8–11 are the surface SEM images for U1–4 respectively. Compared to surface striations observed on U4, small surface cracks, pits, and chipping on coupons U1–3 were mainly caused by drilling during coupon preparation. Elemental analysis data of the U1–4 surfaces indicate enrichment of Fe and losses of Cr and Ni due to HBr attack. SEM data of U5 and 6 surfaces indicate no large changes in morphology and elemental composition after exposure testing. The complete data set is included in Appendix A.

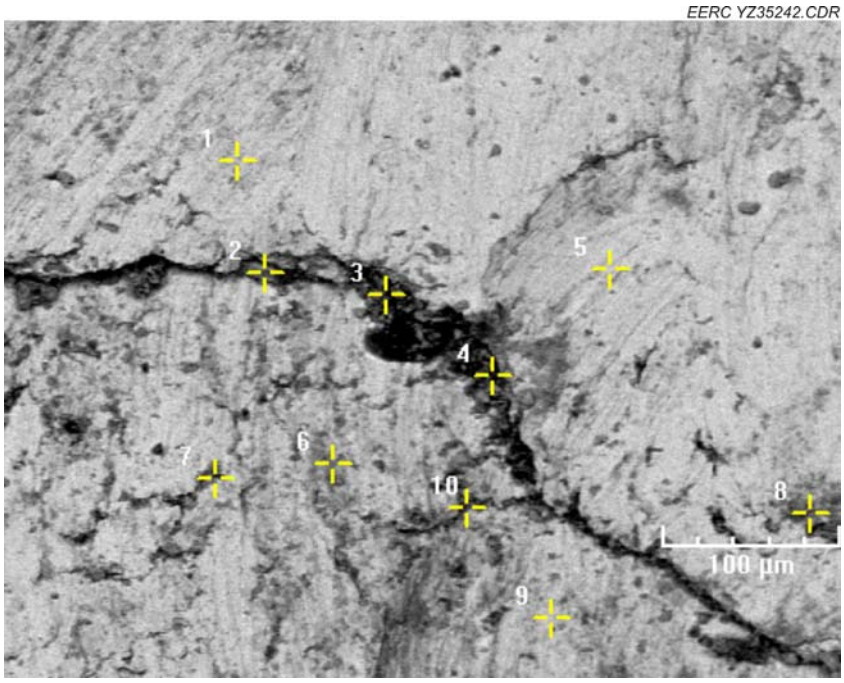

Figure 9. U2 surface SEM image.

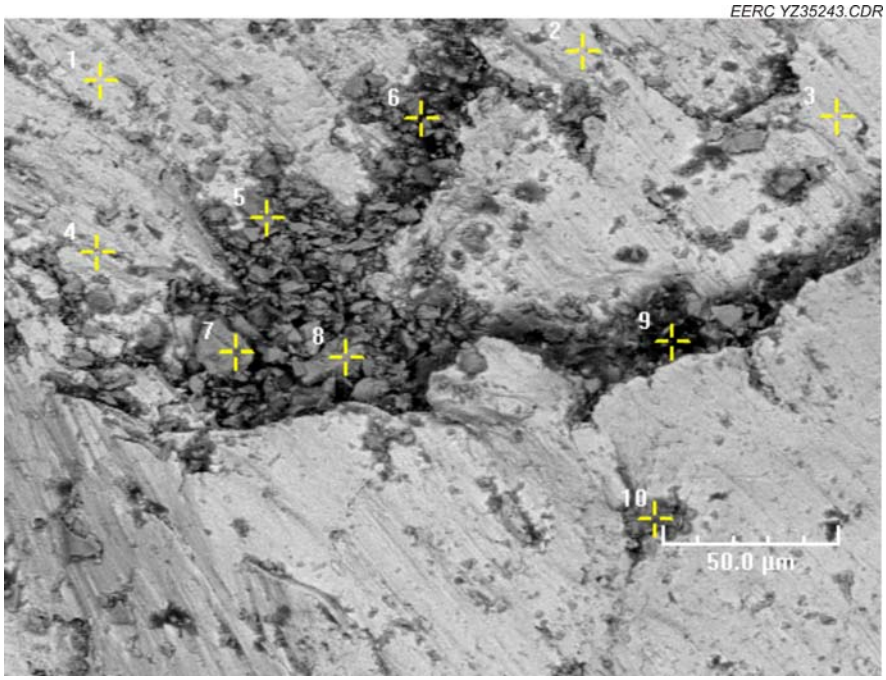

Figure 10. U3 surface SEM image.

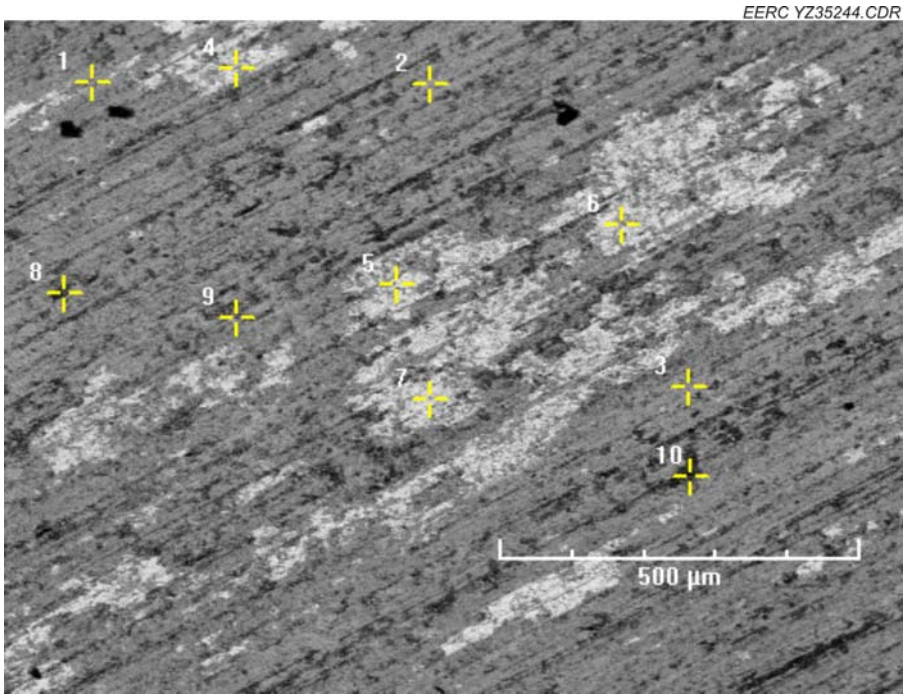

Figure 11. U4 surface SEM image.

The cross-sectional SEM data for United coupons, other than U4, indicate that bromine deposition was confined to the surface of the material and did not impact the elemental composition. Figure 12 is the cross-sectional SEM image for U4, and corresponding elemental distributions are list in Table 7. The SEM data for U4 indicate slight penetration of bromine species with corresponding losses of Ni and Fe below the coupon surface under 500°C testing conditions. Other SEM cross-sectional data are reported in Appendix A.

In summary, all the United coupons showed very little corrosive deterioration after 30 days of exposure testing. None of the United coupon cross sections showed significant bromine penetration beyond the surface. SEM cross sections showed very small surface chips, cracks, and pits on several of the samples, which most likely were caused by drilling the wells. However, it did not seem to induce any additional corrosive activity. The iron oxide/sodium sulfate deposits showed no more corrosion than the flat areas surrounding them. Although the bromine-exposed coupons saw slightly worse corrosion than those not exposed to bromine, cross-sectional SEM analysis indicates that this oxidation did not penetrate beyond the surface of the coupons.

Minorca Coupons

Listed in Table 8 are the averaged elemental compositions on the surfaces of Minorca coupons under different testing conditions.

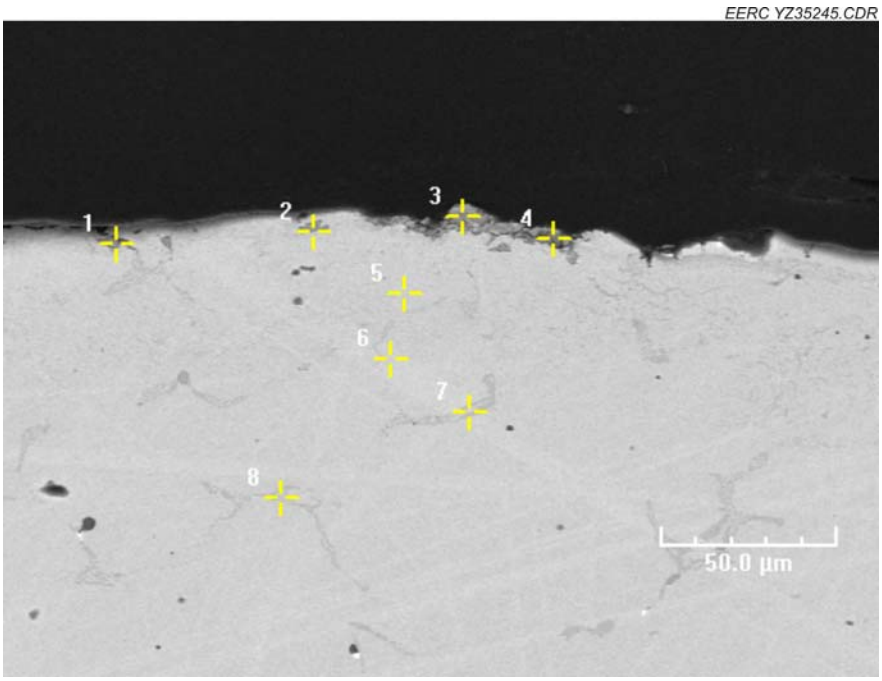

Figure 12. U4 cross-sectional SEM image.

Table 7. Elemental Analysis of U4 Cross Section, wt%

Tag	Si	S	Cr	Mn	Fe	Co	Ni	Br
1	3.09	0.90	16.24	0.00	61.59	0.00	18.08	0.00
2	7.57	0.54	23.58	0.21	50.50	0.00	15.75	1.86
3	5.90	0.58	79.87	3.61	4.82	0.00	1.51	3.71
4	12.35	1.36	55.80	4.43	16.91	0.00	7.38	1.71
5	2.65	0.39	26.22	0.00	55.20	0.00	14.49	0.97
6	3.07	0.51	27.26	0.72	52.08	0.00	14.69	1.66
7	2.40	0.87	60.00	0.07	30.25	0.00	5.32	1.09
8	2.22	0.59	52.67	0.44	35.85	0.01	7.41	0.73

SEM surface analysis of coupons M7–9, which were only exposed to taconite flue gas, indicates gain or loss of Ni, Fe, and Cr, depending on testing conditions. Both Fe and Ni were oxidized or vaporized on the M7 surface under 500°C testing conditions. This resulted in Cr enrichment while little elemental change was observed on M8 at 300°C. The M9 surface appears to have suffered sulfur attack, showing Fe and Cr losses. Plotted in Figures 13–15 are the microscopic surface images of coupons M7–9, respectively. No surface chips, cracks, or pits are visible, but surface striations were observed. Cross-sectional data for M7–9 (reported in Appendix B) show consistent elemental distribution similar to pretest data beyond the coupon surface, proving no penetrated corrosion occurred.

Table 8. Normalized Distribution of Elements on Minorca Coupon Surface, wt%

	Temp., °C	Si	S	Cr	Mn	Fe	Co	Ni	Br
Pretest		5.28	0.31	27.63	0.25	61.66	0.09	4.74	0
M1	500	12.3	0.74	34.95	7.06	41.46	0.06	1.86	1.53
M2	300	1.90	0.24	25.92	0.91	66.94	0.56	2.79	0.76
M3	150	2.67	0.50	14.48	0.43	78.29	0.52	1.86	1.24
M4	500	6.56	0.46	41.54	2.75	43.70	0.43	1.55	3.01
M5	300	3.44	4.25	25.73	0.72	58.61	0.37	3.85	3.03
M6	150	4.35	5.43	26.60	0.38	57.14	0.14	4.03	1.88
M7	500	8.45	0.80	51.78	5.07	32.91	0.00	1.00	0.00
M8	300	3.84	0.39	24.64	0.22	65.90	0.36	4.66	0.00
M9	150	2.96	28.80	15.70	0.50	47.07	0.18	4.39	0.00

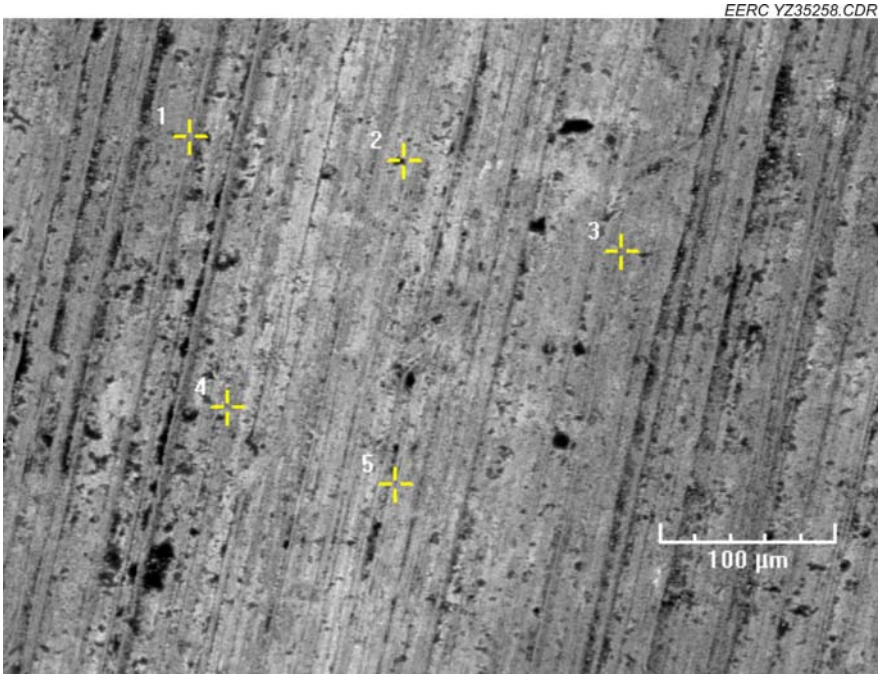

Figure 13. M7 surface SEM image.

The coupons exposed to bromine, M1–6, all showed Br deposition, while bromine concentrations on coupons with iron oxide deposit were less than that without deposition. Plotted in Figures 16–21 are the surface SEM images for coupons M1–6. Small cracking and pitting are observed on M1–3 surfaces, and this was most likely caused by the drilling process. M1 (Figure 16) shows slight blistering, an indication of vaporization at 500°C. Discoloration and striation were seen on M2 and M3. Similar surface striations were also observed for coupons M4–6. As shown in Table 8, consistent losses of Ni were detected on coupon surfaces where they contacted HBr. Iron loss was only detected at the 500°C testing temperature, i.e., M1 and 4.

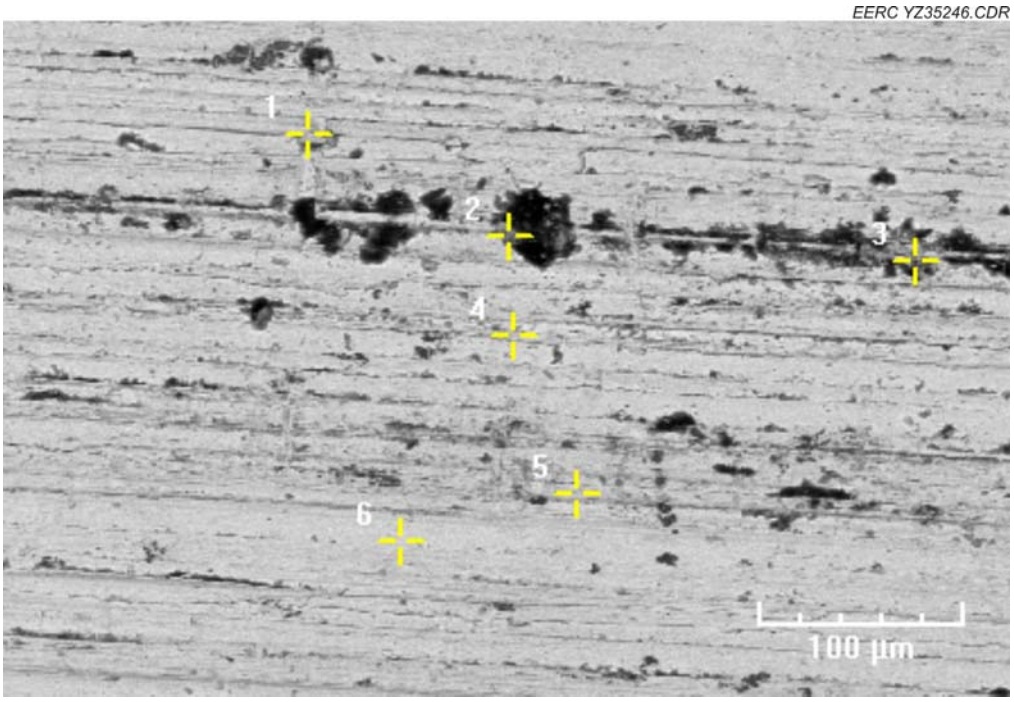

Figure 14. M8 surface SEM image.

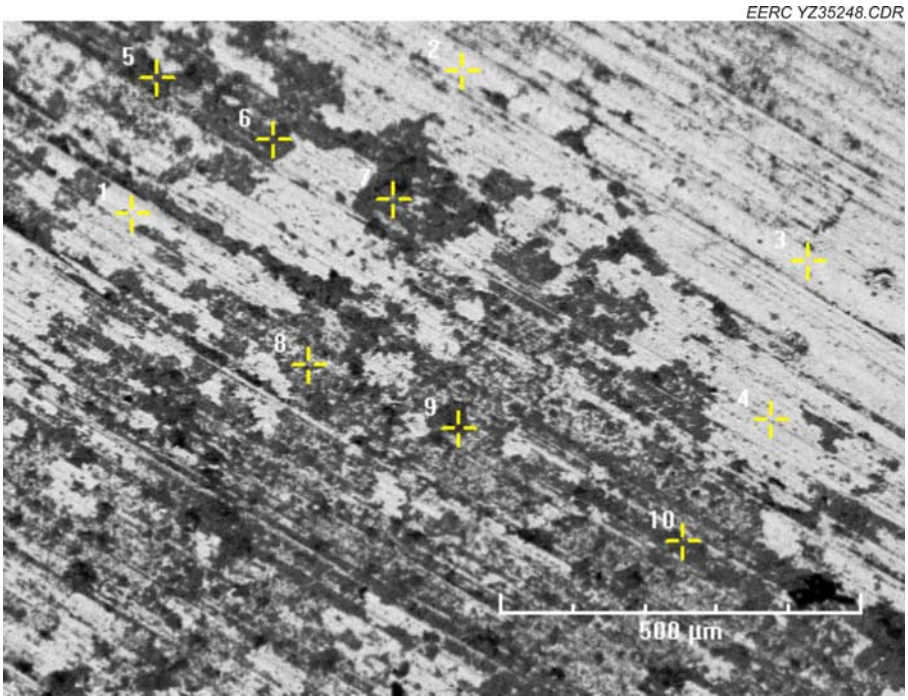

Figure 15. M9 surface SEM image.

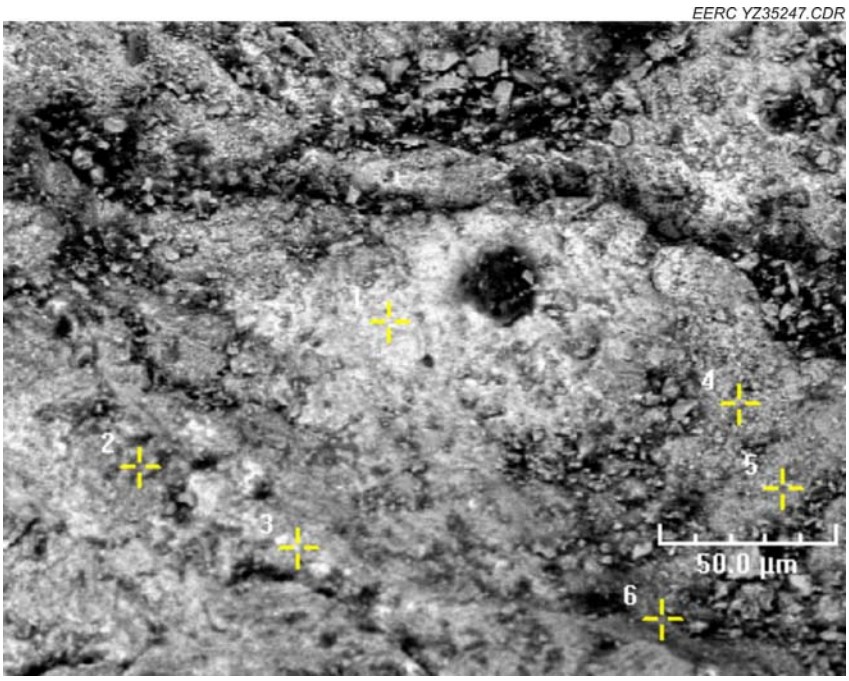

Figure 16. M1 surface SEM image.

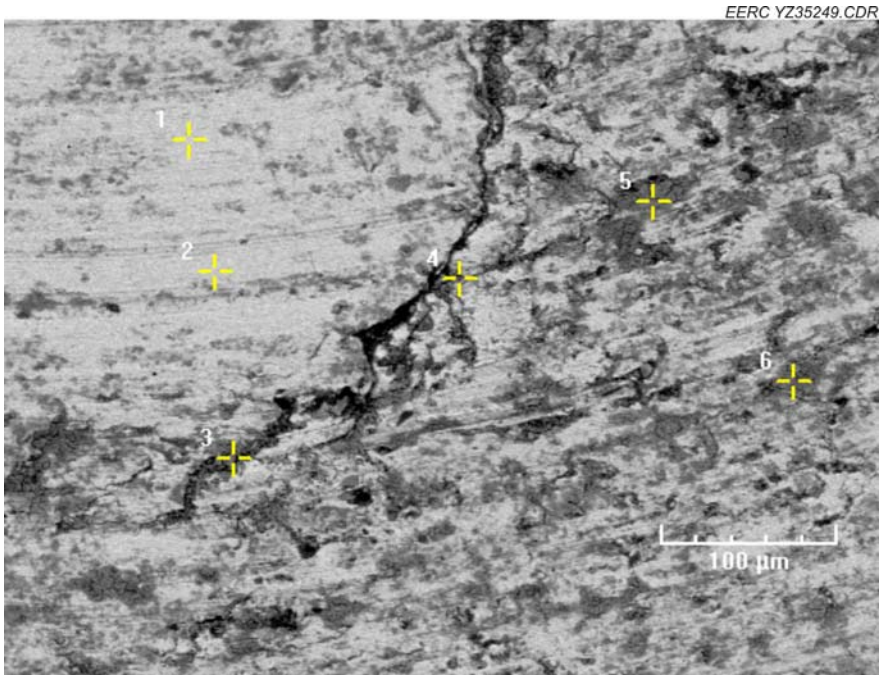

Figure 17. M2 surface SEM image.

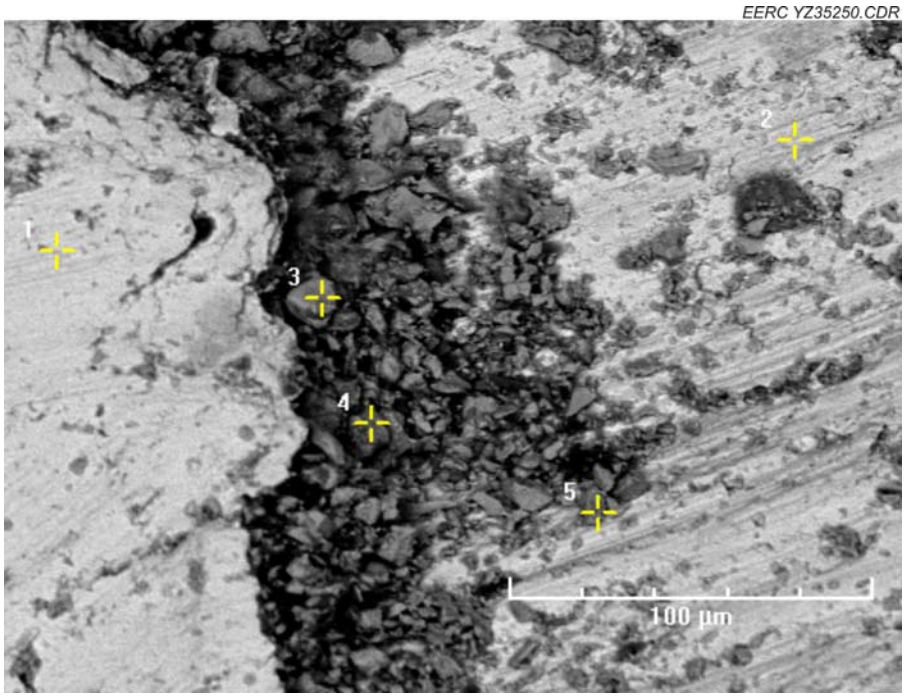

Figure 18. M3 surface SEM image.

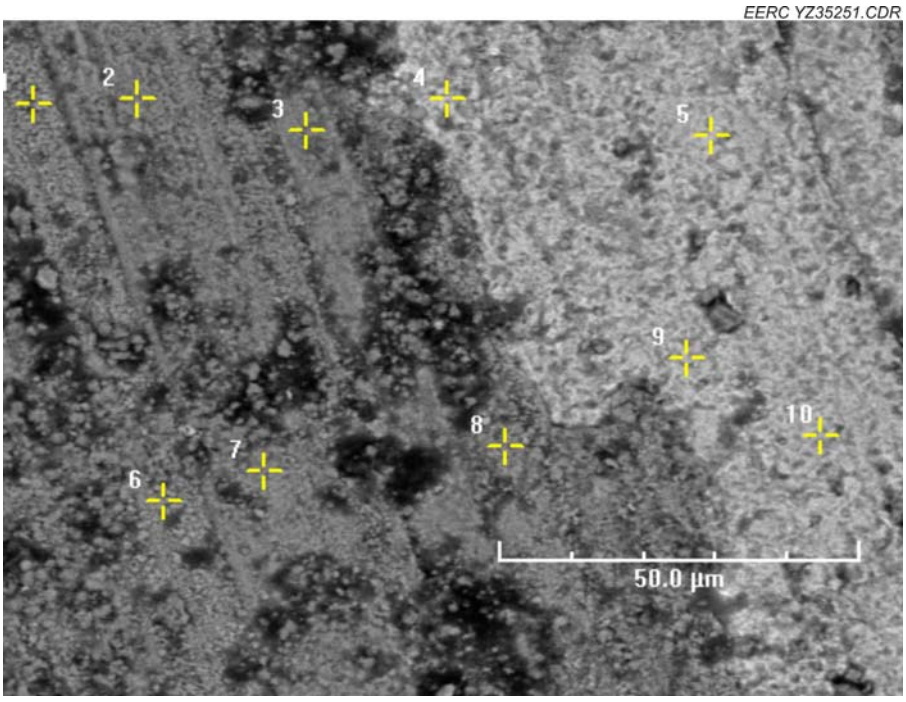

Figure 19. M4 surface SEM image.

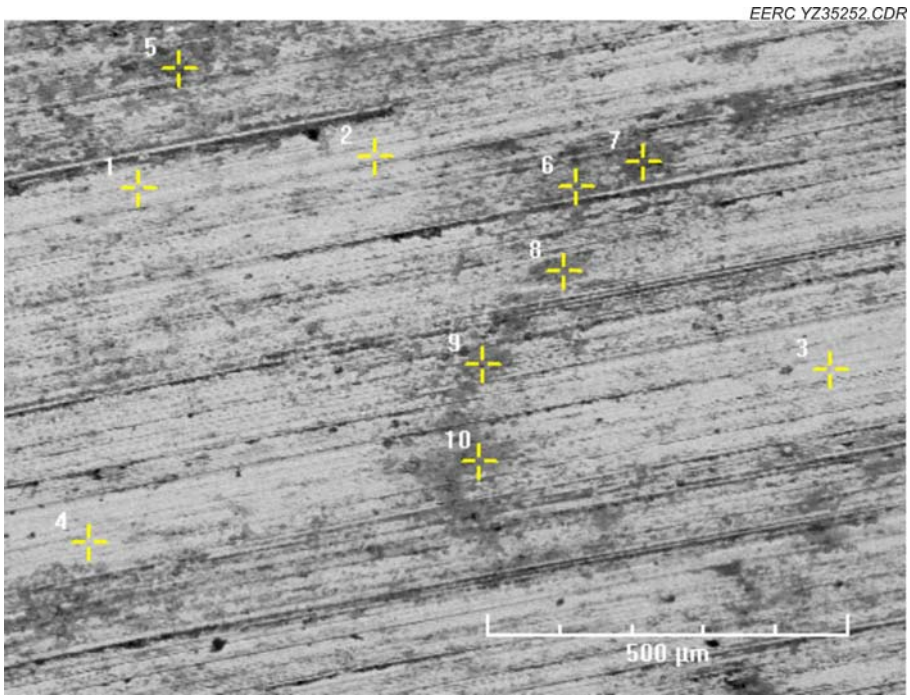

Figure 20. M5 surface SEM image.

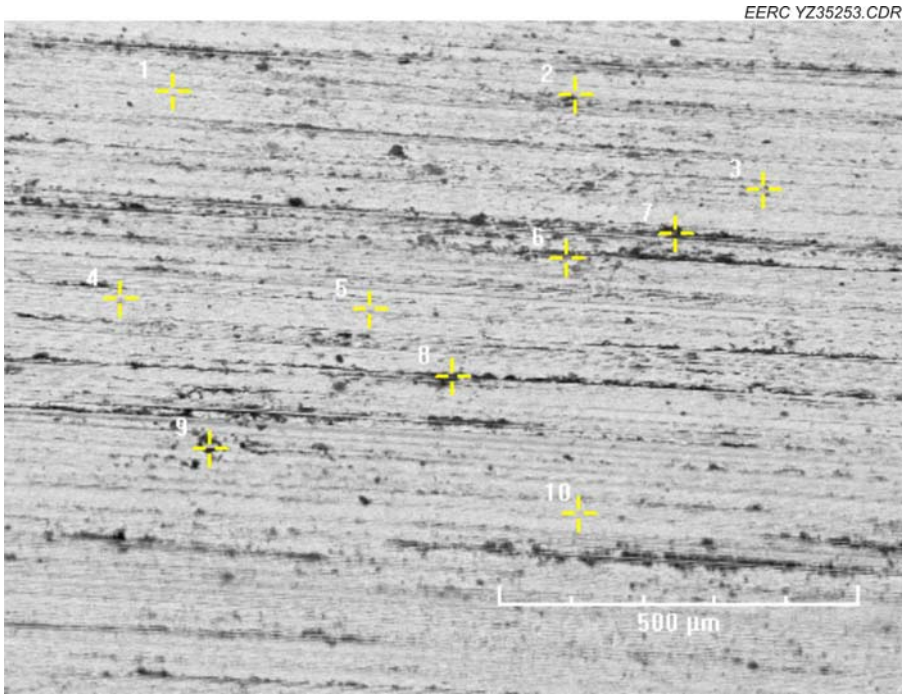

Figure 21. M6 surface SEM image.

Cross-sectional SEM analysis on M1–6 was performed; the complete data set is included in Appendix B. Figures 22–25 are the cross-sectional SEM images for M1, 3, 5, and 6 and show notable changes. M2 and 4 cross-sectional SEMs indicate no corrosion and/or elemental variation compared to pretest data. Cracking through the M1 cross section was due to drilling. However, elemental data (Table 9) show HBr deposits on the surface and no further penetration occurred. Cross-sectional data of M3 (Figure 23 and Table 10) indicate slight Br penetration through intact surface with corresponding Ni loss. Both M5 and M6 cross-sectional SEMs show slight cracking on the coupon surface with elevated Br deposition, but no further elemental changes were observed beyond the surface as listed in Tables 11 and 12.

Overall, microscopic analysis data have confirmed that all bromine attack and corrosion activity did not penetrate beyond the face of the Minorca coupons, although SEM cross sections showed small surface chips, cracks, and pits on several coupons. The wells containing iron oxide/sodium sulfate deposits showed no more corrosion than the flat areas surrounding them. Cracks from drilling the wells were observed in several coupons, although this surface did not attract any additional corrosive activity. All tested coupons have shown minor losses of Fe and Ni on surface, depending on the coupon specific testing conditions. Additional HBr did not induce significant corrosion activities on Minorca coupons under varied testing temperatures.

USS Minntac Coupons

Table 13 shows the averaged elemental compositions on the surfaces of USS Minntac coupons under different testing conditions. The complete SEM data set for surface and cross-sectional analysis are reported in Appendix C.

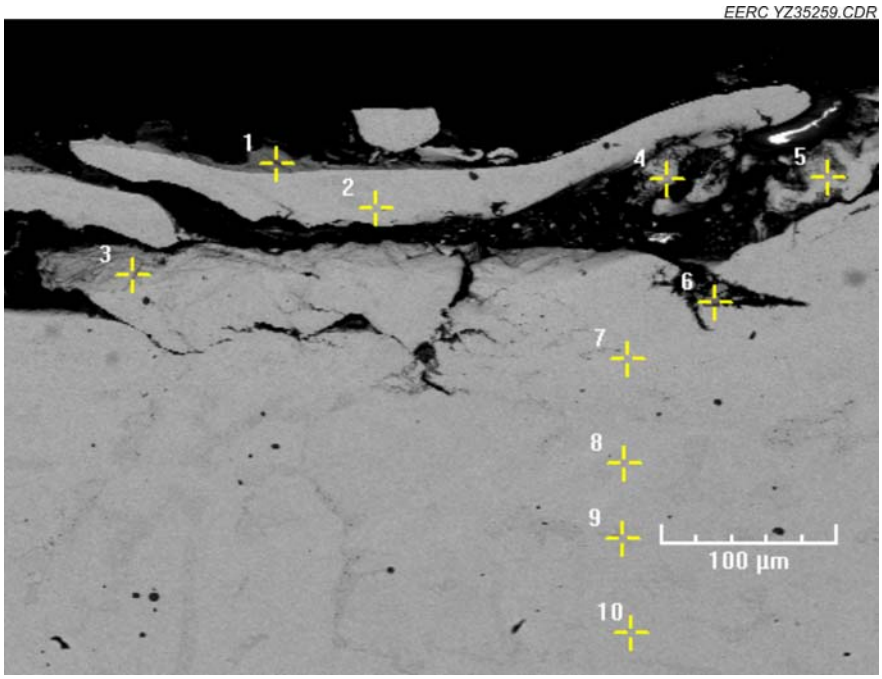

Figure 22. M1 cross-sectional SEM image.

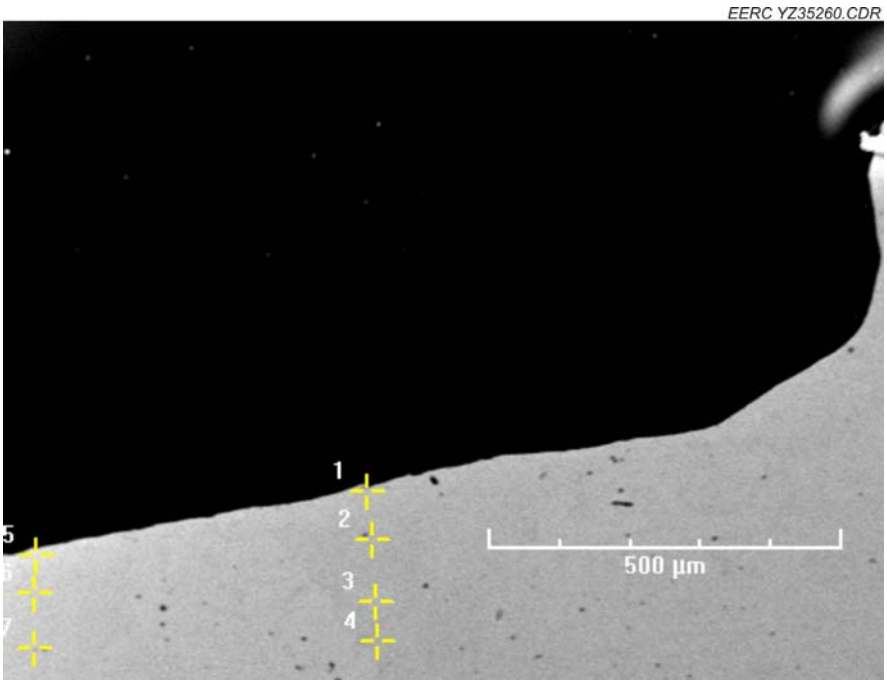

Figure 23. M3 cross-sectional SEM image.

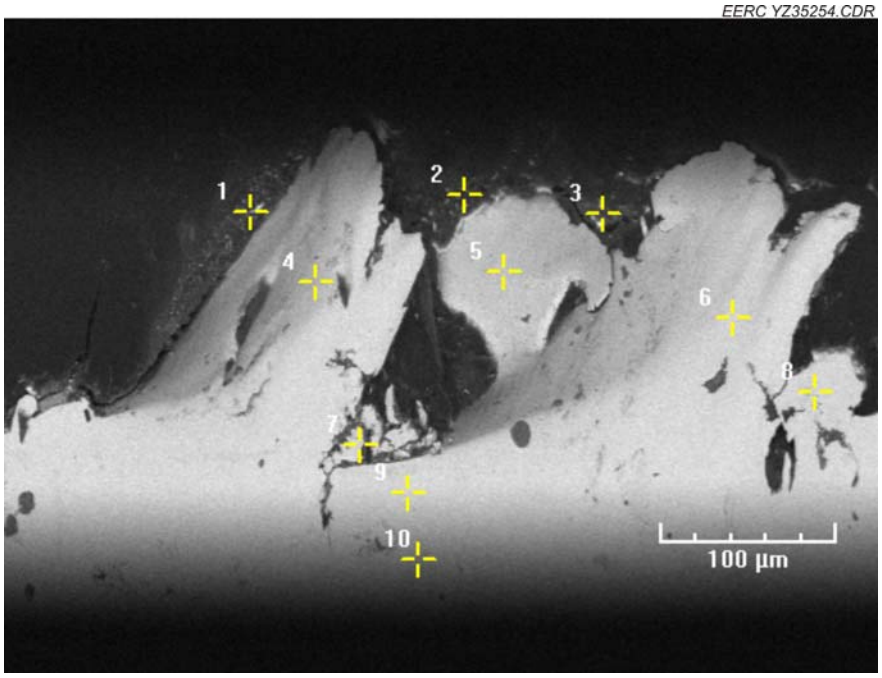

Figure 24. M5 cross-sectional SEM image.

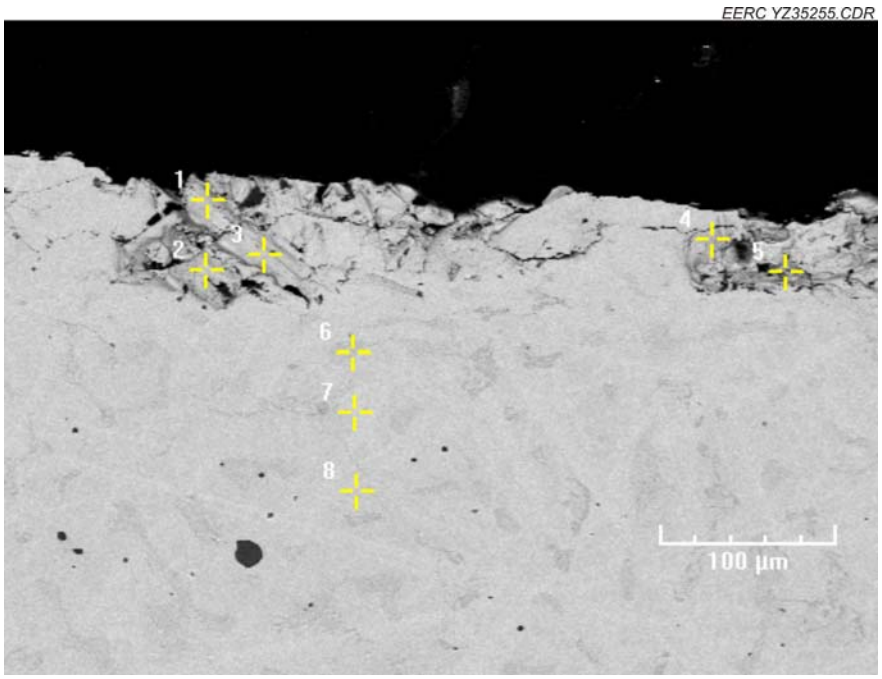

Figure 25. M6 cross-sectional SEM image.

Table 9. Elemental Analysis on M1 Cross Section, wt%

Tag	Si	S	Cr	Mn	Fe	Co	Ni	Br
1	6.14	0.79	22.96	0.00	57.56	0.00	3.55	9.00
2	4.14	0.23	25.42	0.17	63.54	0.00	4.30	2.20
3	4.82	0.32	29.47	0.00	55.97	0.00	3.66	5.76
4	3.32	0.54	16.27	0.00	73.06	0.00	4.58	2.23
5	11.85	0.04	22.64	0.00	62.29	0.00	1.16	2.02
6	1.54	0.57	1.91	0.00	90.98	0.00	0.00	5.00
7	4.13	0.34	26.80	0.09	61.59	0.00	5.19	1.86
8	3.58	0.29	25.38	0.29	64.30	0.02	4.90	1.17
9	3.43	0.28	33.36	0.09	56.94	0.00	4.62	1.25
10	3.39	0.18	26.02	0.18	63.54	0.12	5.13	1.32

Table 10. Elemental Analysis on M3 Cross Section, wt%

Tag	Si	S	Cr	Mn	Fe	Co	Ni	Br
1	9.24	0.00	31.68	0.00	53.12	0.00	1.97	3.86
2	8.07	0.48	28.03	0.00	54.98	0.00	2.30	6.08
3	7.50	0.47	30.11	0.23	55.14	0.00	2.91	3.58
4	7.01	0.13	29.46	0.08	57.41	0.00	2.90	2.81
5	6.88	0.38	27.59	0.00	58.04	0.00	2.50	4.62
6	6.49	0.35	29.54	0.00	58.14	0.00	2.94	2.52
7	6.82	0.15	28.41	0.13	57.49	0.00	2.72	4.28

Table 11. Elemental Analysis on M5 Cross Section, wt%

Tag	Si	S	Cr	Mn	Fe	Co	Ni	Br
1	9.56	1.12	14.04	0.00	33.09	0.00	2.92	39.27
2	19.07	2.54	5.92	0.00	13.68	0.49	3.18	55.12
3	13.59	4.22	7.87	0.81	7.95	0.22	0.32	65.02
4	7.13	0.32	18.97	0.00	46.42	0.00	3.04	24.11
5	5.48	0.45	22.56	0.27	55.29	0.10	4.64	11.20
6	3.75	0.00	25.20	0.06	64.64	0.00	4.86	1.49
7	4.38	0.34	22.22	0.10	65.74	0.08	5.33	1.81
8	3.88	0.24	22.75	0.32	67.42	0.00	4.25	1.00
9	3.08	0.29	24.76	0.17	65.41	0.05	5.08	1.15
10	3.74	0.09	25.84	0.09	63.87	0.00	5.02	1.32

Table 12. Elemental Analysis of M6 Cross Section, wt%

Tag	Si	S	Cr	Mn	Fe	Co	Ni	Br
1	3.57	0.27	25.57	0.06	64.50	0.00	4.68	1.23
2	3.37	0.21	29.81	0.11	61.17	0.00	4.38	0.93
3	3.21	0.25	26.01	0.30	63.89	0.03	5.04	1.25
4	2.84	0.34	27.42	0.13	62.13	0.00	5.23	1.90
5	3.47	0.29	27.54	0.31	61.67	0.00	5.16	1.55
6	3.28	0.26	29.68	0.28	60.28	0.00	5.16	1.01
7	3.14	0.17	24.84	0.36	64.99	0.16	5.13	1.22
8	3.35	0.17	26.06	0.16	65.16	0.00	4.24	0.82

Table 13. Normalized Distribution of Elements on USS Minntac Coupon Surface, wt%

	Temp., °C	Si	S	Cr	Mn	Fe	Co	Ni	Br
Pretest		3.81	0.24	27.24	0.88	50.74	0.03	17.01	0.00
UM1	500	2.34	0.40	19.28	5.30	48.96	0.26	7.20	16.22
UM2	300	2.32	0.91	17.90	0.58	63.86	0.08	9.49	4.80
UM3	150	2.77	0.74	27.26	0.69	48.40	0.05	15.14	4.83
UM4	500	5.76	4.93	48.70	5.54	23.52	0.00	3.63	7.89
UM5	300	2.96	8.71	15.07	0.77	30.64	0.02	11.60	30.09
UM6	150	3.10	41.69	12.70	0.72	27.73	0.09	9.50	3.23
UM7	500	6.59	6.24	56.72	7.24	19.85	0.00	2.62	0.00
UM8	300	5.42	5.00	30.05	1.55	44.98	0.00	12.82	0.00
UM9	150	3.99	8.68	26.63	0.74	46.16	0.00	13.67	0.00

Without HBr in the taconite flue gas, SEM analysis indicates that UM coupons only suffer surface loss of Ni and Fe in a 500°C environment. Discoloration and surface striation were observed for UM7–9. Additional cross-sectional SEM–EDX data show that UM7–9 were well protected and did not experience significant oxidative deterioration.

The coupons exposed to bromine, UM1–6, all showed Br deposition with Ni, Fe, or Cr losses, depending on testing conditions. The highest Br surface concentration was 30.09%, measured on UM5. Figures 26 and 27 and Table 14 are the UM5 microscopic images and cross-sectional analysis, respectively. The UM5 surface shows blistering and cracking, with losses of Ni, Cr, and Fe. Further cross-sectional analysis indicates that although slight Br penetration occurred, no significant elemental disruptions occurred. All other UM coupons exposed to bromine show surface striation but no further corrosion beyond the surface.

Weight Gain/Loss Measurement

Tables 15–17 show the weight gain/loss for each set of coupons during the 30-day testing period.

For the United coupon set, larger weight gains were seen in U1–6, which were exposed to HBr. Coupons U7–9 saw very little weight gain or loss. U1–3 coupons showed a greater weight gain than the non-deposit-containing coupons.

The Minorca coupons exposed to HBr also show a larger weight gain than the non-HBr-exposed coupons. The presence of iron oxide/sodium sulfate deposits on M1–3 did not cause greater weight gain than the M4–6 coupons. For the Minorca coupons, the rate of weight gain was steady throughout the test.

The USS Minntac set showed variable weight gains between the HBr- and non-HBr-exposed coupons.

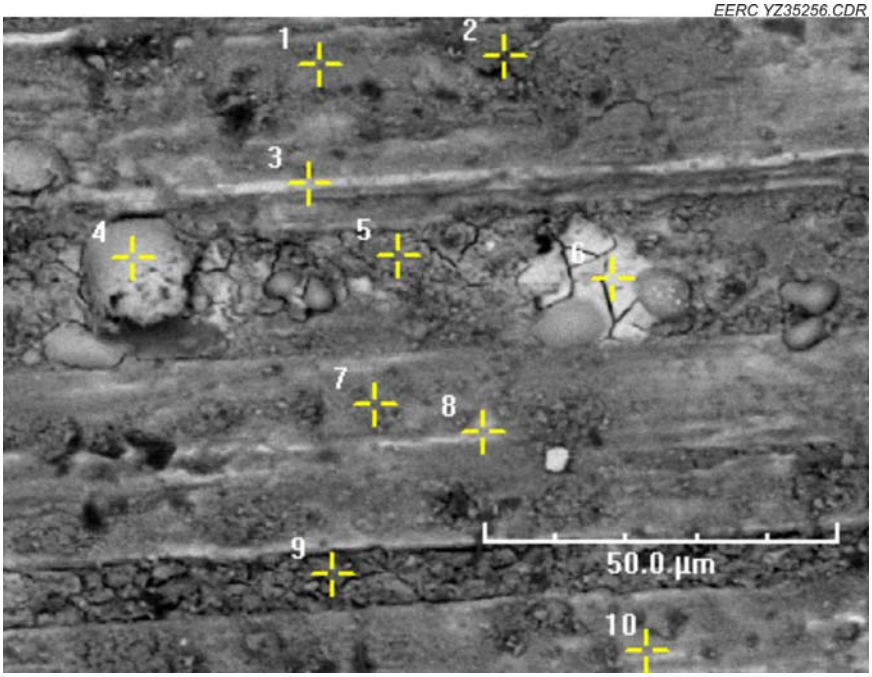

Figure 26. UM5 surface SEM image.

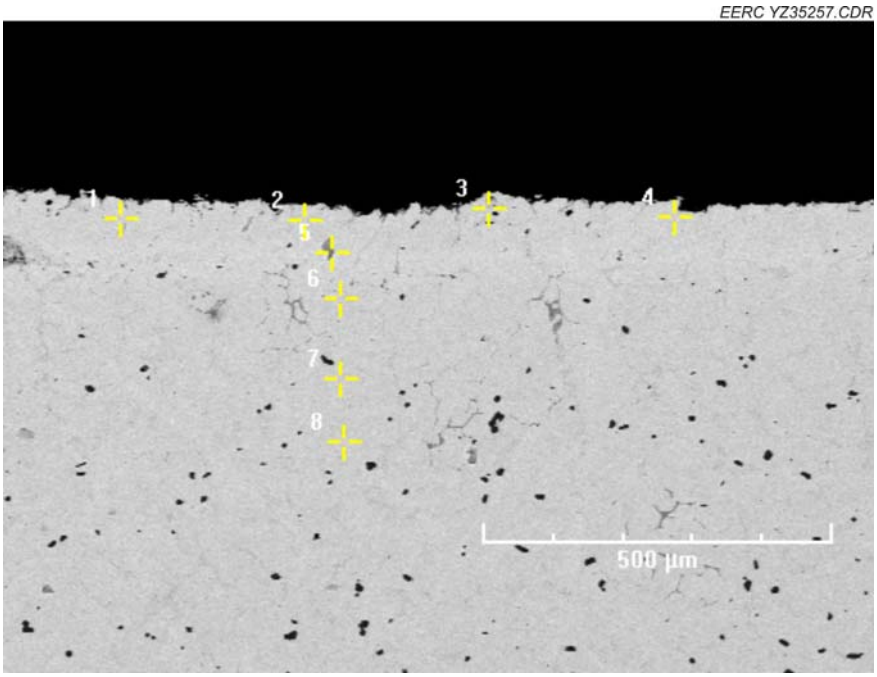

Figure 27. UM5 cross-sectional SEM image

Table 14. Elemental Analysis of UM5 Cross Section, wt%

Tag	Si	S	Cr	Mn	Fe	Co	Ni	Br
1	3.39	0.40	26.51	0.84	46.84	0.00	16.44	5.58
2	2.31	0.31	54.47	0.55	29.91	0.00	9.37	3.09
3	3.04	0.36	24.95	0.19	50.36	0.20	16.47	4.43
4	2.72	0.22	26.61	0.83	48.86	0.00	16.04	4.64
5	3.01	0.12	28.04	0.42	47.69	0.00	15.99	4.73
6	2.84	0.27	27.15	0.75	47.97	0.01	16.23	4.74
7	3.21	0.27	29.13	0.97	44.96	0.00	16.51	4.91
8	2.56	0.31	25.72	0.94	49.02	0.05	16.12	5.20

Table 15. Weight Gain/Loss of United Coupons, mg

Coupon	10 days	20 days	30 days
U1	1.00	2.00	5.00
U2	1.00	4.00	5.00
U3	4.00	3.00	4.00
U4	0.00	−1.00	3.00
U5	0.00	0.00	5.00
U6	0.00	2.00	2.00
U7	1.00	1.00	0.00
U8	−1.00	1.00	−1.00
U9	1.00	0.00	2.00

Table 16. Weight Gain/Loss of Minorca Coupons, mg

Coupon	10 days	20 days	30 days
M1	0.00	2.00	1.00
M2	4.00	7.00	9.00
M3	6.00	4.00	3.00
M4	4.00	6.00	8.00
M5	2.00	5.00	9.00
M6	4.00	5.00	5.00
M7	1.00	2.00	1.00
M8	3.00	2.00	0.00
M9	1.00	2.00	1.00

Table 17. Weight Gain/Loss of USS Minntac Coupons, mg

Coupon	10 days	20 days	30 days
UM1	6.00	3.00	5.00
UM2	0.00	3.00	3.00
UM3	1.00	3.00	1.00
UM4	3.00	3.00	5.00
UM5	−3.00	−2.00	−3.00
UM6	1.00	1.00	−1.00
UM7	7.00	2.00	4.00
UM8	−3.00	−2.00	−2.00
UM9	1.00	−1.00	1.00

COMPARISON

Table 18 provides a summary of relative changes of elements of interest on testing coupon surfaces that experienced different testing conditions. The three coupon sets behaved quite similarly in typical taconite flue gas: limited surface corrosion, mainly with losses of Fe and Ni at 500°C. This corrosion decreased with lowering temperature. As bromine was introduced into the flue gas, all three coupon sets seemed to experience surface attack not only at 500°C but also to some degree at lower temperatures of 300° and 150°C, although corrosion was most obvious at 500°C. The UM coupons seem to indicate more surface reaction than the M and U coupons in bromine-containing taconite flue gas. Iron oxide/sodium sulfate deposition may induce more changes to M and U coupons than UM coupons.

CONCLUSIONS

The EERC was contracted by the Minnesota Department of Natural Resources to perform laboratory corrosion testing on coupons supplied by three Minnesota taconite plants. The bench-scale testing was the first step to determine if the introduction of 40 ppm HBr to flue gas would potentially cause corrosion in taconite facility process equipment. Two simultaneous

Table 18. Relative Elemental Changes of Cr, Fe, and Ni on Testing Coupon Surface

	Cr	Fe	Ni		Cr	Fe	Ni		Cr	Fe	Ni
M1	26.49%	−32.76%	−60.76%	U1	−22.33%	10.66%	−39.64%	UM1	−29.22%	−3.51%	−57.67%
M2	−6.19%	8.56%	−41.14%	U2	−35.63%	29.24%	−52.72%	UM2	−34.29%	25.86%	−44.21%
M3	−47.59%	26.97%	−60.76%	U3	−18.19%	23.64%	-46.88%	UM3	0.07%	−4.61%	−10.99%
M4	50.34%	−29.13%	−67.30%	U4	−22.94%	13.49%	−39.03%	UM4	78.78%	−53.65%	−78.66%
M5	−6.88%	−4.95%	−18.78%	U5	7.80%	−6.96%	−9.26%	UM5	−44.68%	−39.61%	−31.80%
M6	−3.73%	−7.33%	−14.98%	U6	20.35%	−13.26%	−17.10%	UM6	−53.38%	−45.35%	−44.15%
M7	87.40%	−46.63%	−78.90%	U7	42.29%	−25.03%	−78.40%	UM7	108.22%	−60.88%	−84.60%
M8	−10.82%	6.88%	−1.69%	U8	−2.59%	−0.67%	−16.03%	UM8	10.32%	−11.35%	−24.63%
M9	−43.18%	−23.66%	−7.38%	U9	−7.66%	−4.96%	−10.26%	UM9	−2.24%	−9.03%	−19.64%

exposure tests were completed with representative taconite flue gas and flue gas spiked with 40 ppm HBr. The coupon sets were subjected to 30 days of exposure and then analyzed for corrosive activity and bromine deposition. The preliminary test results are given below:

1. Adding 40 ppm HBr to taconite process flue gas appears to cause slight surface corrosion of the test coupons. SEM surface microscopy showed small pitting, cracking, and blistering occurred with bromine deposition and losses of Fe, Cr, and Ni.

2. However, coupon cross-sectional analyses indicated that bromine deposition and losses of Fe, Ni, and Cr were mainly confined to the surface of the coupons, and no significant bromine penetration and subsequent elemental changes were observed below the coupon surface after 30 days of exposure experiments.

3. Coupon surface corrosion appears to be less with decreasing temperature.

4. All three coupon sets show resistance to bromine attack under testing environments during the 30-day testing period.

5. Deposits of iron oxide and sodium sulfate seem to induce slight chemistry changes on U and M coupons but not on UM coupons.

It should be noted that, because of limited time and scope of work, the completed corrosion exposure tests were carried out in simplified simulated flue gas environments that did not represent 100% actual operating conditions in the taconite process. The original objective of this project is to see if bromine could cause any possible corrosion under selected testing conditions, while the 30-day exposure testing period may not necessarily be long enough to attain a complete perspective of possible bromine-induced corrosion issues in a taconite facility. Therefore, the project results can be regarded as the first step in the effort to address potential bromine-induced corrosion as bromine is applied to a taconite facility for mercury reduction. Additional bench-scale coupon corrosion tests under continuous thermal cycling with wider temperature regimes and extended exposure times are needed before any large-scale field testing.

ACKNOWLDGMENT

The EERC acknowledges the financial support of the Minnesota Department of Natural Resources on this project. The EERC would also like to extend its gratitude to the taconite industry that has provided valuable input on this project. Special thanks to Harold Kokal and Jon Maki from ArcelorMital and Global for helping to prepare the testing coupons.

REFERENCES

1. Berndt, M.E. *On the Measurement of Stack Emissions at Taconite Processing Plants*; Progress Report to Minnesota Pollution Control Agency, May 2008.

2. Zhuang, Y.; Thompson, J.S.; Zygarlicke, C.J.; Pavlish, J.H. Impact of Calcium Chloride Addition on Mercury Transformations and Control in Coal Flue Gas. *Fuel* **2007**, *86* (15), 2351–2359.

3. Zhuang, Y.; Zygarlicke, C.J.; Thompson, J.S.; Pavlish, J.H. Chlorine-Induced Mercury Transformation in a High-Temperature Coal Flue Gas. In *Proceedings of Air Quality V: Mercury, Trace Elements, SO_3, and Particulate Matter Conference*; Arlington, VA, Sept 19–21, 2005.

4. Zhuang, Y.; Laumb, J.; Liggett, R.; Holmes, M.J.; Pavlish, J.H. Impacts of Acid Gases on Mercury Oxidation Across SCR Catalyst. *Fuel Process. Technol.* **2007**, *88*, 929–934.

5. Pavlish, J.H. Understanding Mercury Speciation, Variability, and Operational Impact on Mercury Control. Presented at Mercury 2006, 8th International Conference on Mercury as a Global Pollutant, Madison, WI, Aug 6–11, 2006; Paper No. S-662.

6. Pavlish, J.H.; Sondreal, E.A.; Mann, M.D.; Olson, E.S.; Galbreath, K.C.; Laudal, D.L.; Benson, S.A. A Status Review of Mercury Control Options for Coal-Fired Power Plants. *Special Mercury Issue of Fuel Process. Technol*. **2003**, *82* (2–3), 89–165.

7. Liu, S.; Yan, N.; Liu, Z. Using Bromine Gas to Enhance Mercury Removal from Flue Gas of Coal-Fired Power Plants. *Environ. Sci. Technol*. **2007**, *41* (4) 1405–1412.

8. Berndt , M.E.; Engesser, J. Mercury Transport in Taconite Processing Facilities: (III) Control Method Test Results; Iron Ore Cooperative Research Final Report, Dec 2007.

9. Pavlish, J.H.; Zhuang, Y. *Proof-of-Concept Testing of Novel Mercury Control Technology* for a Minnesota Taconite Plant; EERC Technical Report to Minnesota Department of Natural Resources; 2008-EERC-07-02. Energy & Environmental Research Center: Grand Forks, ND, 2008.

10. Zhuang, Y.; Chen, C.; Timpe, R.; Pavlish, J.H. Investigations on Bromine Corrosion Associated Mercury Control Technologies in Coal Flue Gas. *Fuel* **2008**, *88* (9), 1692–1697.

APPENDIX A

UNITED COUPON SEM ANALYSIS

UNITED COUPON SEM ANALYSIS

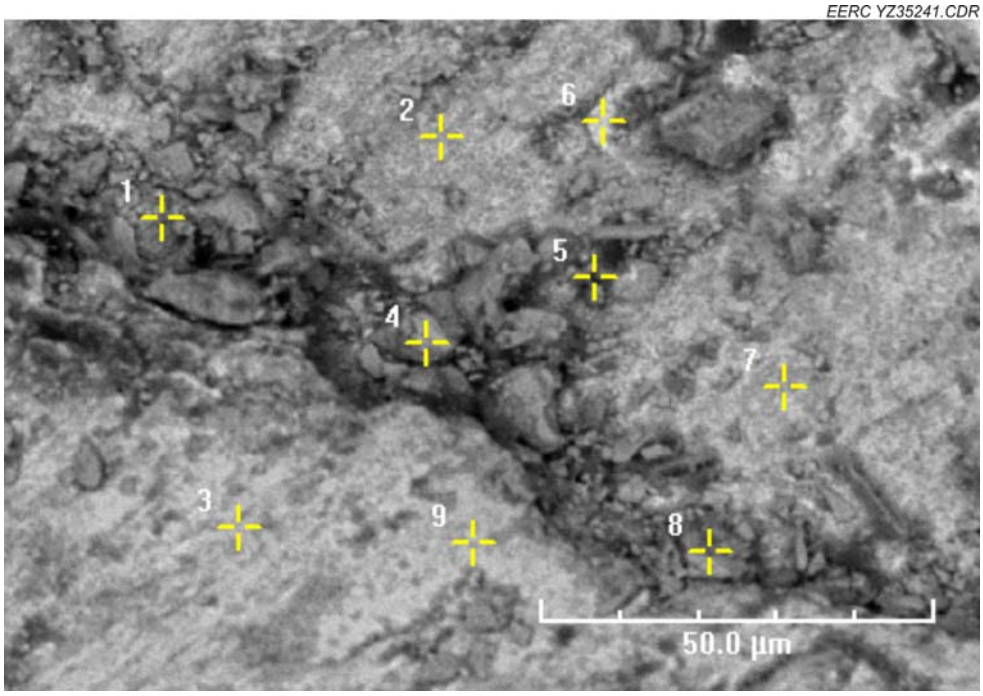

Figure A-1. U1 surface SEM image.

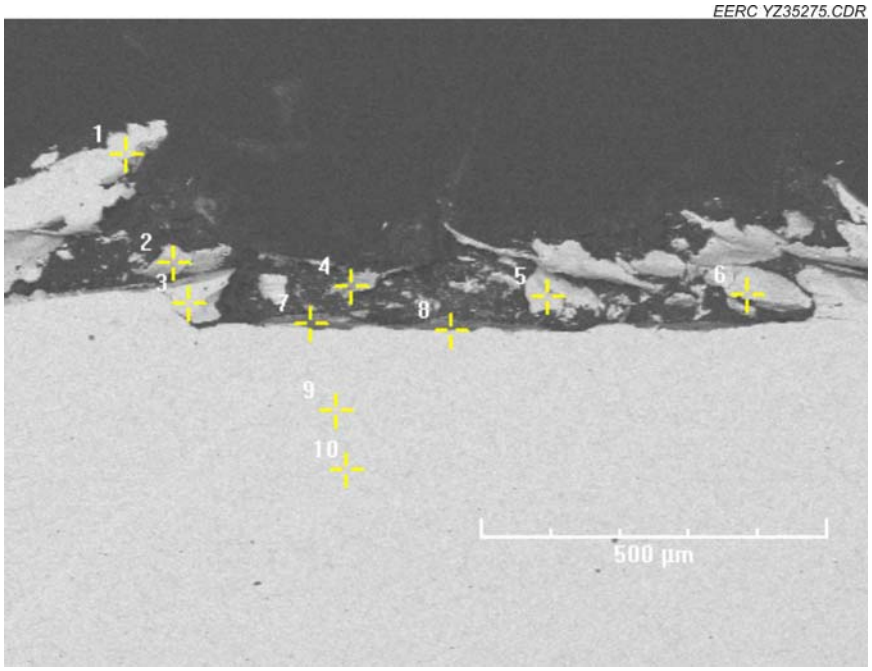

Figure A-2. U1 cross-sectional SEM image.

Table A-1. Elemental Analysis on U1 Cross Section

Tag	Si	S	Cr	Mn	Fe	Co	Ni	Br
1	2.92%	0.52%	24.40%	0.00%	54.96%	0.00%	15.94%	1.24%
2	3.56%	1.03%	28.47%	0.46%	51.50%	0.00%	14.32%	0.65%
3	3.10%	0.89%	28.10%	0.59%	52.33%	0.00%	14.43%	0.57%
4	3.24%	0.70%	29.22%	0.60%	51.62%	0.00%	13.78%	0.84%
5	2.82%	0.32%	25.82%	0.33%	54.85%	0.00%	15.13%	0.73%
6	3.77%	1.10%	39.13%	0.24%	43.24%	0.00%	11.16%	1.35%
7	12.40%	1.01%	47.36%	5.04%	25.36%	0.00%	3.19%	5.49%
8	9.89%	0.88%	30.79%	0.00%	46.92%	0.00%	10.27%	1.25%
9	2.90%	0.25%	25.33%	0.12%	55.07%	0.10%	14.96%	1.26%
10	2.98%	0.41%	26.40%	0.28%	53.73%	0.00%	15.09%	1.12%

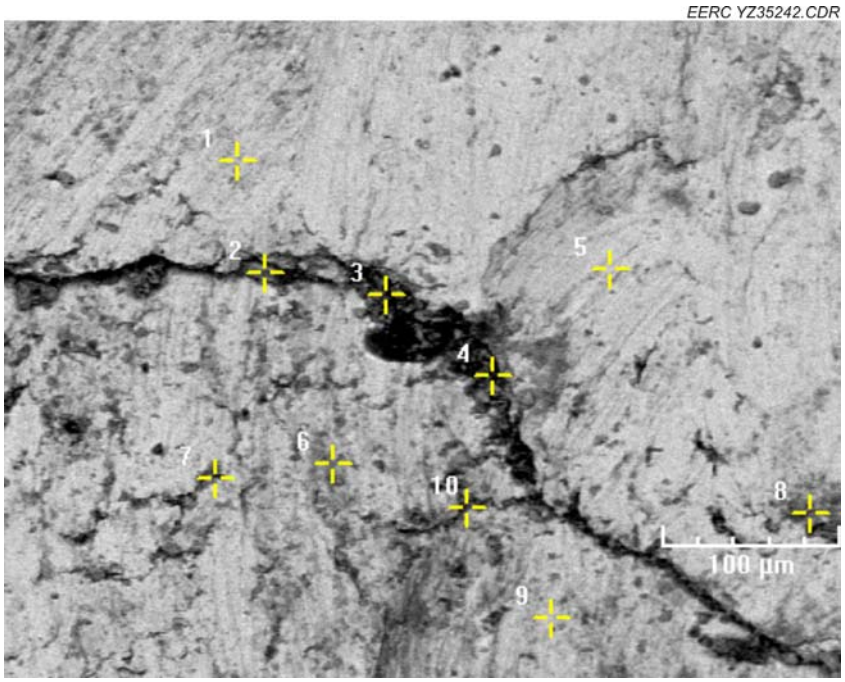

Figure A-3. U2 surface SEM image.

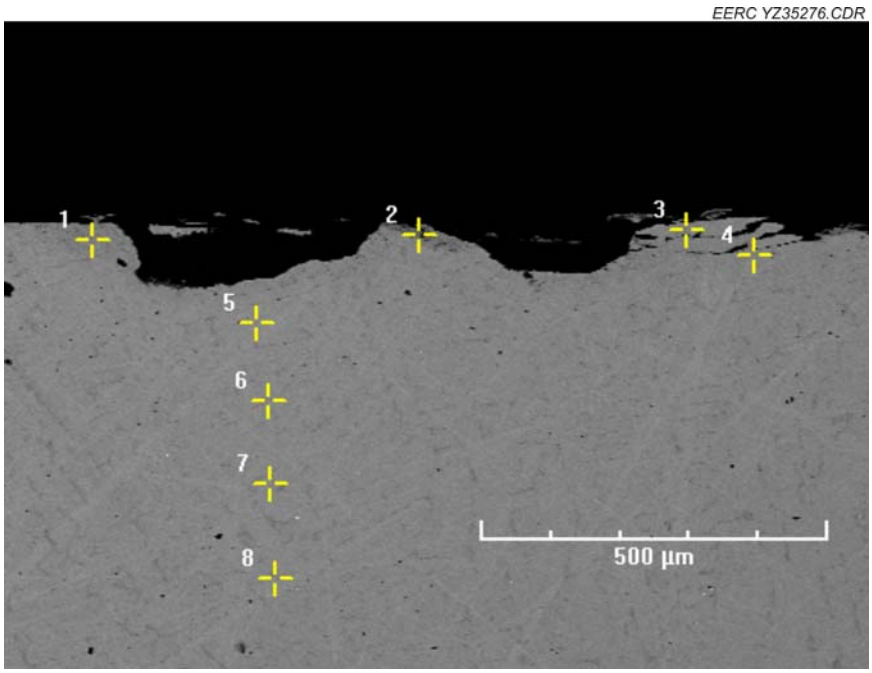

Figure A-4. U2 cross-sectional SEM image.

Table A-2. Elemental Analysis of U2 Cross Section

Tag	Si	S	Cr	Mn	Fe	Co	Ni	Br
1	10.09%	0.58%	26.61%	0.65%	47.72%	0.00%	13.48%	0.82%
2	14.74%	0.48%	26.12%	0.18%	43.42%	0.00%	12.57%	2.40%
3	4.84%	0.37%	24.79%	0.41%	54.39%	0.01%	14.36%	0.81%
4	4.09%	0.39%	27.55%	0.06%	52.58%	0.00%	14.73%	0.60%
5	2.79%	0.39%	27.18%	0.46%	53.14%	0.00%	15.06%	0.97%
6	2.70%	0.26%	26.62%	0.37%	54.42%	0.00%	14.55%	1.05%
7	2.51%	0.38%	25.73%	0.39%	54.63%	0.00%	15.07%	1.23%
8	0.54%	0.68%	85.89%	0.00%	11.45%	0.00%	0.06%	1.33%

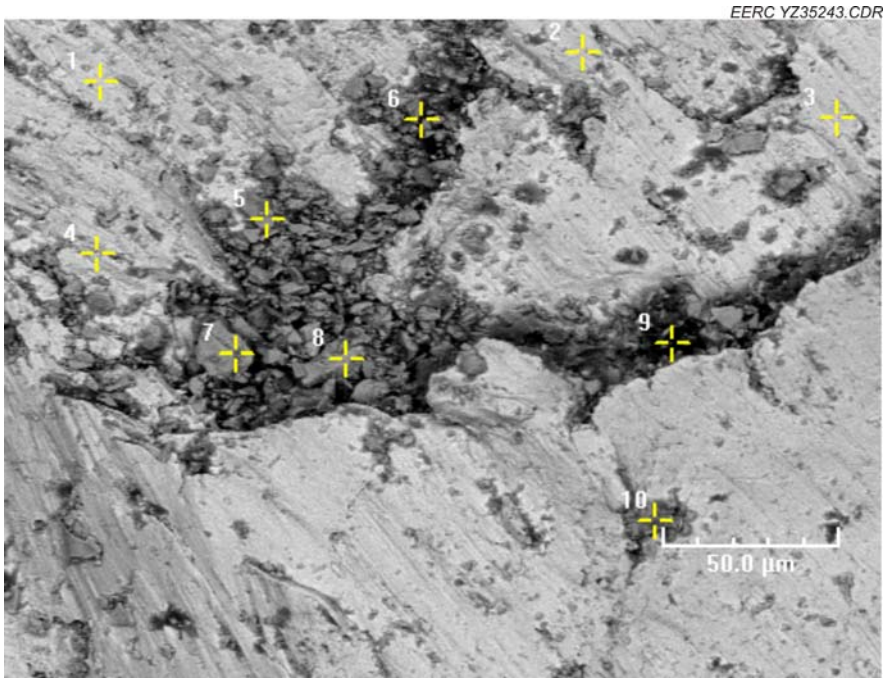

Figure A-5 U3 surface SEM image.

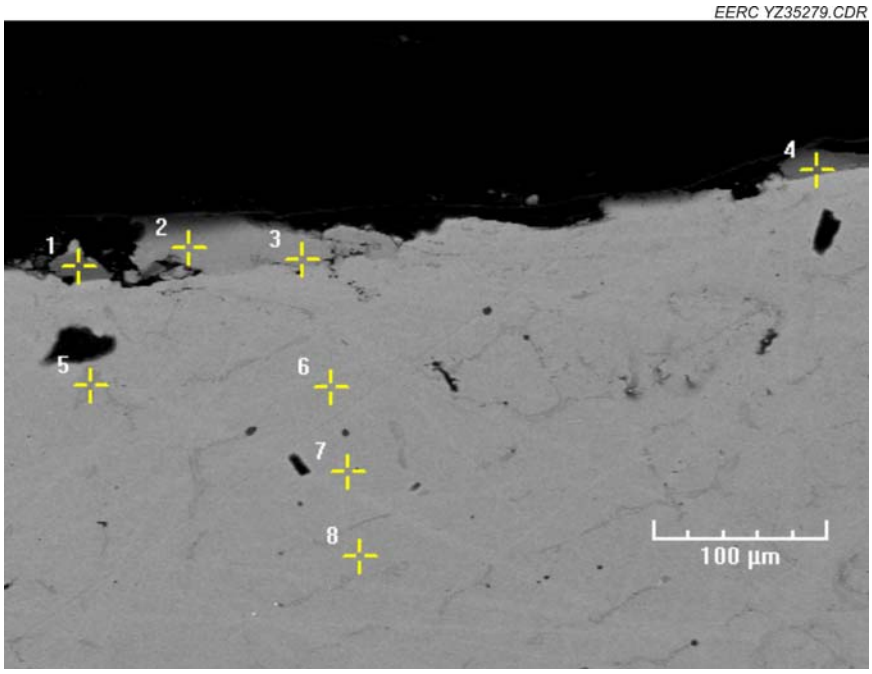

Figure A-6. U3 cross-sectional SEM image.

Table A-3. Elemental Analysis of U3 Cross Section

Tag	Si	S	Cr	Mn	Fe	Co	Ni	Br
1	1.58%	0.04%	30.33%	1.17%	55.04%	0.00%	11.82%	0.00%
2	0.02%	0.00%	25.79%	0.65%	57.47%	0.00%	15.92%	0.00%
3	0.00%	0.00%	26.09%	0.70%	56.22%	0.00%	16.84%	0.00%
4	0.14%	0.00%	27.93%	0.89%	57.51%	0.00%	13.53%	0.00%
5	4.27%	0.44%	26.18%	0.49%	52.59%	0.14%	15.08%	0.80%
6	3.47%	0.40%	26.37%	0.26%	53.70%	0.00%	14.64%	1.14%
7	3.31%	0.38%	30.00%	0.29%	50.71%	0.00%	14.28%	0.92%
8	3.70%	0.34%	25.79%	0.29%	54.65%	0.00%	14.65%	0.59%

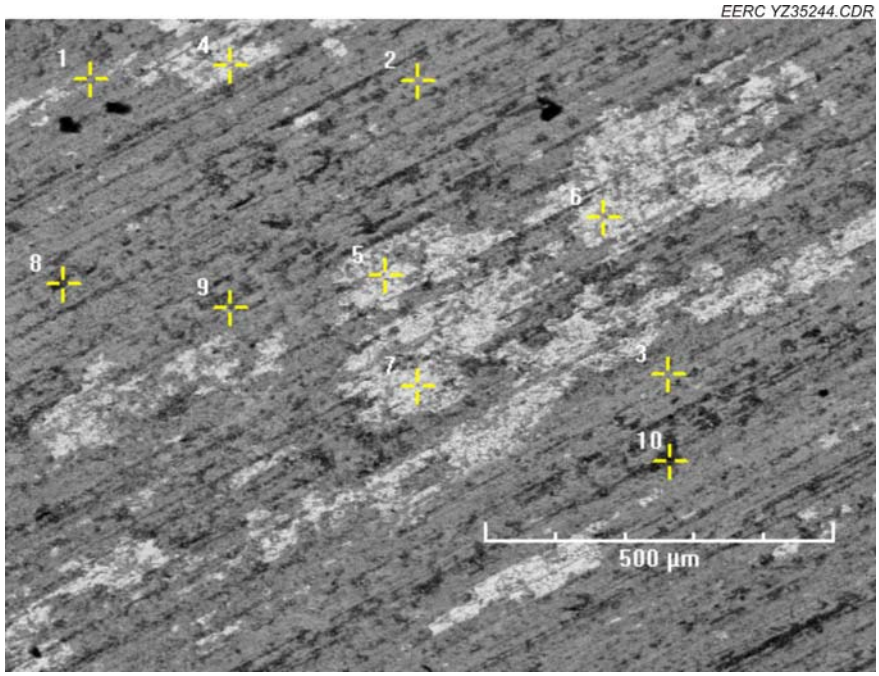

Figure A-7. U4 surface SEM image.

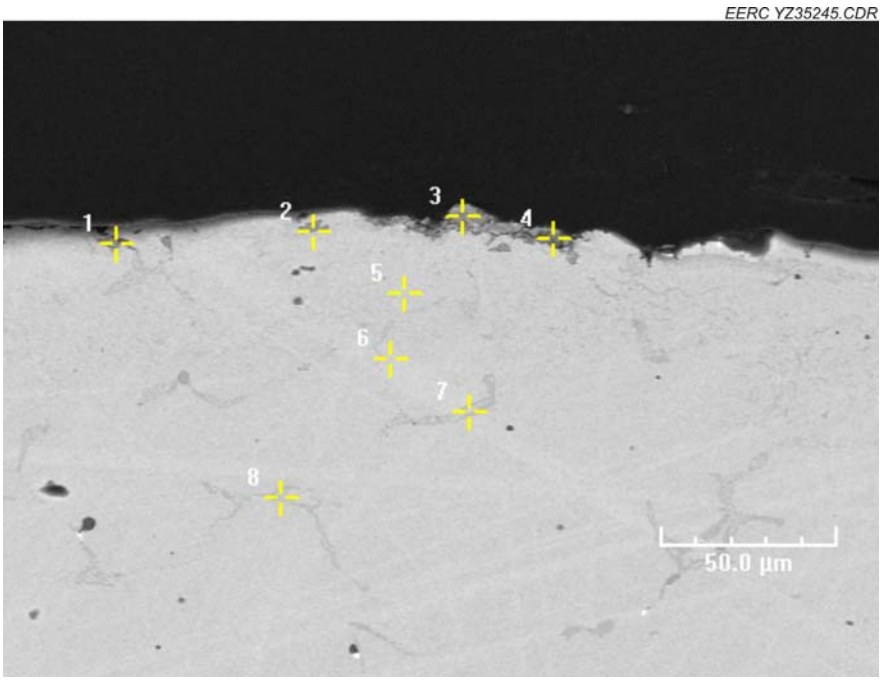

Figure A-8. U4 cross-sectional SEM image.

Table A-4. Elemental Analysis of U4 Cross Section

Tag	Si	S	Cr	Mn	Fe	Co	Ni	Br
1	3.09%	0.90%	16.24%	0.00%	61.59%	0.00%	18.08%	0.00%
2	7.57%	0.54%	23.58%	0.21%	50.50%	0.00%	15.75%	1.86%
3	5.90%	0.58%	79.87%	3.61%	4.82%	0.00%	1.51%	3.71%
4	12.35%	1.36%	55.80%	4.43%	16.91%	0.00%	7.38%	1.71%
5	2.65%	0.39%	26.22%	0.00%	55.20%	0.00%	14.49%	0.97%
6	3.07%	0.51%	27.26%	0.72%	52.08%	0.00%	14.69%	1.66%
7	2.40%	0.87%	60.00%	0.07%	30.25%	0.00%	5.32%	1.09%
8	2.22%	0.59%	52.67%	0.44%	35.85%	0.01%	7.41%	0.73%

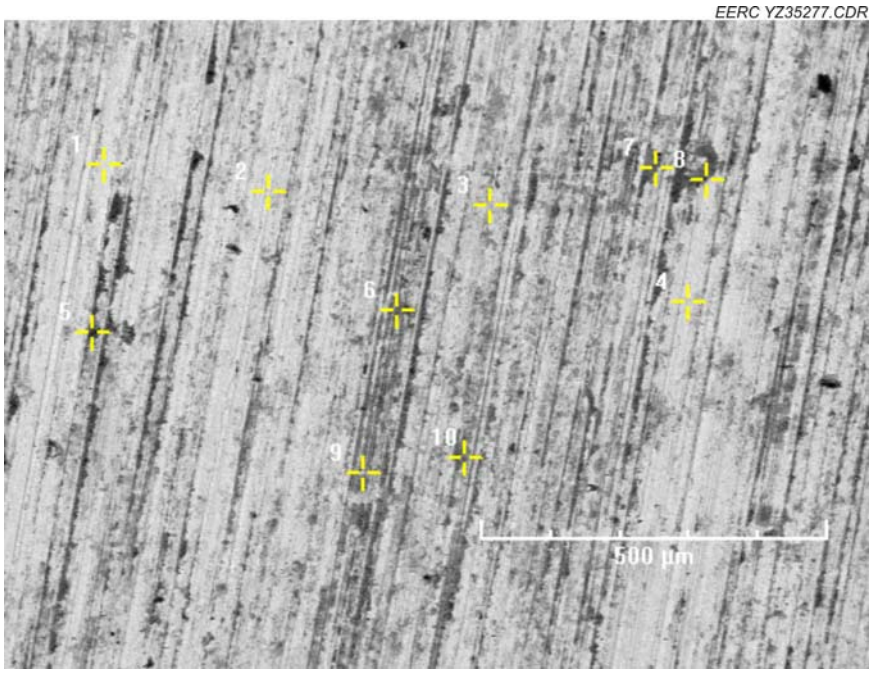

Figure A-9. U5 surface SEM image

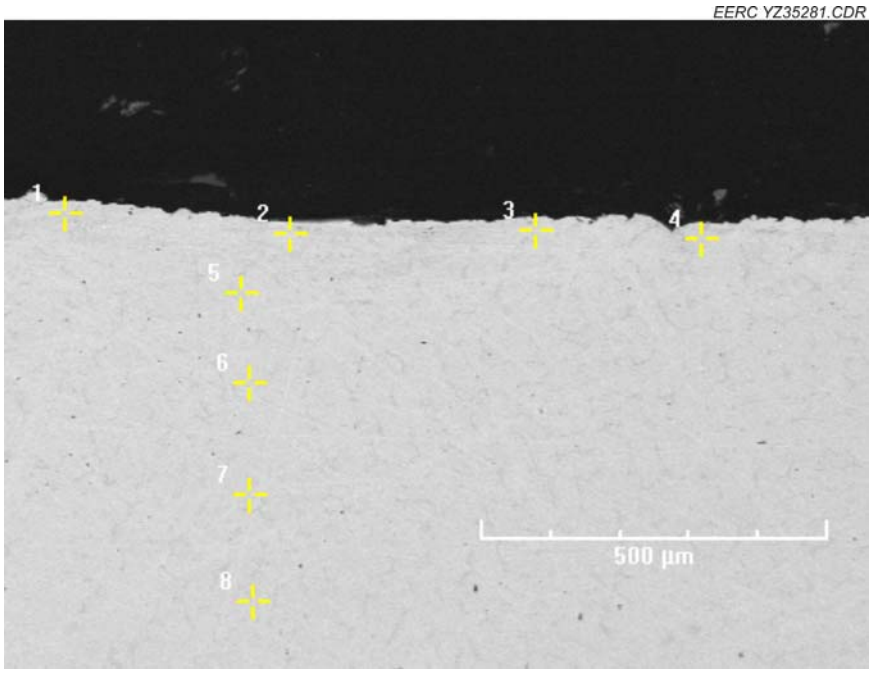

Figure A-10. U5 cross-sectional SEM image.

Table A-5. Elemental Analysis of U5 Cross-Section

Tag	Si	S	Cr	Mn	Fe	Co	Ni	Br
1	3.23%	1.14%	46.18%	0.19%	38.99%	0.00%	9.59%	0.67%
2	4.16%	0.43%	27.70%	0.43%	52.12%	0.00%	13.82%	1.35%
3	3.76%	0.62%	28.76%	0.50%	50.21%	0.00%	15.06%	1.09%
4	2.56%	0.23%	26.44%	0.40%	54.16%	0.00%	14.84%	1.28%
5	2.97%	0.40%	28.62%	0.28%	51.59%	0.00%	15.19%	0.94%
6	2.24%	0.22%	25.64%	0.36%	55.66%	0.00%	14.96%	0.93%
7	2.38%	0.22%	25.56%	0.01%	55.65%	0.00%	15.08%	1.09%
8	2.60%	0.35%	26.02%	0.42%	54.63%	0.00%	14.89%	1.07%

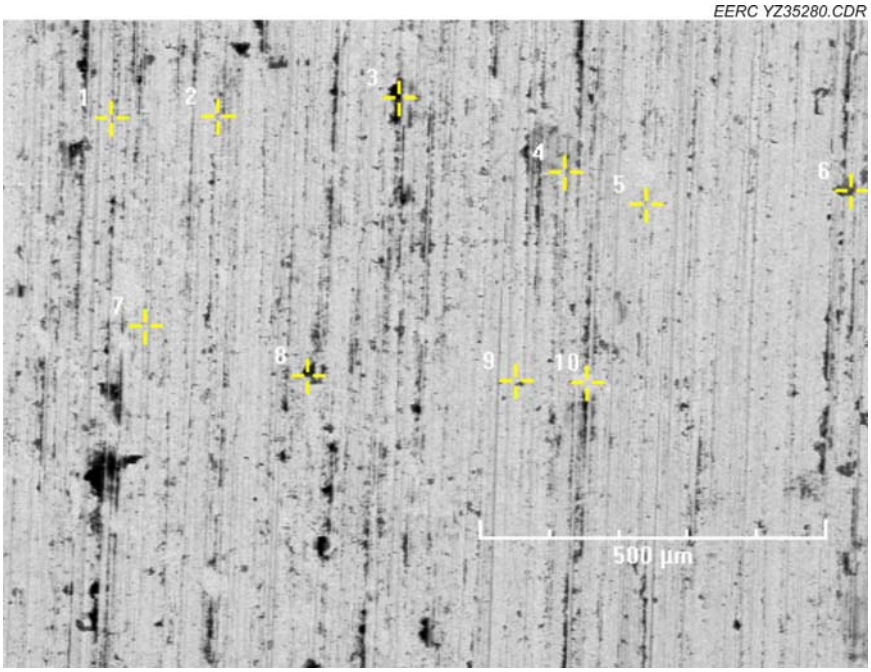

Figure A-11. U6 surface SEM image.

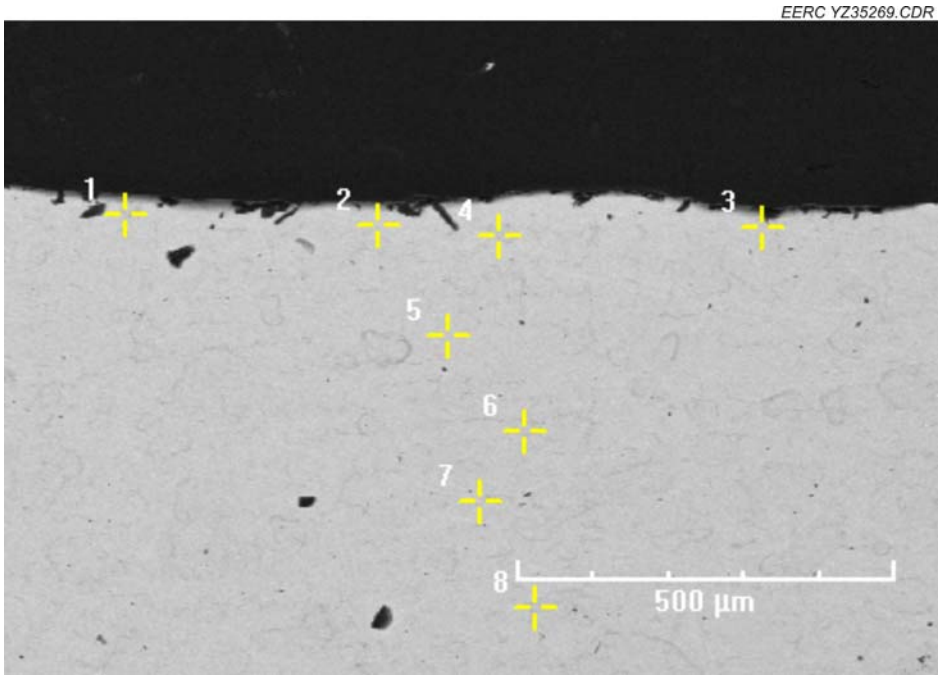

Figure A-12. U6 cross-sectional SEM image.

Table A-6 Elemental Analysis on U6 Cross Section Image

Tag	Si	S	Cr	Mn	Fe	Co	Ni	Br
1	16.33%	1.24%	25.45%	0.27%	44.44%	0.00%	11.66%	0.51%
2	2.97%	0.37%	25.96%	0.34%	54.56%	0.00%	14.92%	0.88%
3	3.30%	0.31%	26.31%	0.54%	53.04%	0.29%	15.06%	1.06%
4	2.52%	0.77%	59.67%	0.00%	29.16%	0.00%	6.95%	0.94%
5	2.55%	0.31%	25.38%	0.39%	54.92%	0.14%	14.96%	1.28%
6	5.30%	0.56%	28.62%	0.56%	48.96%	0.00%	14.56%	1.43%
7	4.41%	0.72%	26.68%	0.51%	51.59%	0.00%	14.76%	1.29%
8	2.96%	0.36%	24.95%	0.43%	55.41%	0.00%	14.69%	1.19%

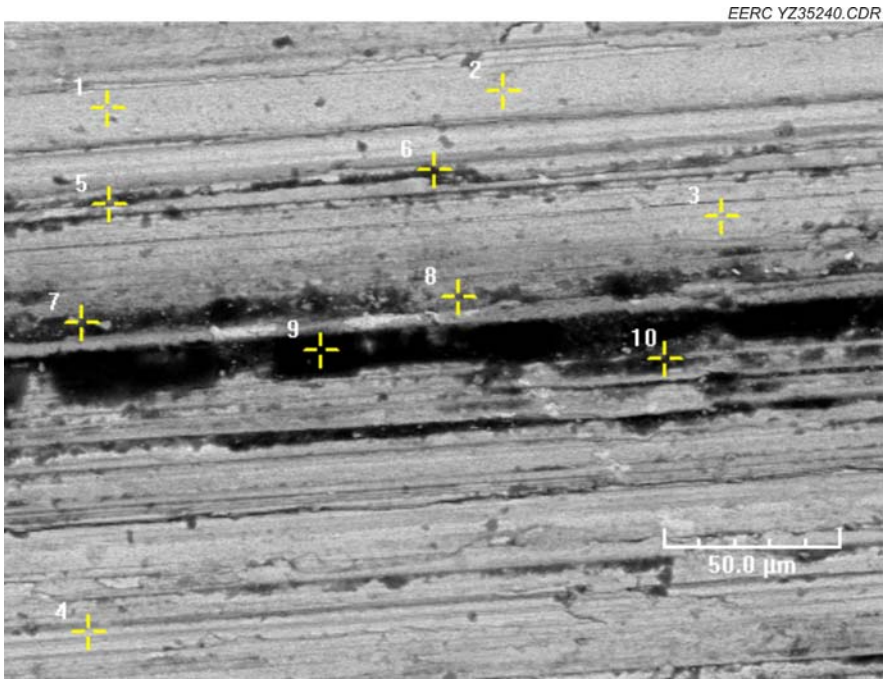

Figure A-13. U7 surface SEM image.

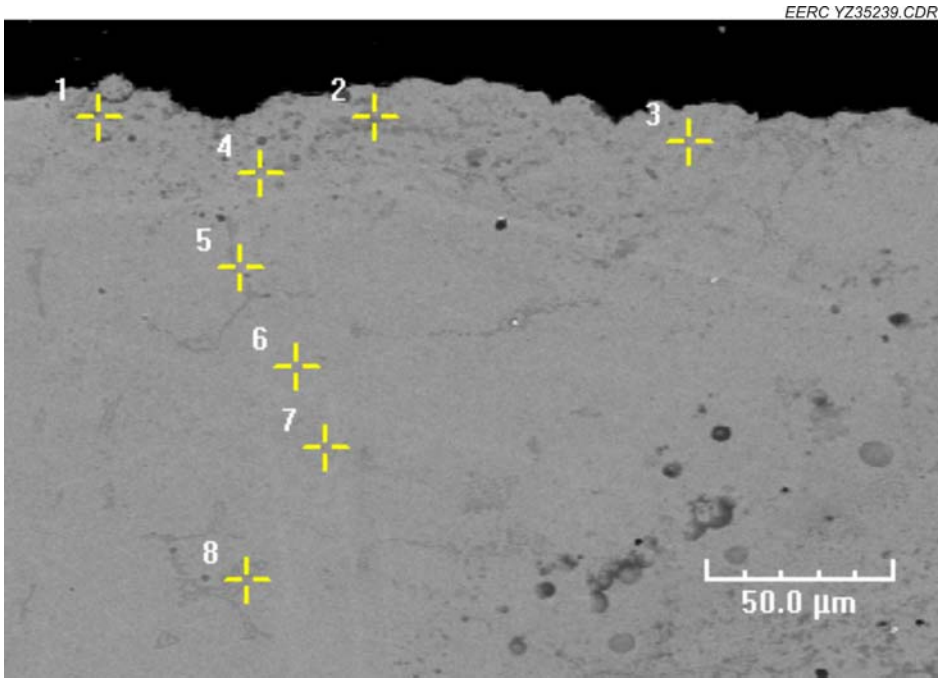

Figure A-14. U7 cross-sectional SEM image.

Table A-7. Elemental Analysis of U7 Cross Section

Tag	Si	S	Cr	Mn	Fe	Co	Ni
1	1.78%	0.50%	50.52%	0.71%	37.11%	0.00%	9.34%
2	5.68%	2.01%	26.56%	0.23%	51.25%	0.00%	14.02%
3	3.19%	0.50%	26.32%	0.43%	54.76%	0.00%	14.71%
4	6.63%	0.52%	26.84%	0.15%	51.56%	0.00%	14.29%
5	4.23%	1.02%	28.45%	0.17%	52.28%	0.00%	13.81%
6	4.69%	0.30%	24.75%	0.37%	55.35%	0.00%	14.45%
7	3.04%	0.45%	26.36%	0.18%	54.15%	0.00%	15.72%
8	3.73%	0.43%	27.20%	0.78%	52.81%	0.00%	14.96%

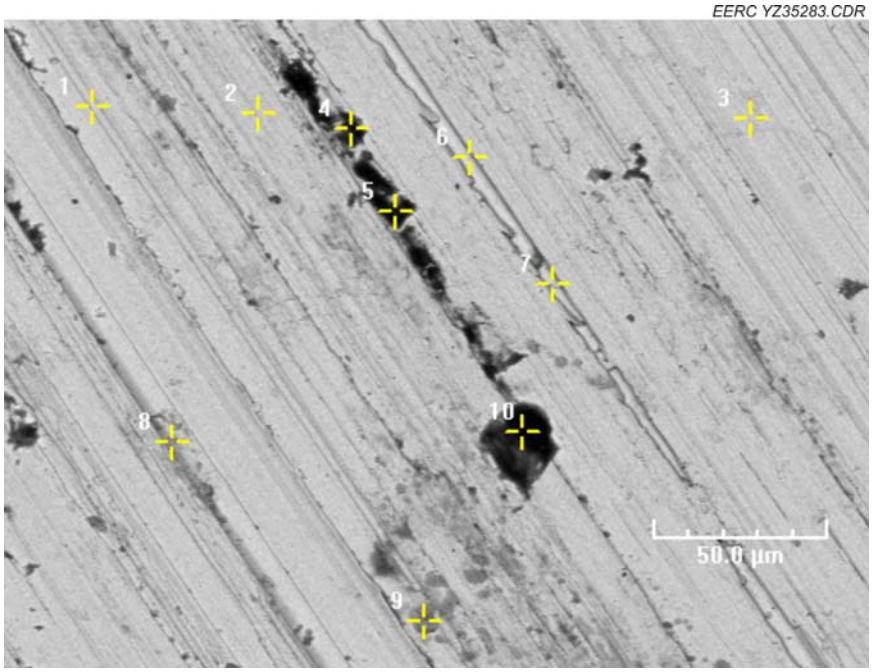

Figure A-15. U8 surface SEM image.

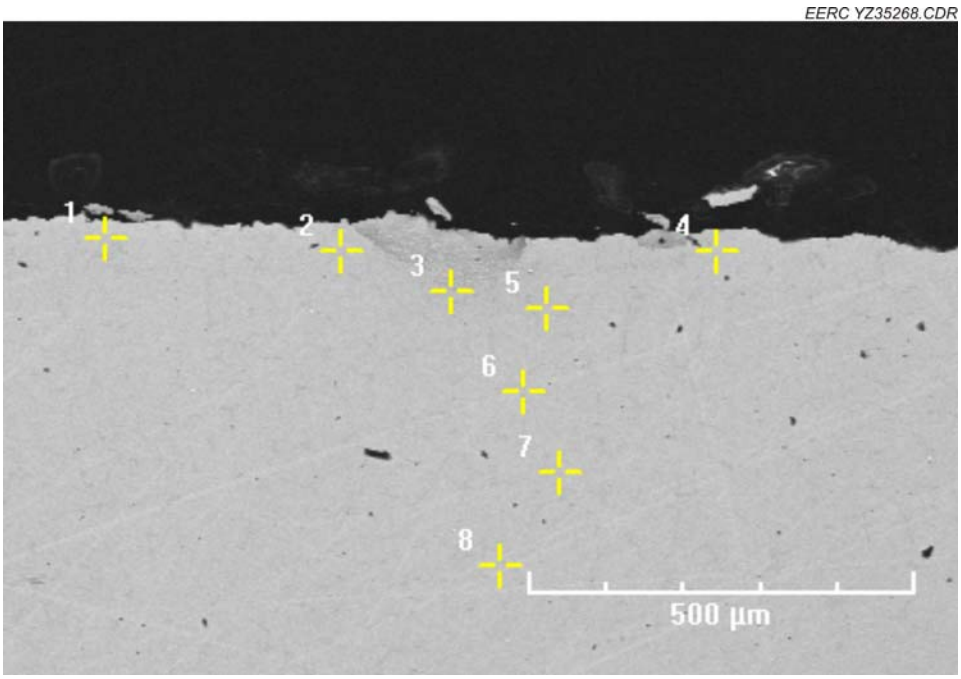

Figure A-16. U8 cross-sectional SEM image.

Table A-8. Elemental Analysis of U8 Cross Section

Tag	Si	S	Cr	Mn	Fe	Co	Ni
1	3.76%	0.62%	45.98%	0.50%	38.91%	0.00%	10.14%
2	5.16%	0.39%	27.95%	0.15%	51.50%	0.00%	14.85%
3	7.39%	0.49%	26.39%	0.61%	50.91%	0.02%	14.18%
4	3.87%	0.20%	26.23%	0.25%	54.65%	0.00%	14.80%
5	4.78%	0.33%	26.00%	0.46%	53.90%	0.00%	14.49%
6	4.00%	0.38%	29.34%	0.13%	51.41%	0.00%	14.75%
7	2.99%	0.31%	27.80%	0.15%	54.19%	0.00%	14.42%
8	2.37%	0.27%	25.48%	0.29%	56.92%	0.00%	14.60%

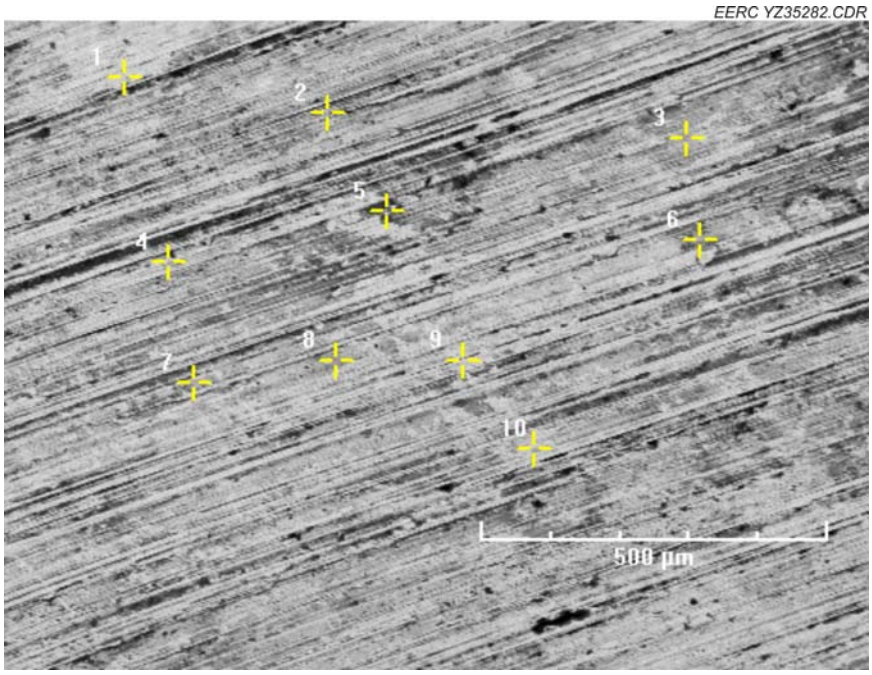

Figure A-17. U9 surface SEM image

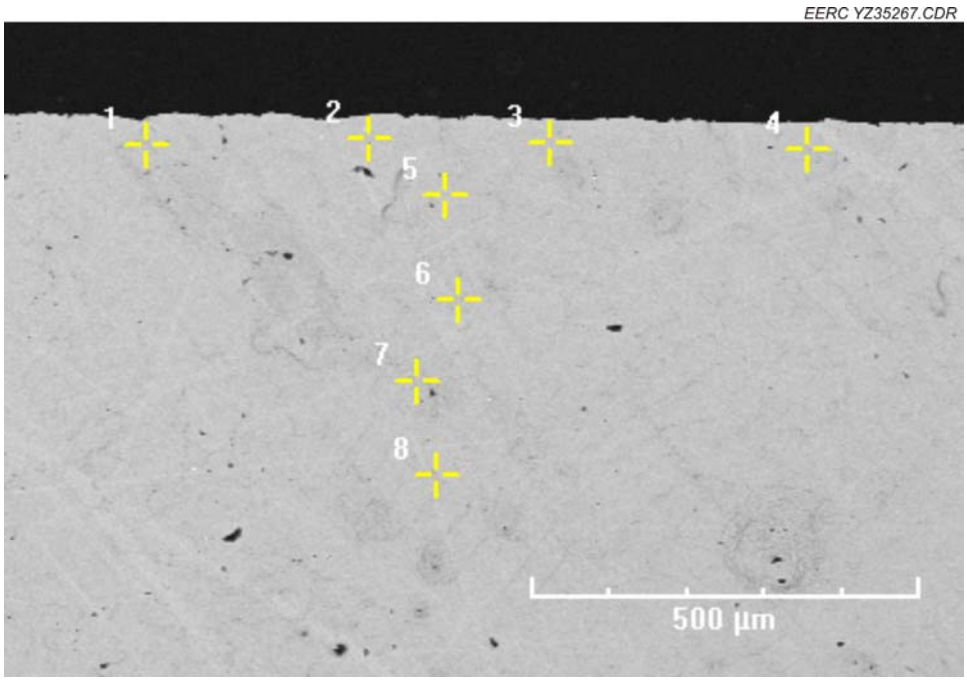

Figure A-18. U9 cross-sectional SEM image.

Table A-9. Elemental Analysis of U9 Cross Section

Tag	Si	S	Cr	Mn	Fe	Co	Ni
1	2.93%	0.32%	25.14%	0.49%	56.54%	0.00%	14.59%
2	3.31%	0.27%	28.23%	0.65%	52.09%	0.19%	15.23%
3	2.94%	0.24%	27.02%	0.21%	54.18%	0.00%	15.42%
4	4.01%	0.53%	29.70%	0.52%	50.64%	0.00%	14.58%
5	4.21%	0.28%	25.78%	0.47%	54.83%	0.00%	14.42%
6	3.43%	0.43%	28.17%	0.42%	51.63%	0.00%	15.83%
7	5.50%	0.56%	29.15%	0.00%	50.16%	0.00%	14.63%
8	4.06%	0.31%	27.86%	0.41%	52.62%	0.00%	14.66%

APPENDIX B

MINORCA COUPON SEM ANALYSIS

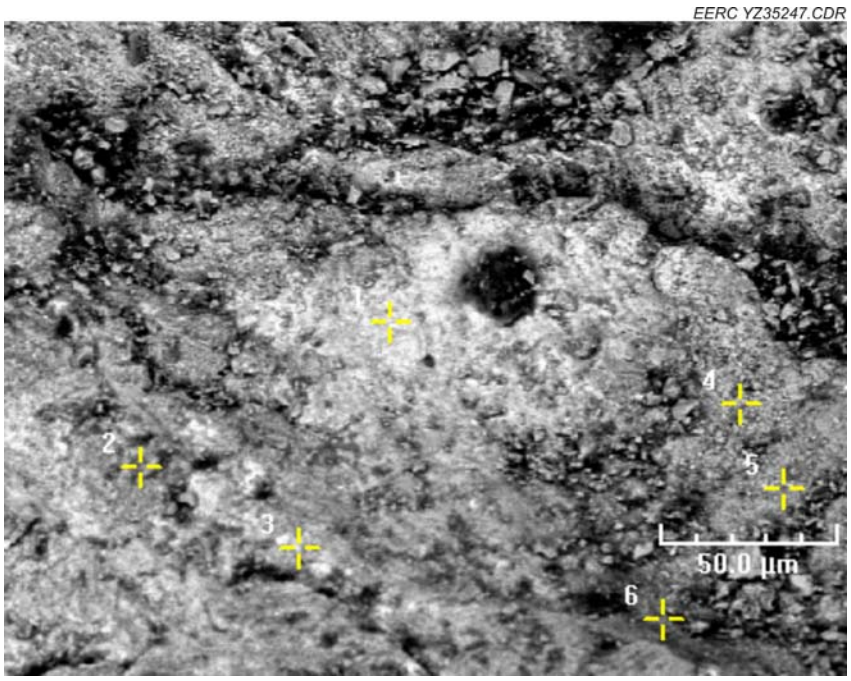

Figure B-1. M1 surface SEM image.

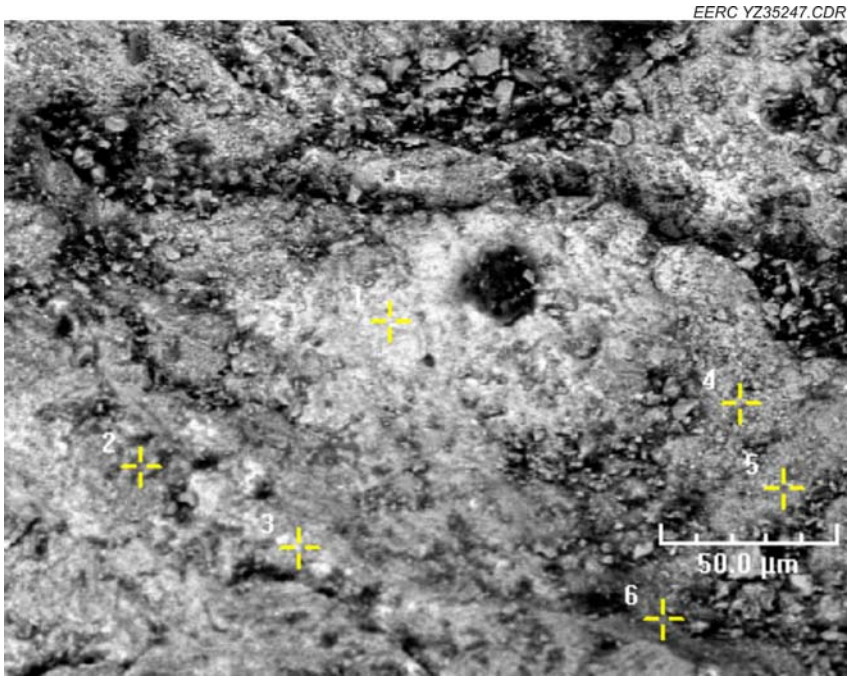

Figure B-2. M1 cross-sectional SEM image.

Table B-1. Elemental Analysis on M1 Cross Section

Tag	Si	S	Cr	Mn	Fe	Co	Ni	Br
1	6.14%	0.79%	22.96%	0.00%	57.56%	0.00%	3.55%	9.00%
2	4.14%	0.23%	25.42%	0.17%	63.54%	0.00%	4.30%	2.20%
3	4.82%	0.32%	29.47%	0.00%	55.97%	0.00%	3.66%	5.76%
4	3.32%	0.54%	16.27%	0.00%	73.06%	0.00%	4.58%	2.23%
5	11.85%	0.04%	22.64%	0.00%	62.29%	0.00%	1.16%	2.02%
6	1.54%	0.57%	1.91%	0.00%	90.98%	0.00%	0.00%	5.00%
7	4.13%	0.34%	26.80%	0.09%	61.59%	0.00%	5.19%	1.86%
8	3.58%	0.29%	25.38%	0.29%	64.30%	0.02%	4.90%	1.17%
9	3.43%	0.28%	33.36%	0.09%	56.94%	0.00%	4.62%	1.25%
10	3.39%	0.18%	26.02%	0.18%	63.54%	0.12%	5.13%	1.32%

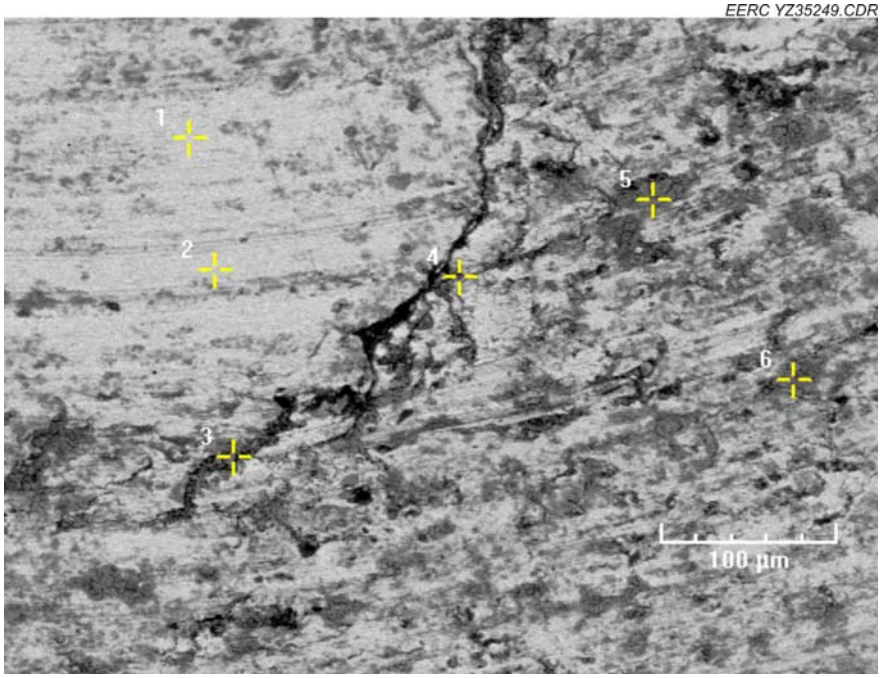

Figure B-3. M2 surface SEM image.

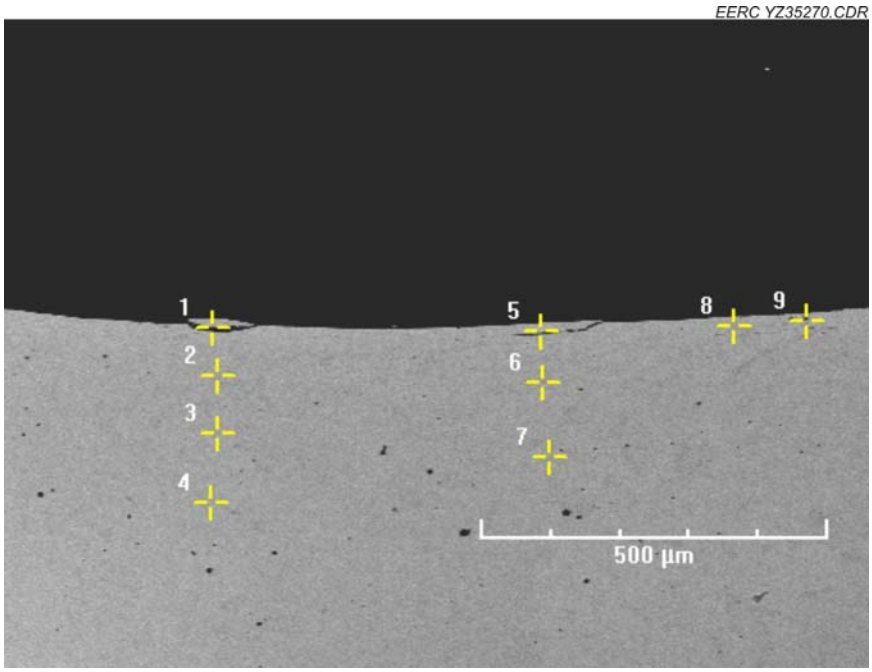

Figure B-4. M2 cross-sectional SEM image.

Table B-2 Elemental Analysis on M2 Cross Section

Tag	Si	S	Cr	Mn	Fe	Co	Ni	Br
1	14.15%	0.20%	10.28%	0.00%	40.67%	0.00%	0.00%	34.66%
2	7.29%	0.43%	29.29%	0.00%	57.24%	0.00%	2.11%	3.64%
3	7.27%	0.37%	29.40%	0.00%	57.35%	0.00%	2.29%	3.33%
4	7.08%	0.27%	29.13%	0.00%	57.32%	0.00%	3.11%	3.01%
5	8.42%	0.00%	25.14%	0.00%	42.16%	0.00%	1.05%	23.23%
6	7.44%	0.25%	30.41%	0.00%	55.06%	0.00%	3.31%	3.53%
7	6.42%	0.16%	28.14%	0.00%	58.75%	0.00%	4.17%	2.36%
8	6.70%	0.14%	31.97%	0.00%	56.49%	0.00%	2.50%	2.17%
9	7.60%	1.10%	29.26%	0.24%	55.55%	0.00%	2.62%	3.63%

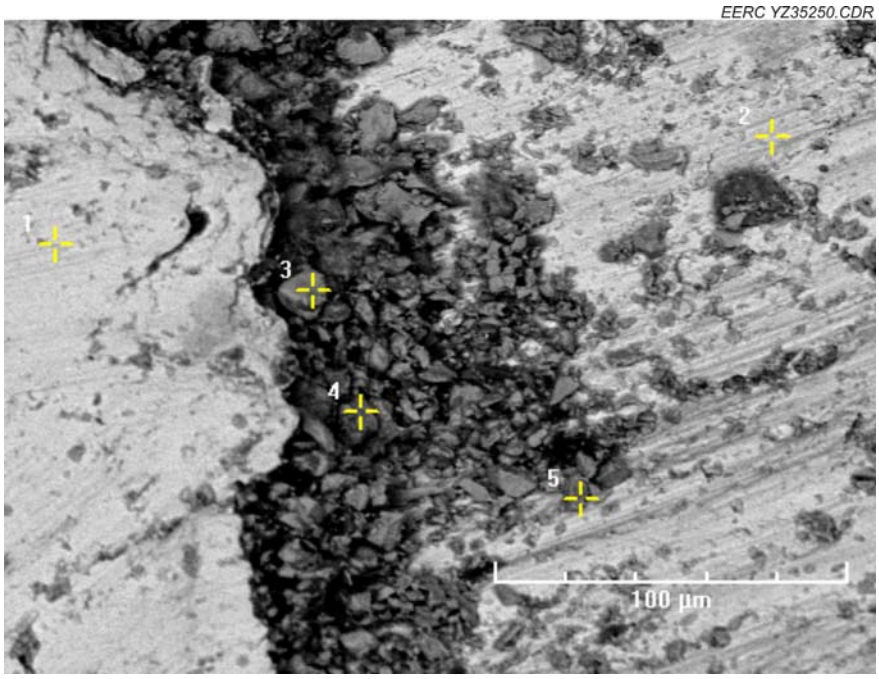

Figure B-5. M3 surface SEM image.

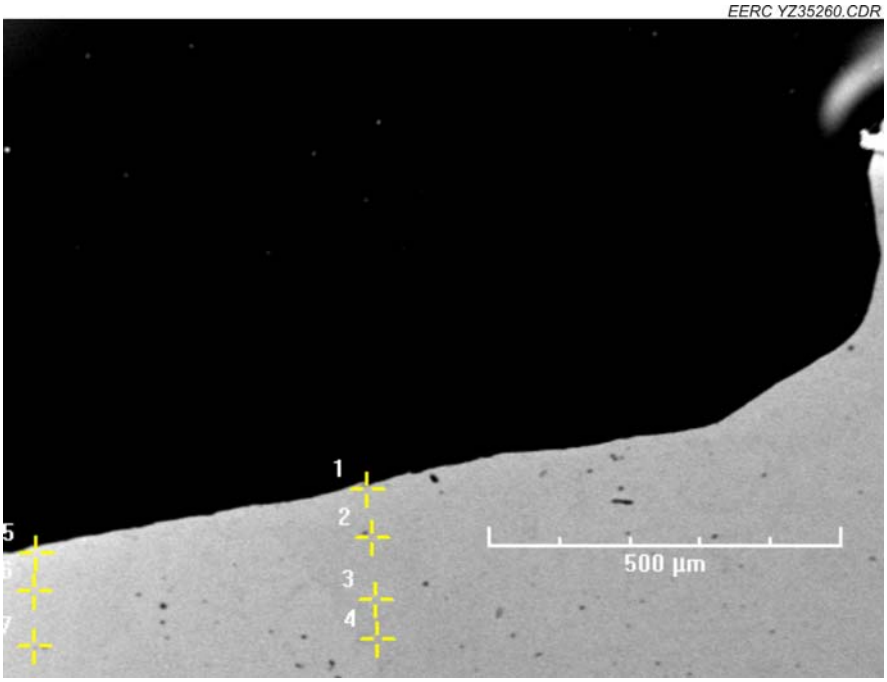

Figure B-6. M3 cross-sectional SEM image.

Table B-3. Elemental Analysis on Cross Section of M3

Tag	Si	S	Cr	Mn	Fe	Co	Ni	Br
1	9.24%	0.00%	31.68%	0.00%	53.12%	0.00%	1.97%	3.86%
2	8.07%	0.48%	28.03%	0.00%	54.98%	0.00%	2.30%	6.08%
3	7.50%	0.47%	30.11%	0.23%	55.14%	0.00%	2.91%	3.58%
4	7.01%	0.13%	29.46%	0.08%	57.41%	0.00%	2.90%	2.81%
5	6.88%	0.38%	27.59%	0.00%	58.04%	0.00%	2.50%	4.62%
6	6.49%	0.35%	29.54%	0.00%	58.14%	0.00%	2.94%	2.52%
7	6.82%	0.15%	28.41%	0.13%	57.49%	0.00%	2.72%	4.28%

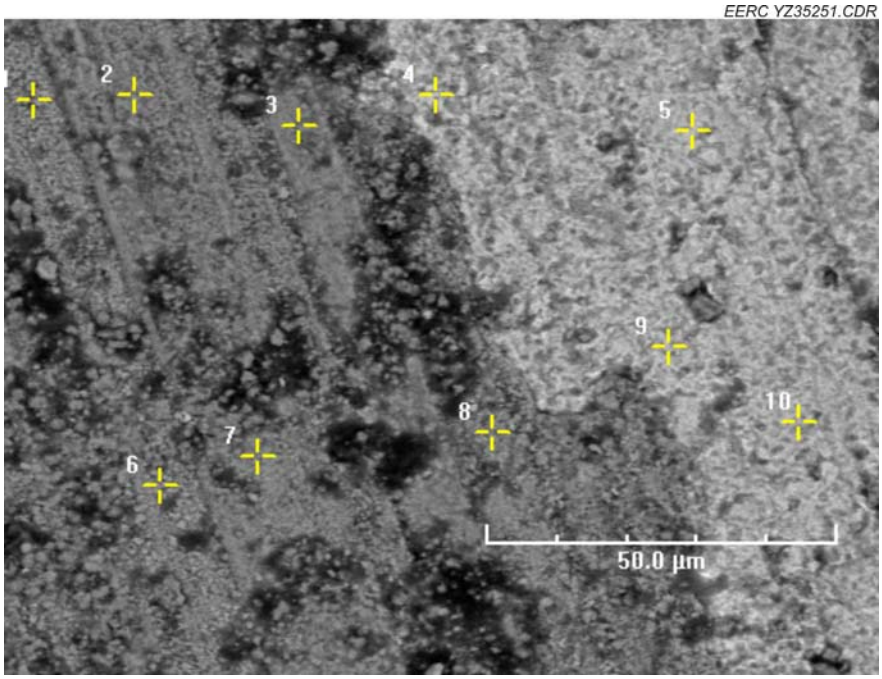

Figure B-7. M4 surface SEM image.

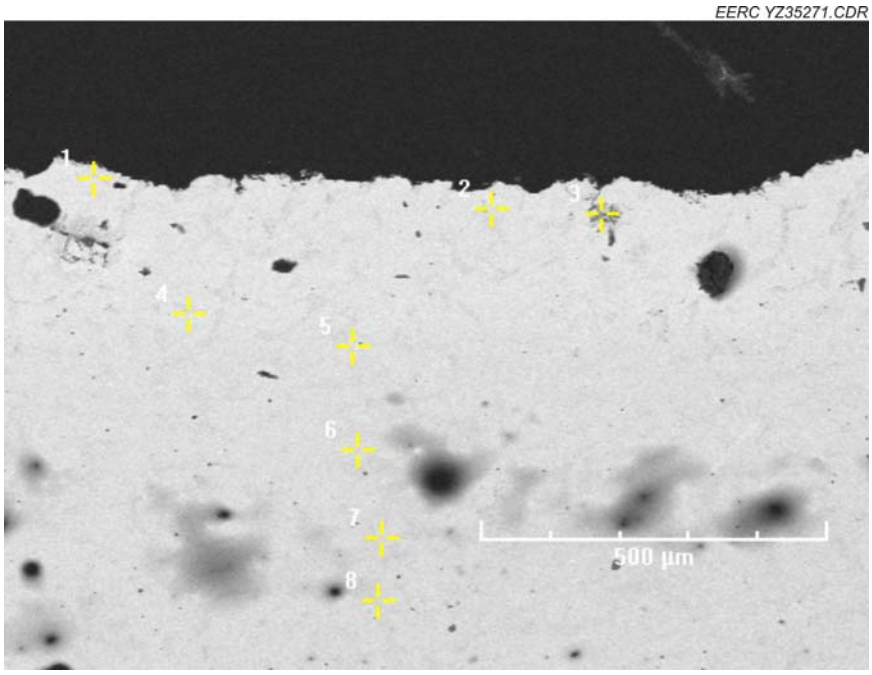

Figure B-8. M4 cross-sectional SEM image.

Table B-4. Elemental Analysis of Cross Section of M4

Tag	Si	S	Cr	Mn	Fe	Co	Ni	Br
1	3.87%	0.35%	24.42%	0.07%	63.83%	0.00%	5.26%	2.15%
2	4.30%	0.16%	25.68%	0.34%	61.38%	0.21%	5.18%	2.76%
3	3.85%	0.58%	26.25%	0.21%	60.70%	0.00%	4.96%	3.46%
4	4.04%	0.08%	25.70%	0.00%	63.82%	0.00%	4.47%	1.80%
5	3.82%	0.19%	27.74%	0.08%	62.15%	0.00%	4.65%	1.36%
6	3.97%	0.37%	26.19%	0.10%	63.11%	0.00%	4.54%	1.69%
7	3.66%	0.25%	26.26%	0.17%	64.73%	0.00%	3.81%	1.06%
8	3.84%	0.28%	27.11%	0.03%	63.50%	0.00%	3.81%	1.40%

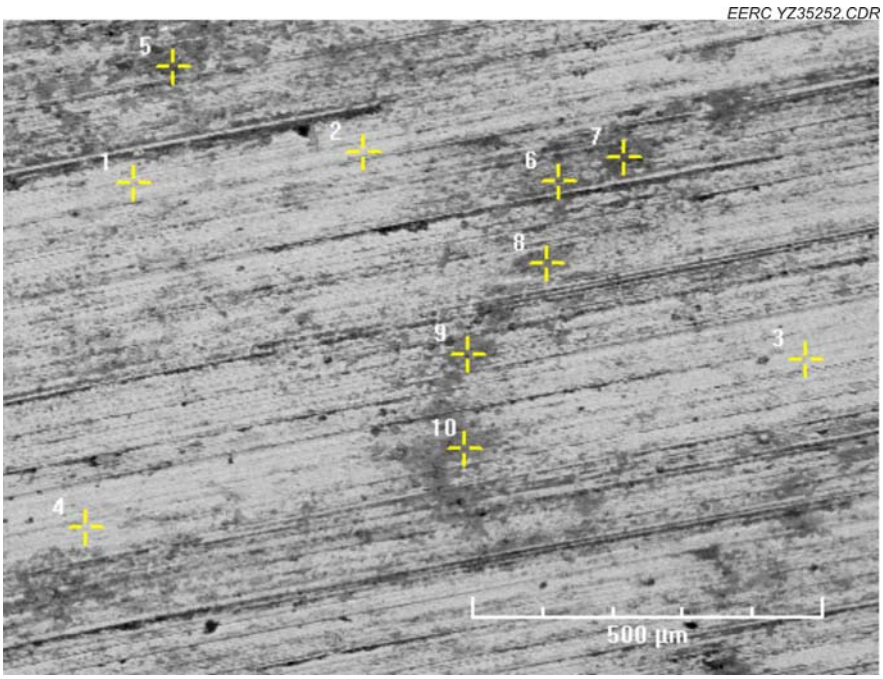

Figure B-9. M5 surface SEM image.

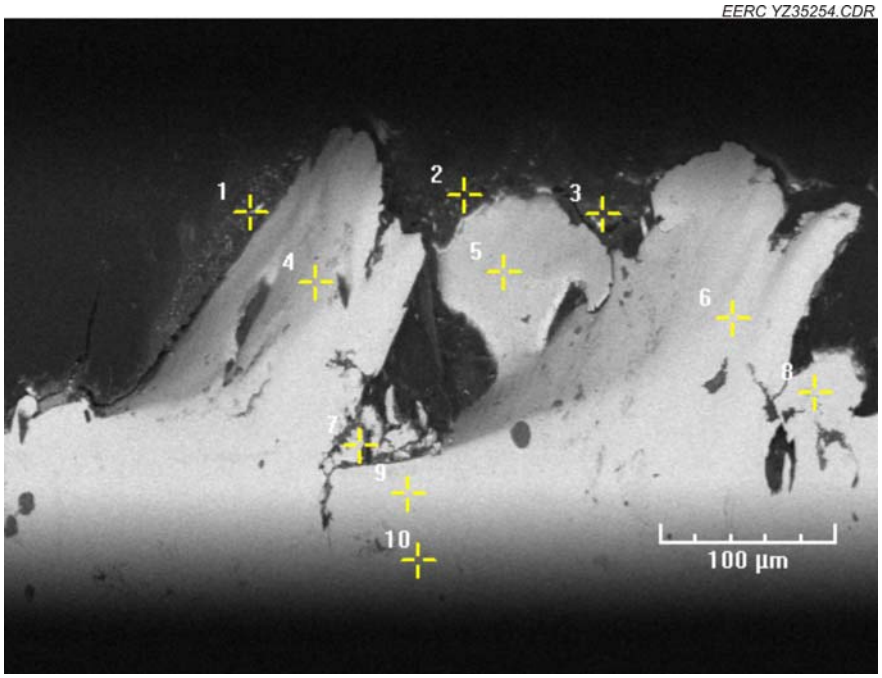

Figure B-10. M5 cross-sectional SEM image.

Table B-5. Elemental Analysis of Cross Section of M5

Tag	Si	S	Cr	Mn	Fe	Co	Ni	Br
1	9.56%	1.12%	14.04%	0.00%	33.09%	0.00%	2.92%	39.27%
2	19.07%	2.54%	5.92%	0.00%	13.68%	0.49%	3.18%	55.12%
3	13.59%	4.22%	7.87%	0.81%	7.95%	0.22%	0.32%	65.02%
4	7.13%	0.32%	18.97%	0.00%	46.42%	0.00%	3.04%	24.11%
5	5.48%	0.45%	22.56%	0.27%	55.29%	0.10%	4.64%	11.20%
6	3.75%	0.00%	25.20%	0.06%	64.64%	0.00%	4.86%	1.49%
7	4.38%	0.34%	22.22%	0.10%	65.74%	0.08%	5.33%	1.81%
8	3.88%	0.24%	22.75%	0.32%	67.42%	0.00%	4.25%	1.00%
9	3.08%	0.29%	24.76%	0.17%	65.41%	0.05%	5.08%	1.15%
10	3.74%	0.09%	25.84%	0.09%	63.87%	0.00%	5.02%	1.32%

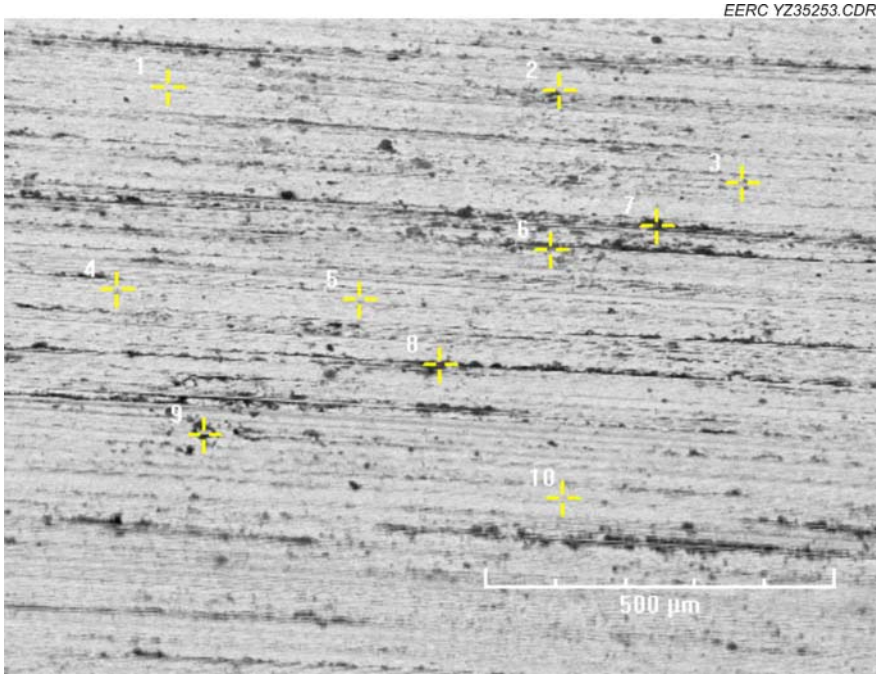

Figure B-11. M6 surface SEM image.

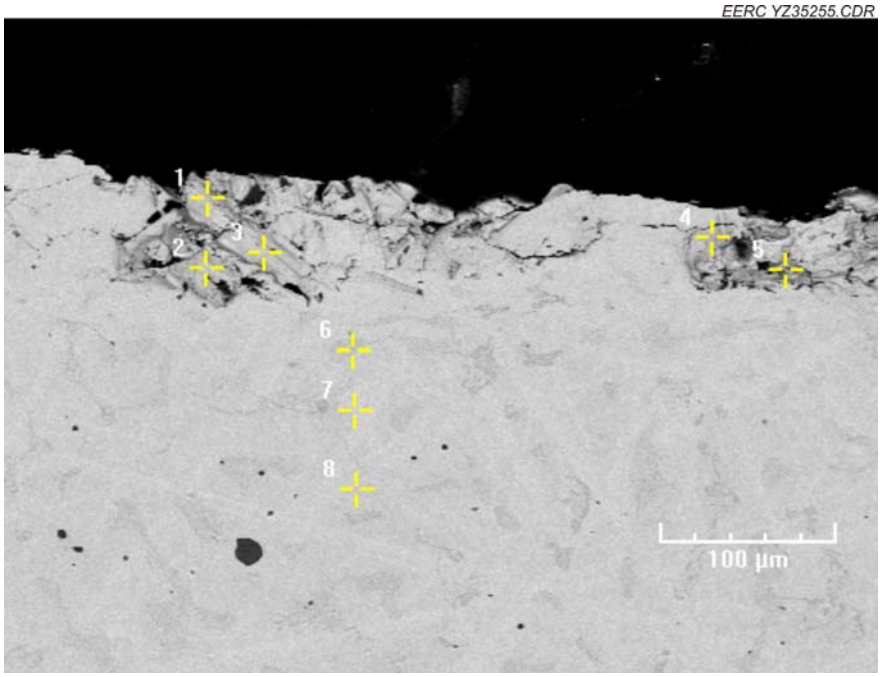

Figure B-12. M6 cross-sectional SEM image.

Table B-6. Elemental Analysis of M6 Cross Section

Tag	Si	S	Cr	Mn	Fe	Co	Ni	Br	K
1	3.57%	0.27%	25.57%	0.06%	64.50%	0.00%	4.68%	1.23%	0.12%
2	3.37%	0.21%	29.81%	0.11%	61.17%	0.00%	4.38%	0.93%	0.01%
3	3.21%	0.25%	26.01%	0.30%	63.89%	0.03%	5.04%	1.25%	0.01%
4	2.84%	0.34%	27.42%	0.13%	62.13%	0.00%	5.23%	1.90%	0.02%
5	3.47%	0.29%	27.54%	0.31%	61.67%	0.00%	5.16%	1.55%	0.00%
6	3.28%	0.26%	29.68%	0.28%	60.28%	0.00%	5.16%	1.01%	0.04%
7	3.14%	0.17%	24.84%	0.36%	64.99%	0.16%	5.13%	1.22%	0.00%
8	3.35%	0.17%	26.06%	0.16%	65.16%	0.00%	4.24%	0.82%	0.05%

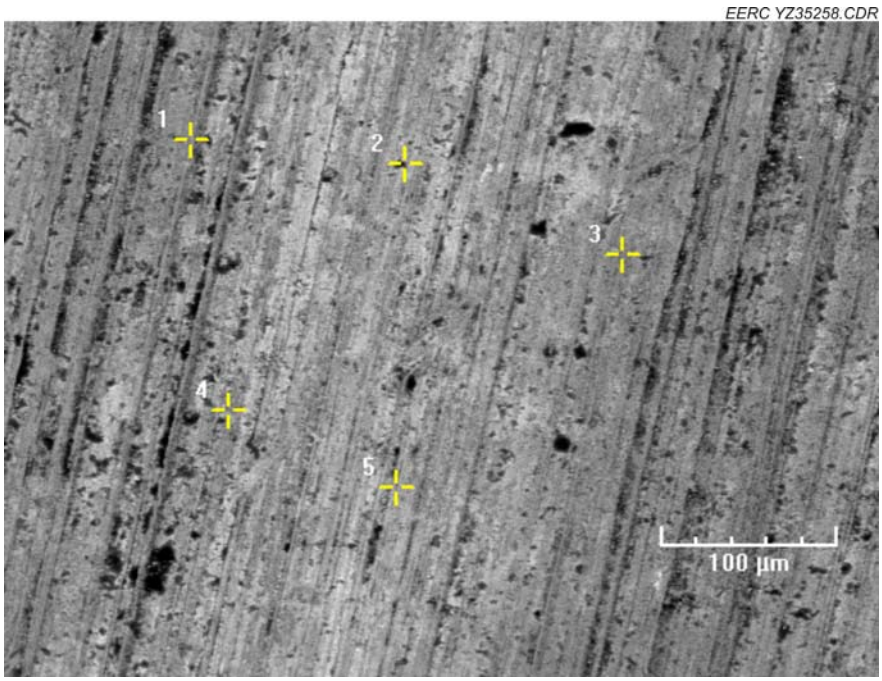

Figure B-13. M7 surface SEM image.

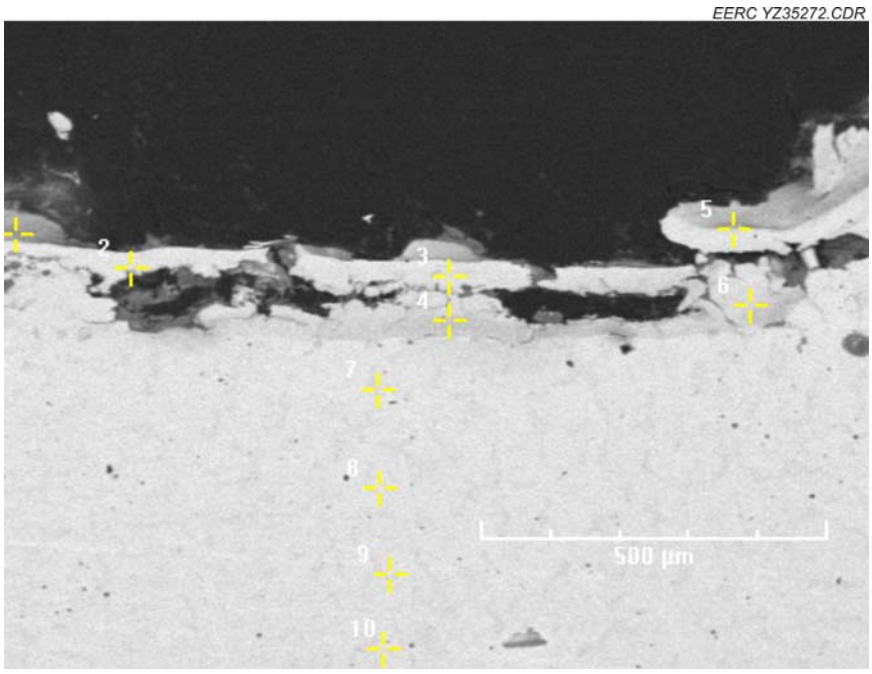

Figure B-14. M7 cross-sectional SEM image.

Table B-7. Element Analysis on M7 Cross Section

Tag	Si	S	Cr	Mn	Fe	Co	Ni	K
1	4.03%	0.43%	26.33%	0.00%	64.44%	0.00%	4.77%	0.00%
2	3.39%	0.17%	27.30%	0.51%	64.00%	0.00%	4.62%	0.00%
3	3.30%	0.23%	25.39%	0.31%	65.68%	0.00%	5.07%	0.01%
4	3.12%	0.44%	26.17%	0.04%	64.91%	0.00%	5.31%	0.00%
5	4.27%	1.11%	28.66%	0.34%	60.61%	0.00%	5.00%	0.00%
6	2.83%	0.32%	25.55%	0.23%	65.64%	0.00%	5.28%	0.16%
7	3.65%	0.15%	30.55%	0.00%	60.45%	0.00%	5.20%	0.00%
8	3.42%	0.24%	26.13%	0.10%	65.55%	0.12%	4.43%	0.00%
9	3.66%	0.28%	24.98%	0.22%	64.95%	0.57%	5.35%	0.00%
10	3.64%	0.10%	26.22%	0.15%	64.81%	0.00%	4.96%	0.12%

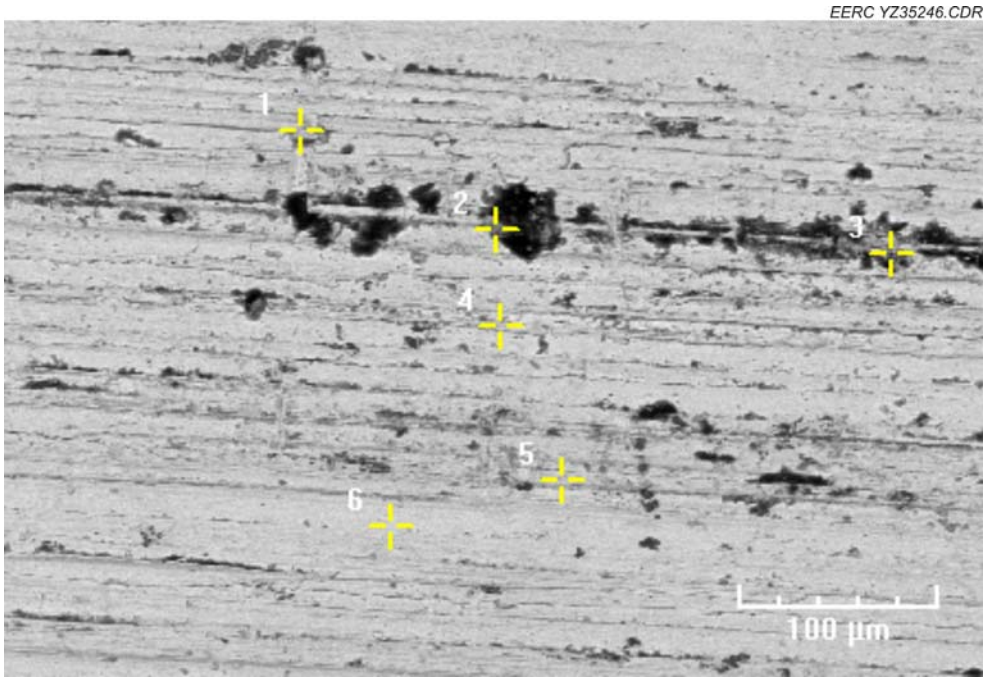

Figure B-15. M8 surface SEM image.

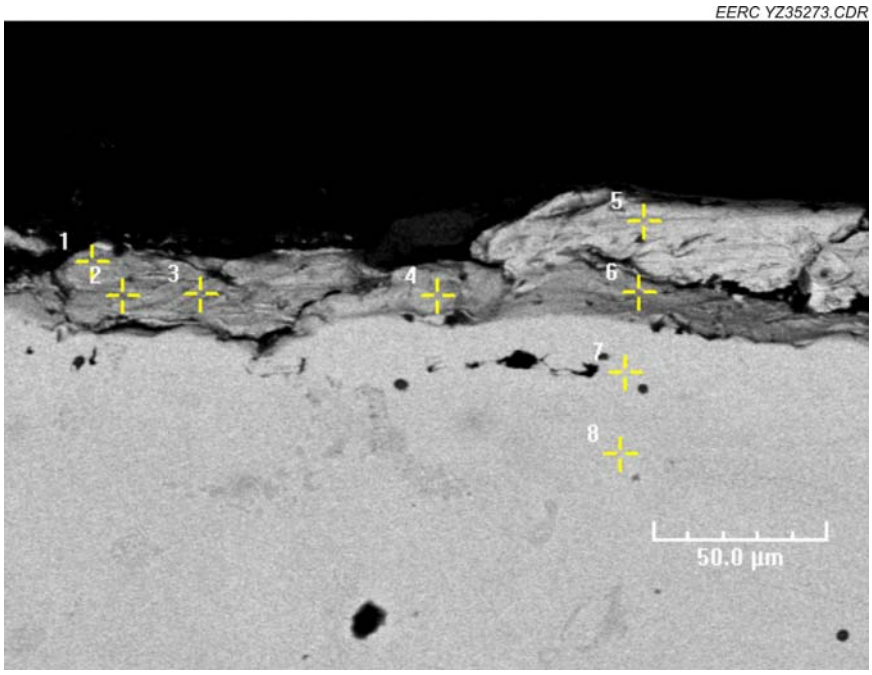

Figure B-16. M8 cross-sectional SEM image.

Table B-8. Elemental Analysis of M8 Cross Section

Tag	Si	S	Cr	Mn	Fe	Co	Ni
1	6.32%	0.41%	26.21%	0.00%	62.00%	0.00%	5.06%
2	3.91%	0.43%	25.67%	0.34%	64.43%	0.00%	5.16%
3	5.01%	0.20%	26.69%	0.35%	63.00%	0.15%	4.60%
4	3.78%	0.20%	26.43%	0.00%	64.82%	0.00%	4.77%
5	3.77%	0.27%	25.95%	0.42%	64.76%	0.00%	4.71%
6	4.47%	0.30%	27.11%	0.17%	63.19%	0.00%	4.76%
7	3.24%	0.28%	24.74%	0.30%	65.82%	0.11%	5.51%
8	3.21%	0.12%	25.93%	0.00%	66.10%	0.00%	4.64%

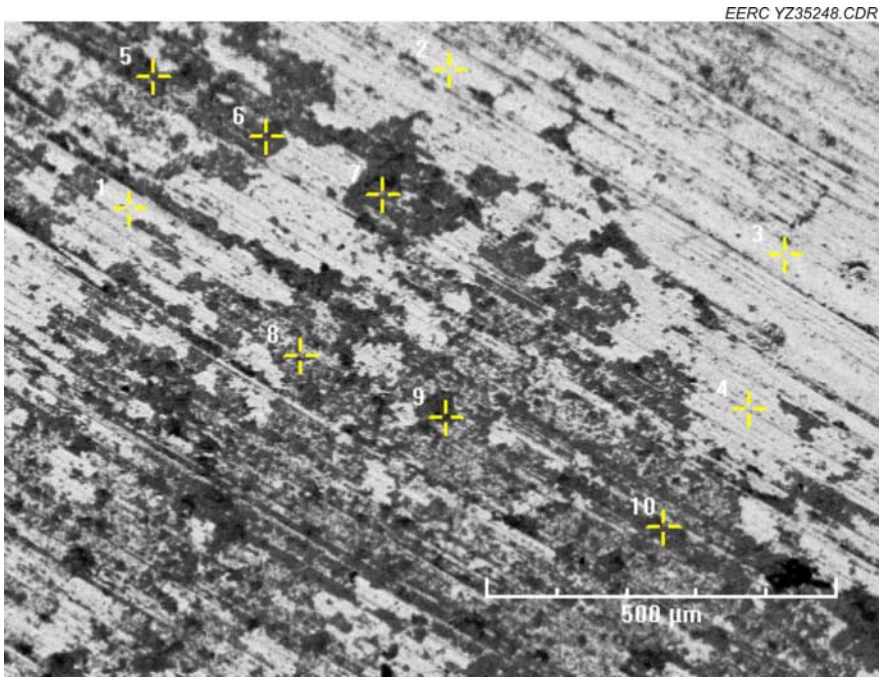

Figure B-17. M9 surface SEM image.

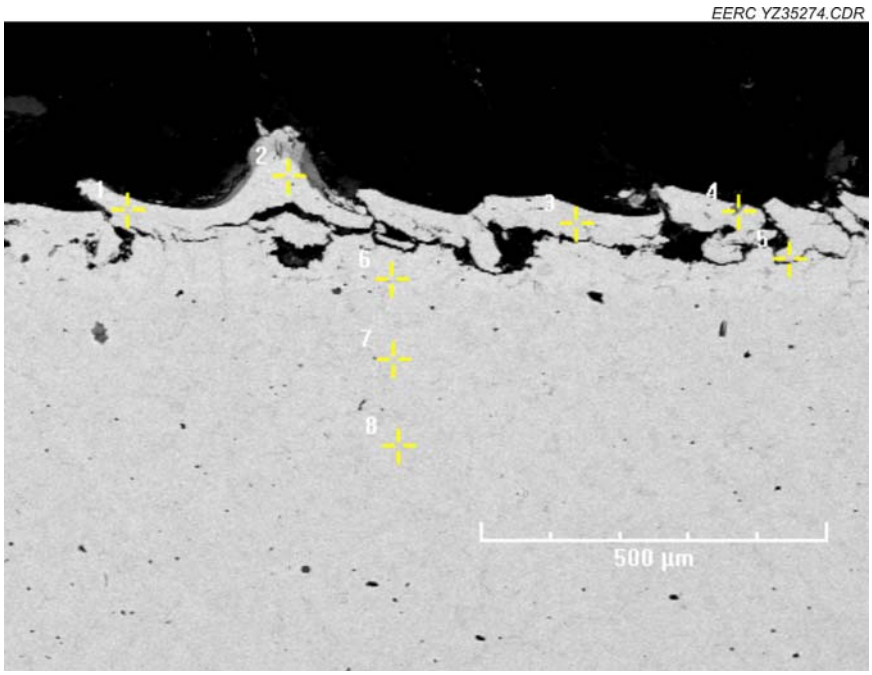

Figure B-18. M9 cross-sectional SEM image.

Table B-9. Elemental Analysis on M9 Cross Section

Tag	Si	S	Cr	Mn	Fe	Co	Ni
1	3.26%	0.23%	28.33%	0.20%	63.27%	0.00%	4.71%
2	3.16%	0.28%	25.36%	0.30%	65.74%	0.00%	5.17%
3	5.43%	0.33%	24.00%	0.31%	66.99%	0.25%	2.67%
4	4.90%	0.24%	25.95%	0.00%	63.31%	0.00%	5.59%
5	3.47%	0.20%	27.13%	0.16%	63.55%	0.00%	5.49%
6	4.32%	0.45%	27.40%	0.00%	63.05%	0.00%	4.74%
7	3.30%	0.32%	25.70%	0.34%	64.83%	0.07%	5.41%
8	3.13%	0.34%	25.83%	0.46%	65.25%	0.00%	4.99%

APPENDIX C

USS MINNTAC COUPON SEM ANALYSIS

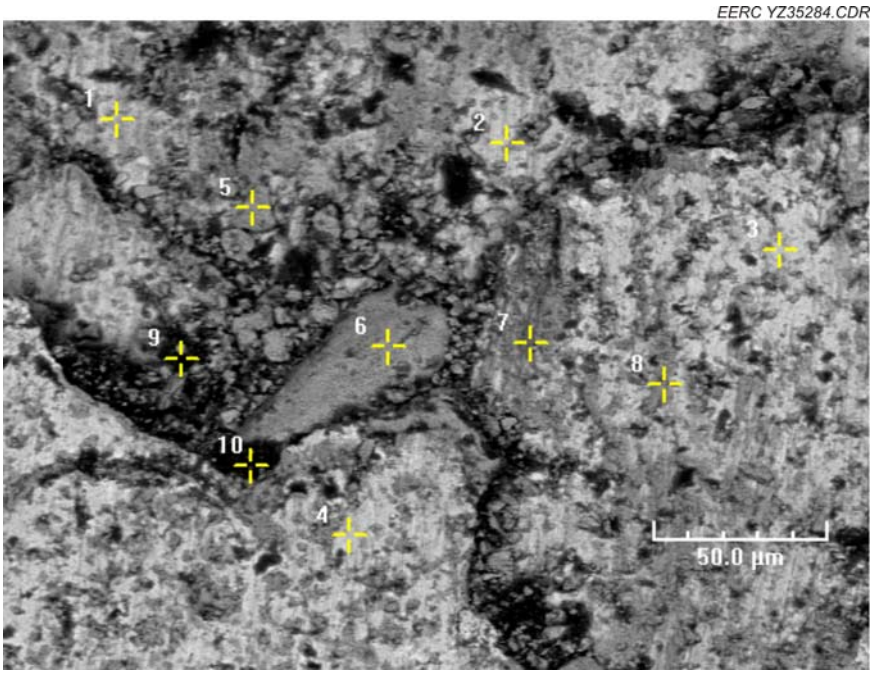

Figure C-1. UM1 surface SEM image.

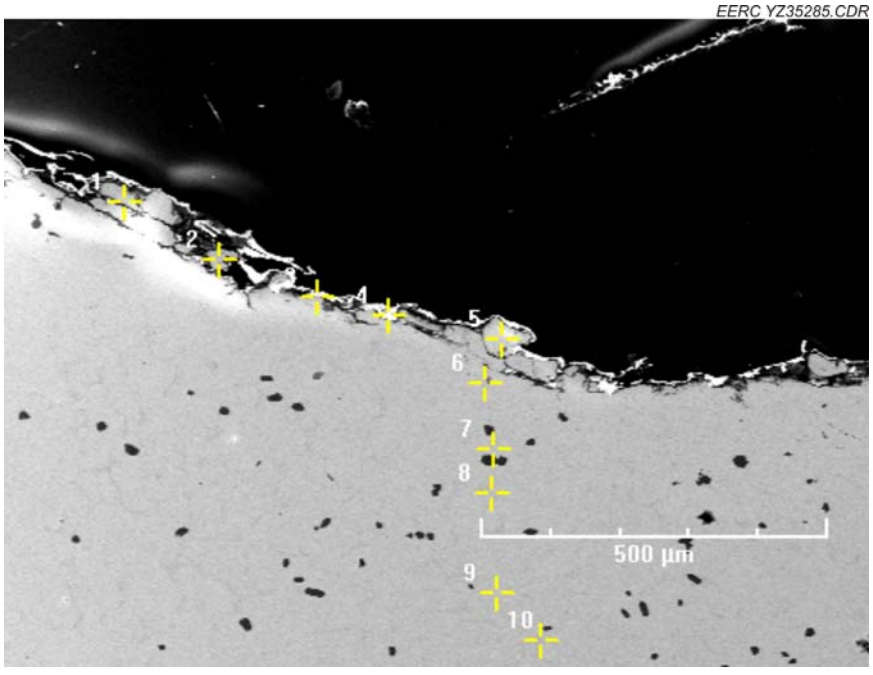

Figure C-2. UM1 cross-sectional SEM image.

Table C-1. Elemental Analysis of UM1 Cross Section

Tag	Si	S	Cr	Mn	Fe	Co	Ni	Br
1	9.38%	0.44%	36.13%	0.23%	35.27%	0.00%	3.99%	14.57%
2	11.97%	0.92%	36.25%	0.00%	34.76%	0.00%	3.35%	12.57%
3	18.72%	0.72%	5.97%	1.62%	10.74%	0.00%	0.76%	61.46%
4	28.82%	0.00%	1.77%	0.00%	14.50%	0.00%	0.46%	54.45%
5	9.66%	1.09%	33.90%	0.00%	36.44%	0.00%	5.10%	13.81%
6	7.33%	0.46%	25.50%	0.25%	37.15%	0.00%	7.00%	22.30%
7	7.75%	0.85%	31.95%	0.61%	40.22%	0.00%	5.93%	12.59%
8	8.53%	0.18%	34.25%	0.33%	37.44%	0.00%	6.09%	13.19%
9	7.24%	0.42%	30.38%	0.63%	40.59%	0.00%	5.43%	15.30%
10	7.67%	0.58%	42.35%	1.33%	31.71%	0.00%	4.51%	11.86%

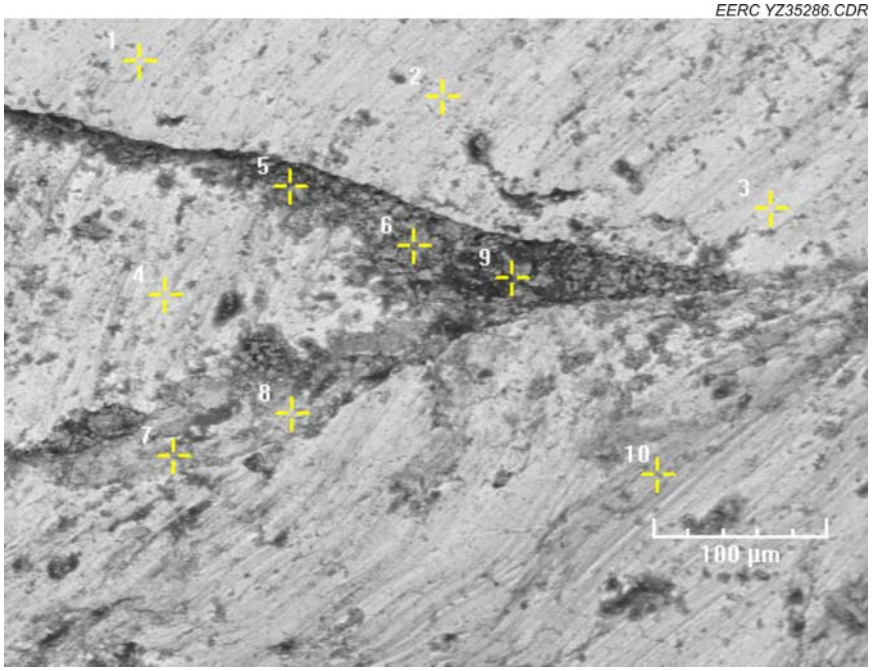

Figure C-3. UM2 surface SEM image.

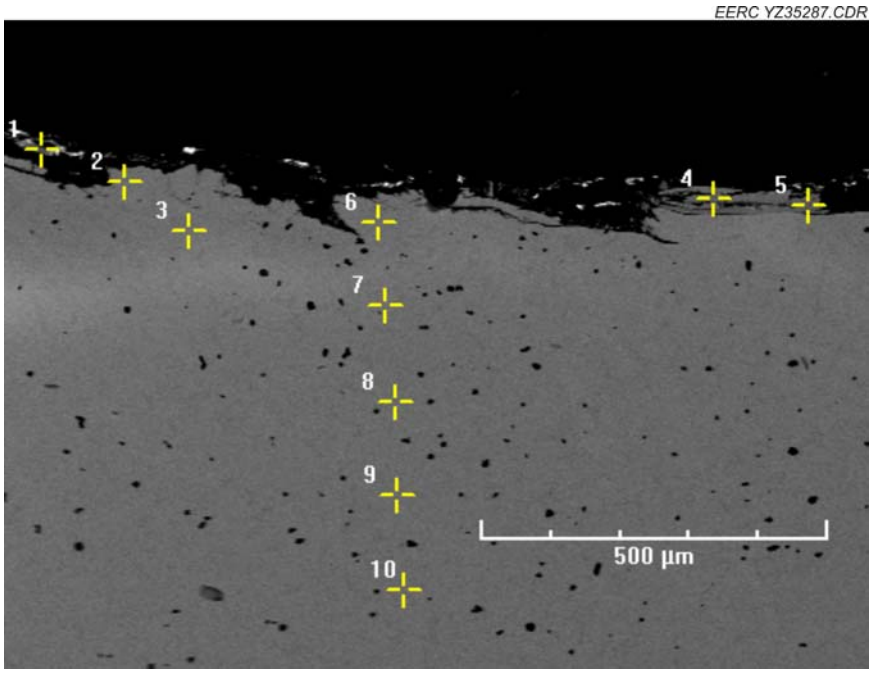

Figure C-4. UM2 cross-sectional SEM image.

Table C-2. Elemental Analysis of UM2 Cross Section

Tag	Si	S	Cr	Mn	Fe	Co	Ni	Br
1	11.82%	0.00%	13.76%	3.77%	19.19%	0.00%	0.00%	51.46%
2	4.64%	0.32%	28.80%	0.68%	44.07%	0.00%	13.46%	8.00%
3	4.04%	0.24%	28.98%	0.95%	44.44%	0.10%	13.57%	7.70%
4	3.82%	0.50%	38.45%	0.34%	39.56%	0.00%	10.79%	6.52%
5	1.26%	0.00%	33.80%	1.79%	48.58%	0.93%	10.17%	3.38%
6	3.65%	0.20%	30.60%	0.87%	44.58%	0.00%	13.58%	6.51%
7	4.39%	0.47%	45.14%	0.86%	34.77%	0.00%	8.58%	5.73%
8	3.92%	0.27%	29.19%	0.49%	46.00%	0.00%	13.45%	6.67%
9	2.96%	0.29%	27.48%	0.38%	48.42%	0.06%	14.44%	5.88%
10	3.46%	0.29%	41.21%	0.40%	39.03%	0.00%	10.45%	5.16%

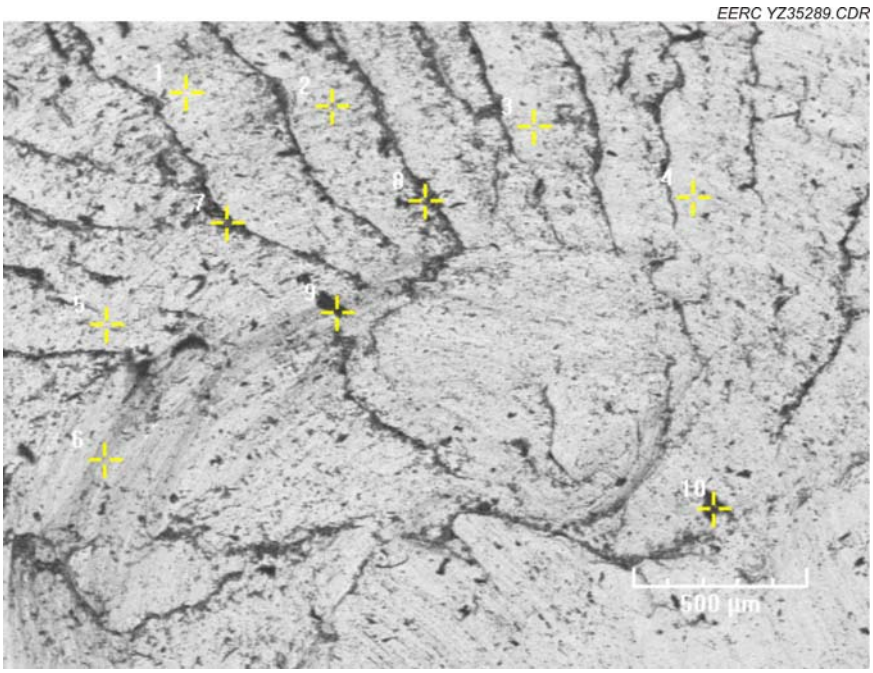

Figure C-5 UM3 surface SEM image.

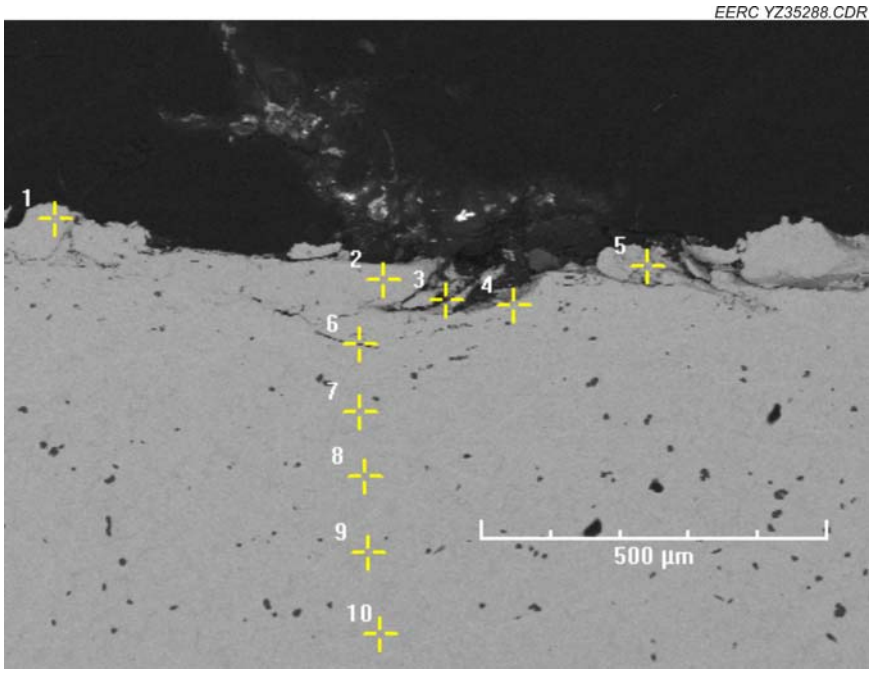

Figure C-6. UM3 cross-sectional SEM image.

Table C-3. Elemental Analysis of UM3 Cross Section

Tag	Si	S	Cr	Mn	Fe	Co	Ni	Br
1	3.39%	0.24%	29.03%	0.69%	45.31%	0.00%	16.15%	5.14%
2	2.81%	0.25%	27.54%	0.65%	48.19%	0.00%	15.61%	4.92%
3	0.25%	0.00%	45.62%	1.48%	45.75%	0.00%	6.19%	0.58%
4	3.13%	0.24%	27.74%	0.68%	46.20%	0.00%	15.90%	6.11%
5	3.60%	0.33%	28.12%	0.33%	46.13%	0.00%	13.98%	7.51%
6	2.98%	0.29%	26.70%	0.80%	47.18%	0.22%	16.14%	5.69%
7	2.50%	0.29%	26.13%	0.66%	49.66%	0.00%	15.80%	4.96%
8	2.88%	0.38%	26.24%	0.70%	47.61%	0.15%	16.56%	5.48%
9	2.77%	0.37%	38.04%	0.75%	40.10%	0.00%	13.65%	4.28%
10	2.48%	0.15%	26.73%	0.73%	49.29%	0.19%	15.21%	5.23%

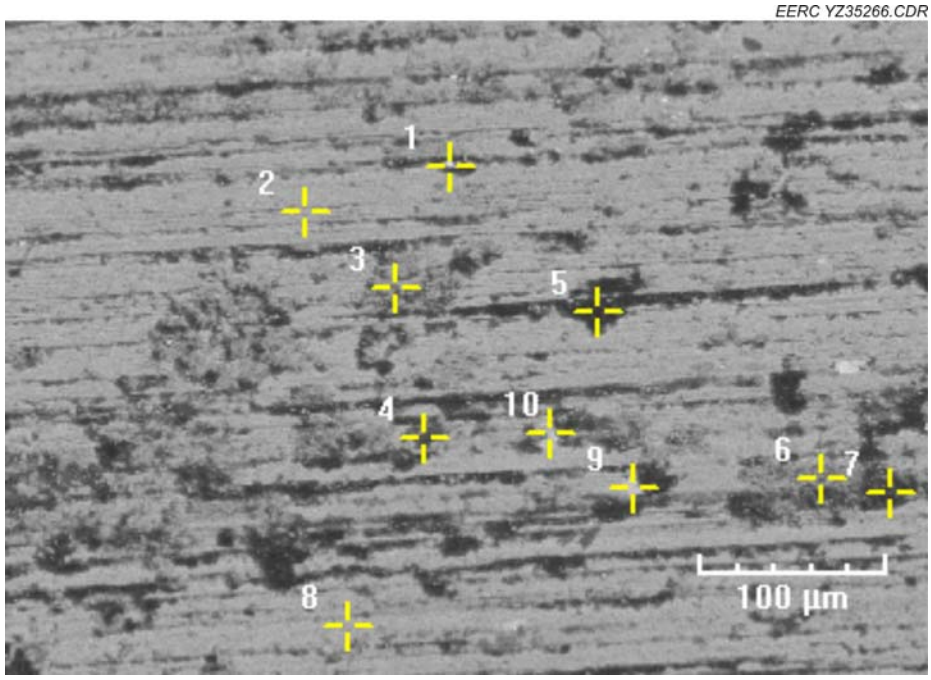

Figure C-7. UM4 surface SEM image.

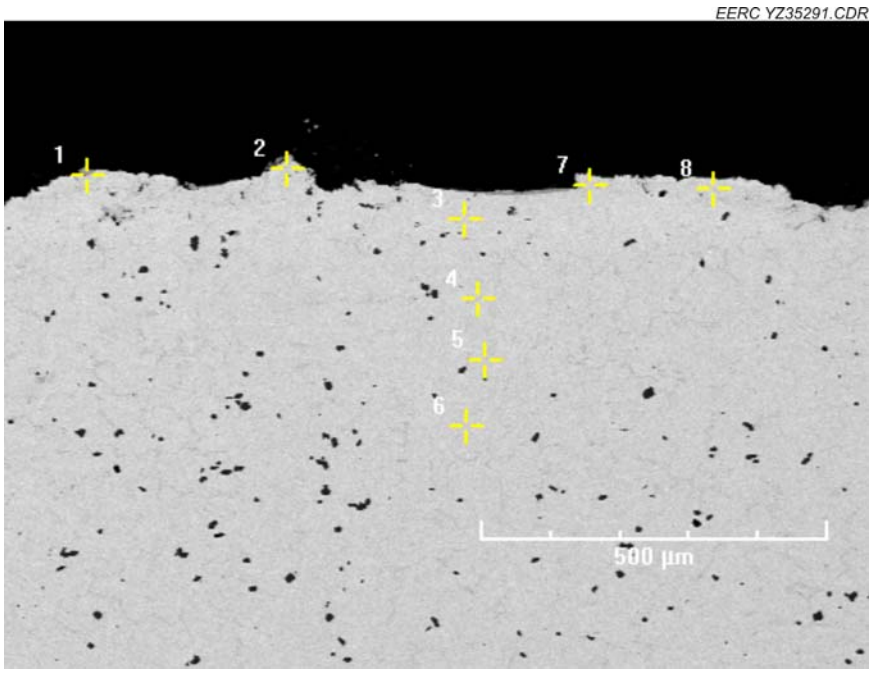

Figure C-8. UM4 cross-sectional SEM image.

Table C-4. Elemental Analysis of UM4 Cross Section

Tag	Si	S	Cr	Mn	Fe	Co	Ni	Br
1	3.28%	0.40%	25.70%	0.28%	49.05%	0.00%	14.33%	6.97%
2	3.25%	0.24%	26.95%	0.24%	47.57%	0.00%	14.90%	6.86%
3	2.99%	0.33%	29.72%	0.54%	47.33%	0.00%	14.16%	4.91%
4	2.96%	0.16%	28.79%	0.57%	47.38%	0.00%	16.07%	4.02%
5	4.44%	0.18%	30.14%	0.41%	52.77%	0.00%	7.21%	4.72%
6	3.22%	0.28%	28.40%	0.84%	45.59%	0.06%	16.87%	4.69%
7	2.56%	0.21%	26.62%	0.65%	48.96%	0.00%	15.73%	5.22%
8	3.02%	0.24%	27.05%	0.63%	47.70%	0.00%	16.06%	5.31%

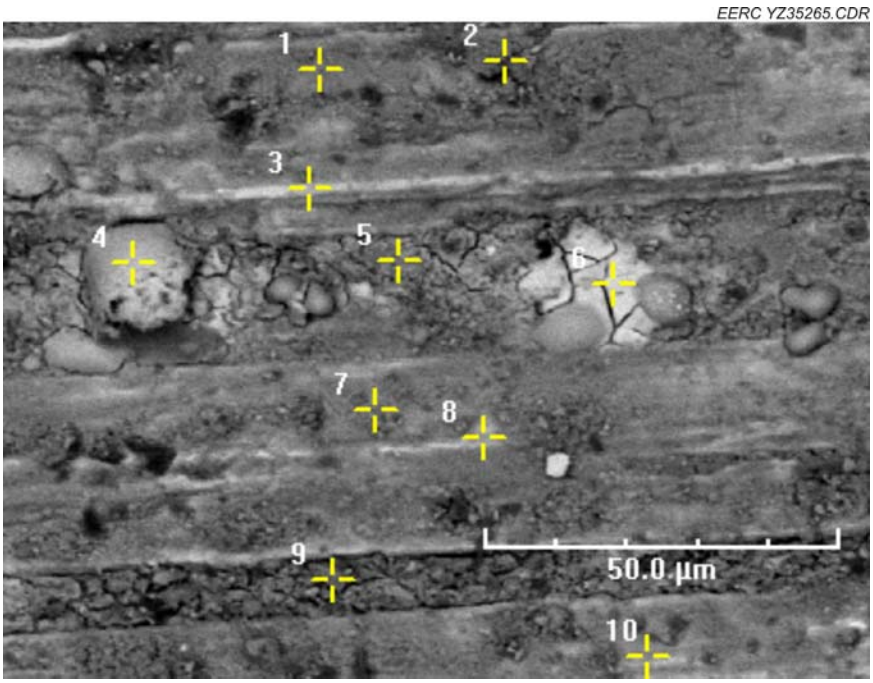

Figure C-9. UM5 surface SEM image.

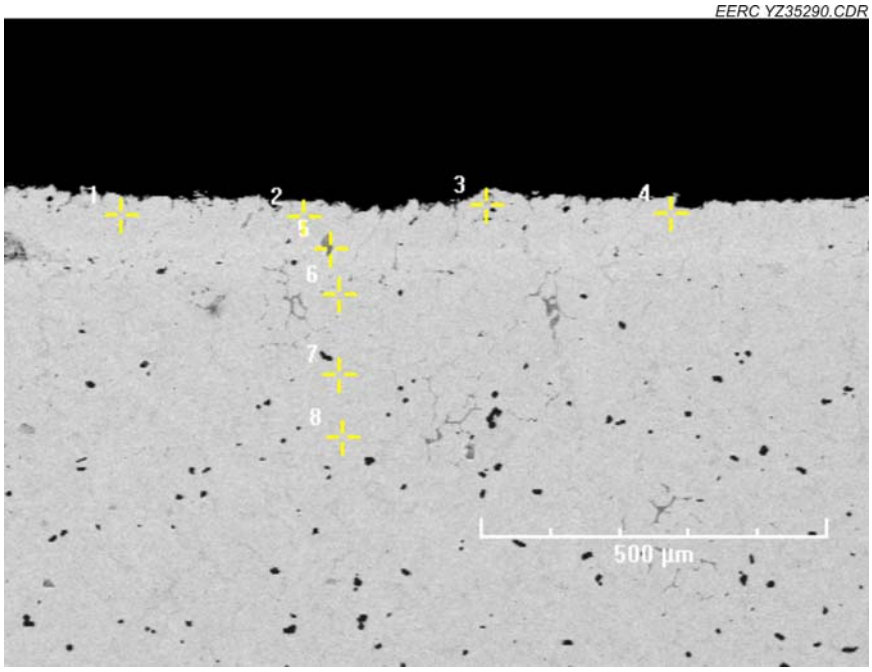

Figure C-10. UM5 cross-sectional SEM image.

Table C-5. Elemental Analysis of Cross-Sectional of UM5

Tag	Si	S	Cr	Mn	Fe	Co	Ni	Br
1	3.39%	0.40%	26.51%	0.84%	46.84%	0.00%	16.44%	5.58%
2	2.31%	0.31%	54.47%	0.55%	29.91%	0.00%	9.37%	3.09%
3	3.04%	0.36%	24.95%	0.19%	50.36%	0.20%	16.47%	4.43%
4	2.72%	0.22%	26.61%	0.83%	48.86%	0.00%	16.04%	4.64%
5	3.01%	0.12%	28.04%	0.42%	47.69%	0.00%	15.99%	4.73%
6	2.84%	0.27%	27.15%	0.75%	47.97%	0.01%	16.23%	4.74%
7	3.21%	0.27%	29.13%	0.97%	44.96%	0.00%	16.51%	4.91%
8	2.56%	0.31%	25.72%	0.94%	49.02%	0.05%	16.12%	5.20%

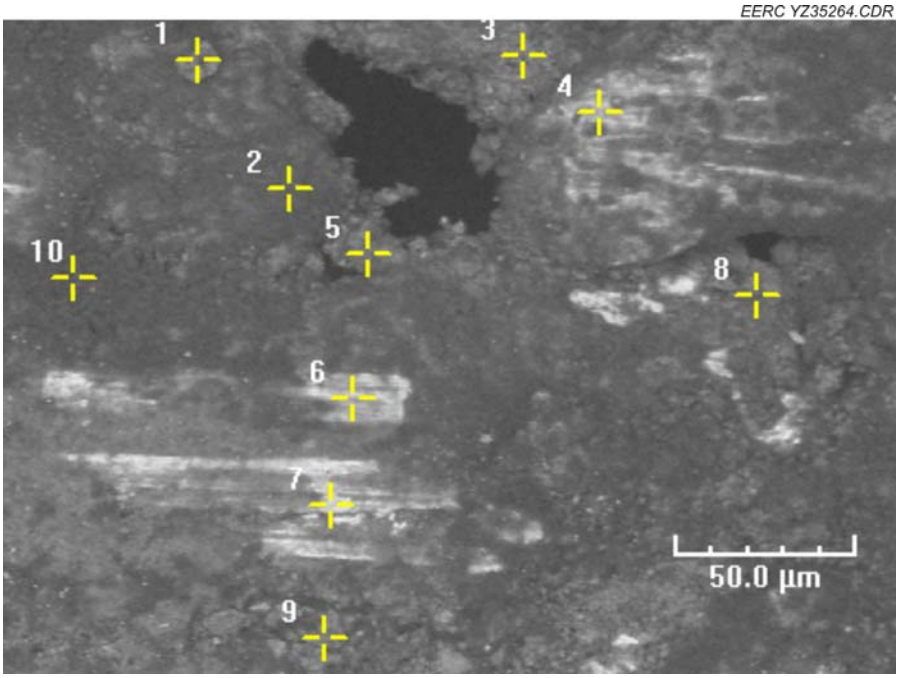

Figure C-11. UM6 surface SEM image.

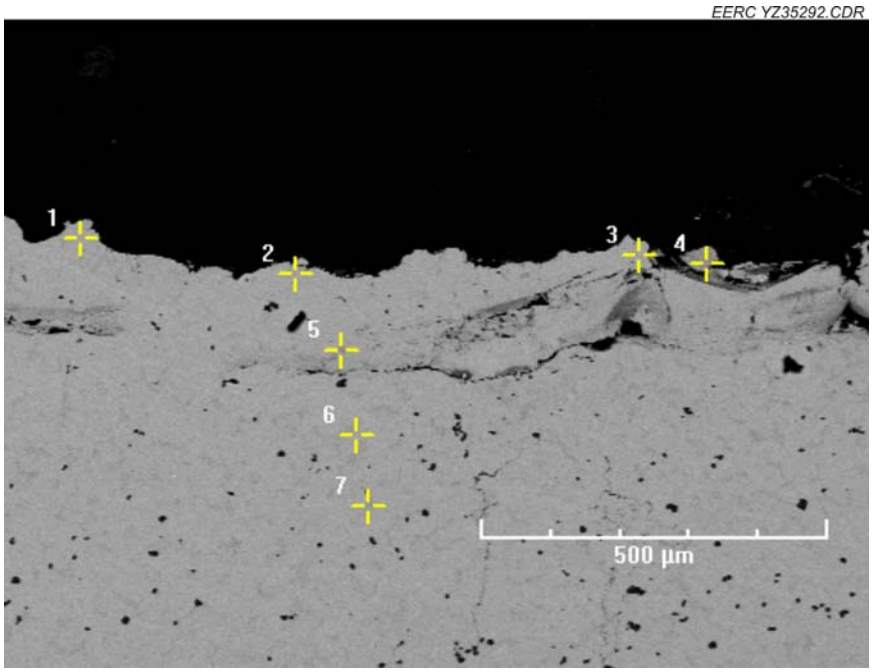

Figure C-12. UM6 cross-sectional SEM image.

Table C-6. Elemental Analysis of UM6 Cross Section

Tag	Si	S	Cr	Mn	Fe	Co	Ni	Br
1	2.88%	0.33%	26.37%	0.39%	47.55%	0.23%	16.87%	5.26%
2	3.27%	0.28%	27.42%	0.41%	48.98%	0.00%	14.60%	4.95%
3	2.84%	0.16%	27.99%	0.33%	48.98%	0.00%	15.73%	3.97%
4	4.44%	0.37%	26.20%	0.66%	45.13%	0.00%	15.47%	7.72%
5	2.59%	0.32%	23.32%	0.75%	43.14%	0.00%	13.73%	16.14%
6	3.25%	0.21%	29.25%	0.58%	46.44%	0.00%	16.02%	4.25%
7	0.78%	0.69%	86.55%	0.38%	9.83%	0.00%	0.10%	1.68%

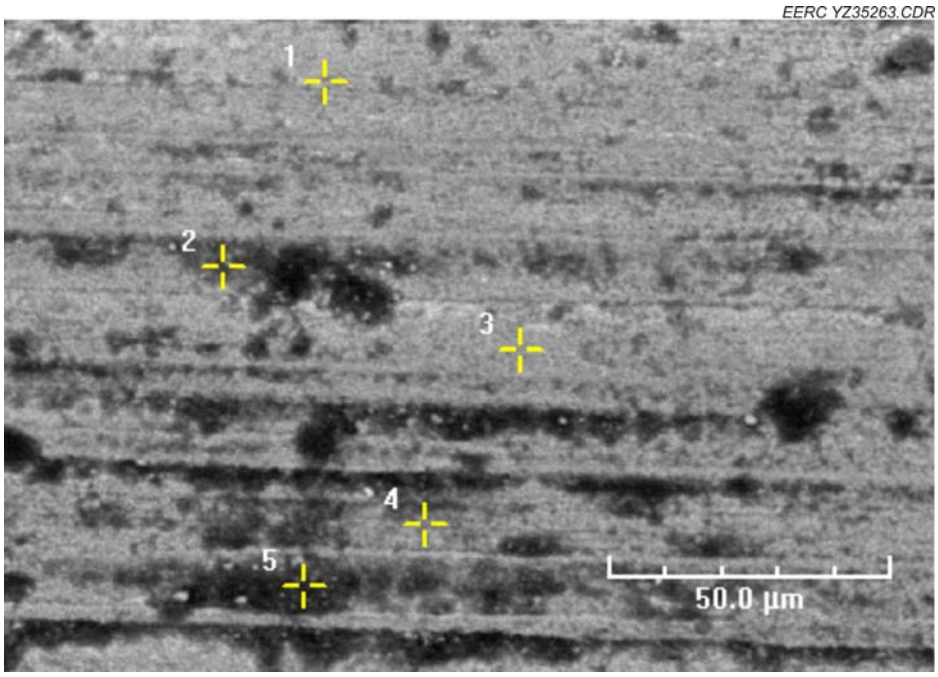

Figure C-13. UM7 surface SEM image.

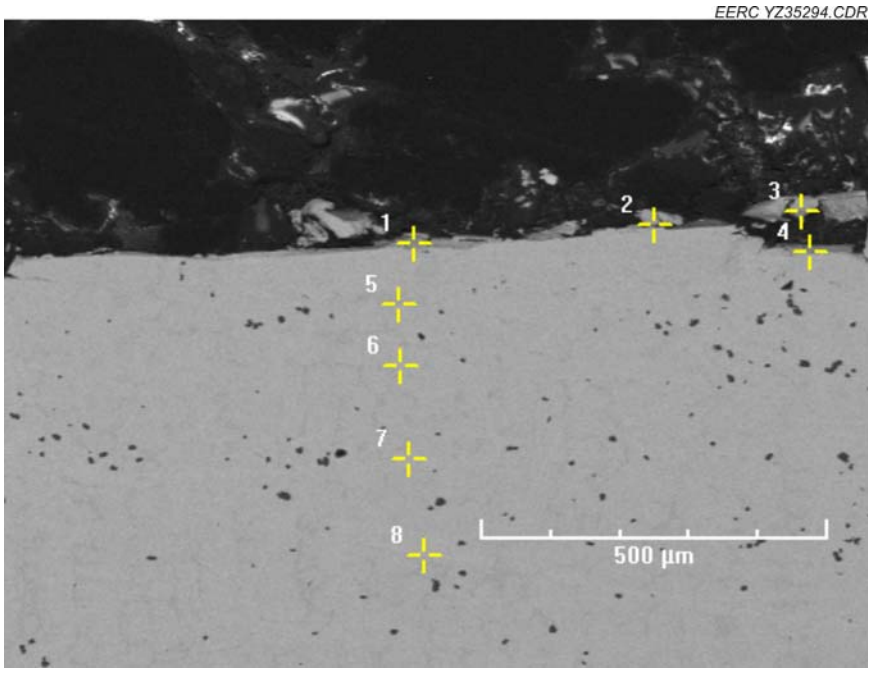

Figure C-14. UM7 cross-sectional SEM image.

Table C-7. Elemental Analysis of UM7 Cross Section

Tag	Si	S	Cr	Mn	Fe	Co	Ni
1	4.34%	0.58%	35.74%	0.58%	43.40%	0.00%	15.37%
2	3.38%	0.39%	29.70%	0.99%	49.54%	0.00%	15.99%
3	3.90%	0.29%	27.36%	0.49%	51.39%	0.00%	16.57%
4	3.88%	0.78%	29.34%	0.83%	49.35%	0.00%	15.81%
5	4.00%	0.85%	37.09%	0.87%	41.46%	0.00%	15.73%
6	2.94%	0.24%	28.50%	0.62%	50.73%	0.00%	16.94%
7	3.06%	0.19%	27.76%	1.09%	51.20%	0.00%	16.69%
8	3.24%	0.30%	28.19%	0.78%	50.71%	0.11%	16.67%

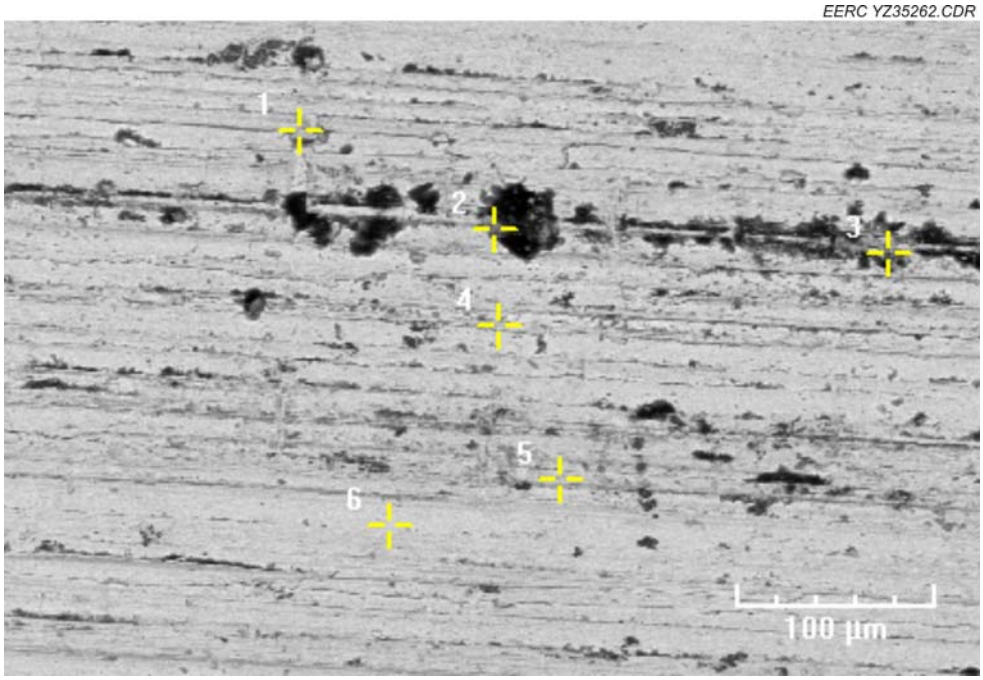

Figure C-15. UM8 surface SEM image.

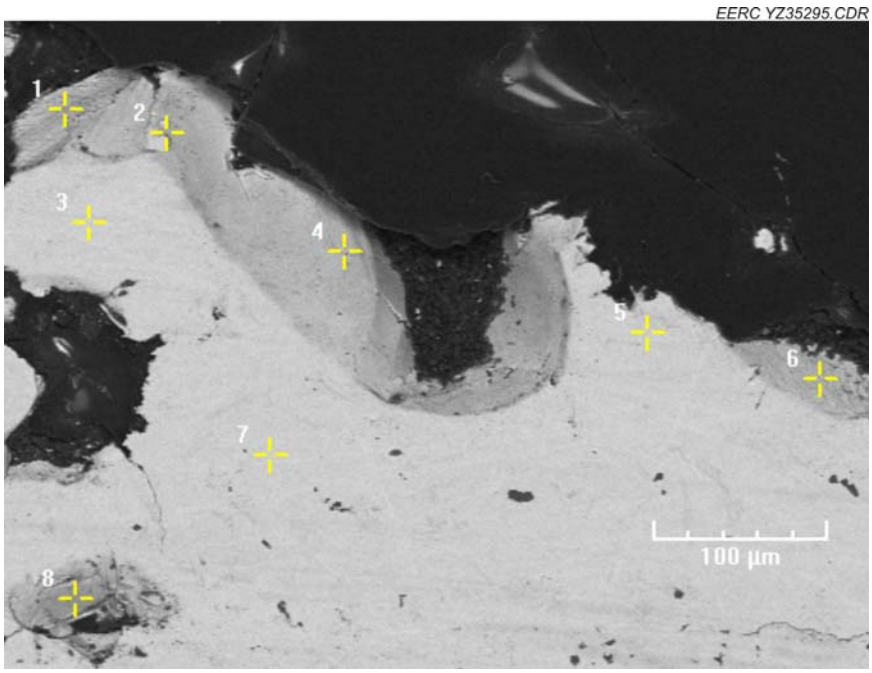

Figure C-16. UM8 cross-sectional SEM image.

Table C-84. Elemental Analysis of Cross-Sectional of UM8

Tag	Si	S	Cr	Mn	Fe	Co	Ni
1	2.86%	0.93%	64.27%	0.26%	25.74%	0.00%	5.95%
2	3.55%	0.49%	29.62%	0.62%	50.78%	0.00%	14.94%
3	3.14%	0.26%	28.05%	0.42%	51.63%	0.00%	16.49%
4	4.13%	0.51%	29.28%	0.09%	50.76%	0.00%	15.21%
5	6.86%	0.66%	35.90%	0.84%	48.36%	0.00%	7.38%
6	3.96%	0.49%	28.62%	0.25%	51.90%	0.00%	14.78%
7	3.58%	0.19%	29.38%	0.78%	49.58%	0.00%	16.50%
8	2.72%	0.46%	35.40%	0.88%	47.15%	0.00%	13.33%

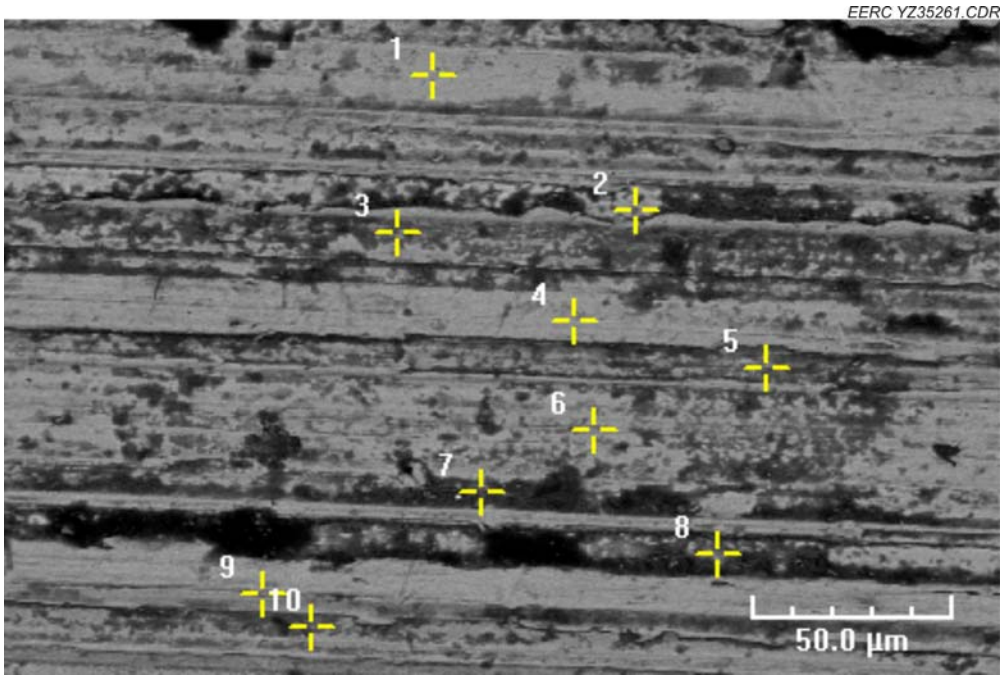

Figure C-17. UM9 surface SEM image.

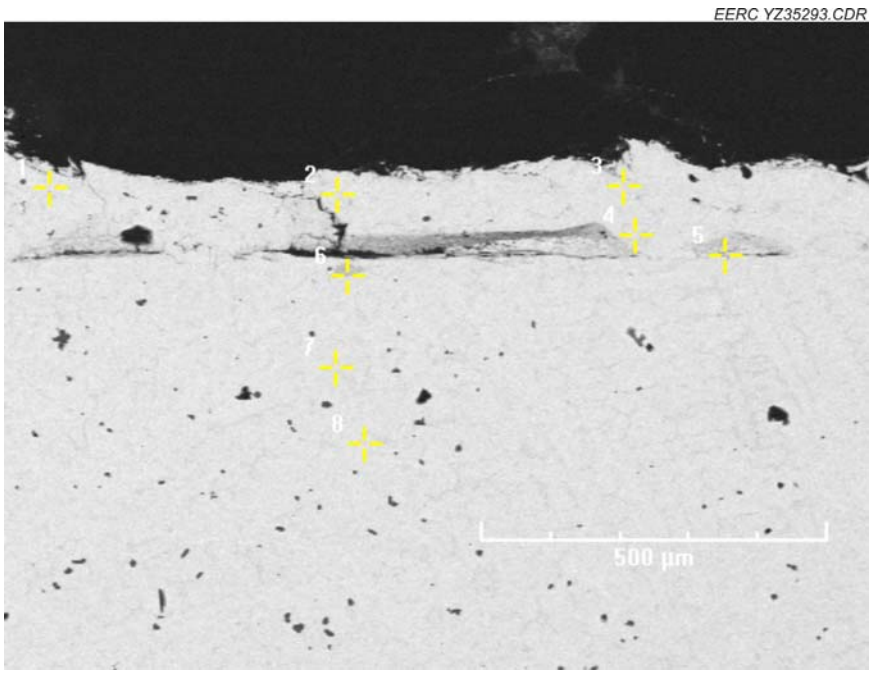

Figure C-18. UM9 cross-sectional SEM image.

Table C-9. Elemental Analysis of UM9 Cross Section

Tag	Si	S	Cr	Mn	Fe	Co	Ni
1	3.05%	0.15%	29.47%	0.86%	49.42%	0.00%	17.06%
2	3.44%	0.30%	29.75%	0.99%	48.71%	0.00%	16.80%
3	2.98%	0.21%	28.54%	0.60%	50.56%	0.00%	17.10%
4	3.17%	0.50%	28.81%	0.75%	49.51%	0.20%	17.06%
5	3.31%	0.26%	28.11%	0.25%	50.49%	0.00%	17.51%
6	4.27%	0.33%	29.07%	0.57%	47.46%	0.07%	18.23%
7	4.07%	0.32%	28.24%	0.97%	49.11%	0.00%	17.29%
8	2.81%	0.20%	27.72%	0.97%	51.36%	0.00%	16.94%